Smoothness of color transformations

Anna Aristova

Smoothness of color transformations

Anna Aristova

2010/07/01

Abstract

Color image quality is an important factor in various media such as digital cameras, displays and printing systems. The employment of different color imaging media leads to a constant problem that each device produces color differently. In this case the image reproduction quality depends on processes of device characterization. Color look-up tables (LUTs) are the most common empirical approach for device characterization, and are the basis for ICC profiles. Correct 3DLUT-based color conversion in device characterization is an important factor for achieving high quality of the reproduced color image. Such factors as LUTs size, interpolation methods and unavoidable noise in color measurement process and unstable printing process influence on smoothness of 3DLUT-based color transforms, and may result in the appearance of artifacts in the final reproduced images. It is quite common to evaluate the quality of color transforms in terms of colorimetric accuracy, but smoothness is often neglected, even through its importance is now generally agreed on (Olson, 1999).

The main goal of this project was to find a way of quantifying to which extent different transforms smooth or not smooth output images through analysis of LUT-based device characterization process, investigating factors which affect on color transformations and testing different existed methods. There are some scientific studies dedicated to evaluating smoothness of color transforms but the proposed algorithms were applied and tested only on well-designed 3D-LUTs, device characterization process and experimental data. So these metrics still require testing and evaluation using complex images and on profiles obtained during different measurements and in different environments.

A new method of evaluating smoothness of color transformations was proposed based on extension of second derivative method suggested earlier (Green, 2008). The algorithm is based on considering 3DLUTs of ICC profiles (AToB# table) as set of color planes in the printer color space and corresponding to them values in CIELAB color space. Each color plane in CIELAB color space presents set of color transitions in horizontal and vertical directions. The second derivative of ΔL^*, Δa^* and Δb^* between adjusted points of each vertical and horizontal transitions was found. Statistical estimations were used for deriving general result among color planes for profiles. The metric values were computed in 2 ways for one channel PM L^* and for three channels PM L^*, a^*, b^*.

In this research it was proposed approaches using image difference metrics for evaluating smoothness of color transformations. For these goals 45 ICC profiles were generated from measurements with different repeatability and from measurements of consecutive printed charts on substrates of the same paper type for providing 3DLUTs with various noise characteristics. The process of profiling was designed to be close to a real practical case. Four test images containing smooth transitions of colors were converted using the profiles for obtaining images with varying smoothness. A psychophysical experiment involving 20 observers was conducted for evaluating perceived difference in smoothness

between softcopy of original image and softcopies of images' reproductions using a category scale from perfect match to worst match in smoothness.

The proposed method have shown better performance in predicting smoothness of color transformation by particular profiles – compare with previous metrics by Green (2008), Kim et al. (2010). Full-reference image quality metrics SSIM, GSSIM, pixel wise CIELAB Delta E, sCIELAB, Adaptive bilateral filter, Edge similarity, and Structural content - were compared for evaluating difference in smoothness between original and reproduced images. GSSIM have shown higher Pearson correlation with visual judgments and representation than the other metrics.

Keywords: Device characterization, look up tables, smoothness, color transform, color difference, color quality.

Preface

This master thesis had been carried out together with the Department of Computer Science and Media Technology at Gjøvik University College and The Norwegian Color Research Laboratory. The main aim of this project is to find a way of quantifying smoothness of color transforms.

In first order I would like to thank my supervisors, postdoctoral researcher Zhaohui Wang and professor Jon Yngve Hardeberg, for their excellent supervision, good advices, motivation, control of thesis work and patience. Then I want to say thanks to everyone who participate in my experiments, color engineer in The Norwegian Color Research Laboratory Aditya Suneel Sole for assistance with experimental setup and equipment and Eric Garcia for test images. Thanks to Hilde Bakke and Rune Hjelsvold, teachers and stuff for their good work in organizing "Master thesis 2010" spring semester. Thanks to my friend Thomas Snoen and classmates for their support and care during this time.

My special gratitude turns to Gjøvik University College and Norwegian government for opportunity to study here.

Anna Aristova, 2010/07/01

Contents

List of Figures

List of Tables

1   Introduction

This chapter is dedicated to present master thesis topic, problem description, research questions and justification for carrying out thesis.

1.1   Topics covered

The main goal of this project is to find a way of quantifying smoothness of color transforms through analysis of 3D LUTs based device characterization process and the factors which affect on it and test different image quality metrics. It requires conducting a number of experiments for determining and estimating thresholds of factors for predicting unsmooth transform and corresponding human perceptual evaluation of smoothness of color transforms in comparison with quantitative evaluation results provided by different image quality metrics.

1.2   Problem description

The rapid development of the image reproduction digital devices makes them accessible for large group of users. Growing color imaging industry leads to increasing user's expectations and requirements to quality of reproduced images. Different color imaging devices reproduce same color differently, so they employ different reproduction approaches and use own device color spaces. The same color primaries RGB would be presented differently on various displays or printers. Users often look for pleasantness, consistency and predicatibility of colors on reproduced image rather than accuracy of reproduced colors.

There are three main processes which influence on quality reproduced and transmitted color between device: device calibration, characterization and conversion (presented on figure 1 from [1]). In literature, generally,these definition are integrated in one term device characterization.

Calibration guarantees that device (scanner, monitor or printer) conform to an established state or condition often specified by manufacturer. Characterization is a way of determining the output of a system in response to a known input where input and output are defined colors or system signals. Characterization process allows deriving the color gamut and reproduction characteristics of a particular device in calibrated state. Conversion or color transformation defines translating color from device-dependent color space to device-independent (intermediate) under known conditions.

The image reproduction depends on several limitations of processes in a device characterization. The one of the widely used approaches for device characterization is multi-
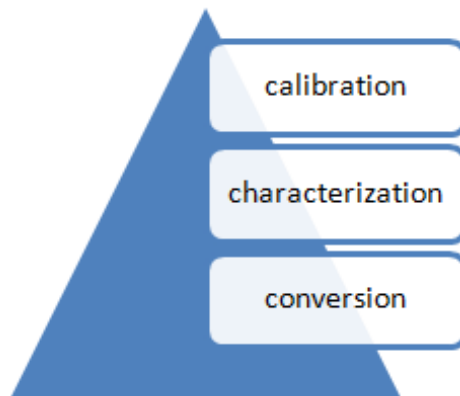
Figure 1: Device characterization.

dimensional look up tables (LUTs) color transformations which are basis for ICC (International Color Consortium) profiles. Profiles play important role in device characterization process and in color management systems. They allow transfer color information between different devices. 3D LUT is a table or matrix of n3 color patches at the lattice points of source space(device-dependent) and corresponding to them measured color specifications of output color space(device-dependent). Special color charts and color targets with known device-dependent primaries are measured by instruments for getting device-independent primaries. In this thesis printer characterization is in scope of attention.

Smoothness of color transform is also desirable property of color transform, often given ranking in visual evaluations of color reproductions [2]. Jon Y.Hardeberg gave definitions of smoothness of a color look up tables as image quality factor [3]. The smoothness means that there should be no abrupt steps in the LUTs: the values should vary smoothly in the entire LUT.

In this project smooth transforms are determined as transforms which provide output smooth color transitions without artifacts (bounding, gains, stripes, color shift, contours). For example smooth transform should guarantee smoothly varying ramp between two colors as shown on figure 2. It can be met frequently in business graphic, natural scenes images.

The unavoidable noise in measurements, interpolation method, look up tables size and precision errors during computation are factors which influence on smoothness of LUT-based color transforms and consequently on quality of reproduced image [4],[5].

So one of main problem in this area is to find a way to quantify that one or another color transform gives smooth or not smooth output result. There are some scientific studies dedicated to evaluating smoothness of color transforms by T.Olson[6], P.Green[7] and Y.J.Kim et all[8]. But proposed algorithms in these research works are based on well-designed 3D-LUTs, device characterization process and experimental data. So these

2

a) Smooth transition between green and red;

b) Smoothnees distortions on ramp between green and red.
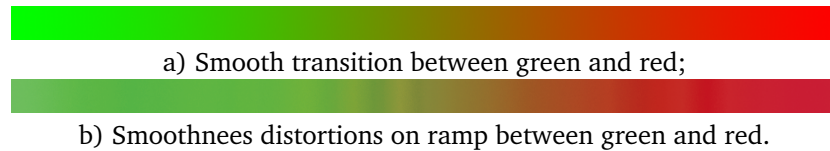
Figure 2: Smoothness of color transitions

metrics still require testing and evaluation with more complex images than ramps and on profiles obtained during different measurements and different environment.

It is worth to notice that image quality assessment is not easy task and depends on personal subjective opinion of observer and many different factors. Special algorithms or metrics are used to quantitatively measure perceptual difference between original and reproduced image simulating human visual system. These primitive models of complex human visual system cannot allow predicting the perceived image difference very well. Then there are also possibilities to test many image differences and image quality metrics as candidates for quantifying smoothness of color transforms. So evaluation of color transform can be considered as open question for research.

1.3 Motivation and benefits

The growing number of color imaging digital devices leads to increasing requirements of users to color image quality reproduction. Devices' manufactures are interested in achieving best possible color reproduction by produced devices. They try to improve technology processes which underlie of color reproduction.

The process responsible for transmitting color information is device characterization. The color transformations using multi-dimensional LUTs (look up tables) in ICC profiles are commonly applied method of device characterization. Manufactures supplies with factory profiles for produced devices. But it is happened very often when professionals in art, design, photography, print-press industry and other users have to change factory specified setup for device and have to conduct device characterization again. So after this moment process of device characterization cannot be controlled by manufacturers, and result depends on measuring instruments, color charts, software for profiling, surrounding environment and experience of person conducting it. Measurement noise is error which inescapable during measurement process though on significant progress in instrument design and manufacture[9]. The measurements instruments are evolved in reliability, stability and convenience of using. But random noise in measurements takes a place the random errors because of unpredictable variations during color measurement. The precision and uncertainty of the color measurement are mainly represented in the LUTs. So it became increasable important to identify which profile allows getting smooth or unsmooth transform and output result.

Image difference and quality metrics are also taken to consideration in this project. The final result of color transforms is output image which estimated by human. There are many image difference and image quality metrics for predicting perceived difference

between original and processed image which simulated human visual system in simple way.

Obtaining and finding metric for evaluating smoothness color transformation allow predict unsmooth results and prevent them during process of device characterization. The evaluation of smoothness of color transform will allow building a bridge between approaches for improving device characterization methods based on 3DLUTs and observers' percieved color image reproduction output image as result of this transform.

It will allow continue work in direction of getting qualitative reproduction of color images fast and economically and developing technology advances for obtaining it.

1.4   Research questions

The following research questions have been formulated for research in this thesis:

- Q1. Which factors during device characterization mainly affect on smoothness of color transforms? For evaluating and predicting unsmooth transform origin of problem must be determined and learned. There are many studies which considered accuracy of color transforms[5] reasons of smoothness distortions related to problems of building 3LUTs in profiling process and methods of smoothing 3D LUTs [4],[9], [10].

  The influence of three main factors of LUT-based color transforms and respectively on color quality of reproduced image is considered in this project as in related work:

  1. 3D LUTs size or quantization interval;
  2. interpolation method for mapping non-lattice (not included to LUTs) points from device-dependent to device-independent color space;
  3. measurements noise during profiling.

- Q2. How to quantify which color transformation gives smooth or unsmooth output result (or quantitatively evaluate) closely to human visual assessment? The idea is to find quantitative method which allow identify unsmooth transform and quality of profile in term of smoothness. The performance of existed metrics should be tested or new algorithm should be proposed for evaluating perceived smoothness of image dataset based on 3LUTs color transforms (ICC profiles).

1.5   Thesis structure

Chapter 2 gives introduction to the state of art in field considered in the thesis and covers though the most important aspects related to this thesis. **Chapter 3** describes methodolody and project workflow for solving existed problem. **Chapter 4** dedicated to analysis of factors which affects on 3DLUT-based smoothness of color transformations:

3DLUT size, noise and interpolation method. In **Chapter 5** conducting color measurements for printer profiling and profile generation process are considered. Evaluation of smoothness of color transformation fully considered in **Chapter 6** including description of psychophysical experiment, visual judgements analysis, method of color planes algorithm and analysis of different metrics performance for evaluating smooothness of color transformations. In **Chapter 7** a conclusion is given followed by further research opportunities and a bibliography. The last sections are **Appendixes** containing supplementary data for this thesis.

2 State of the art

In this chapter overview of previous work and research in area of evaluating smoothness of color transforms. The research questions in this master project requires overview in different fields as LUTs-based device characterization, image quality, color conversion methods and precision and accuracy measurements.

2.1 Device characterization

The definition of device characterization process was mentioned in Introduction of this thesis. So device characterization is complex process interconnected with process of calibration and color conversion.

Device calibration (according [11],272) is the process of maintaining the device with a fixed or known characteristic color response. The main target of this process to make the device behave consistently so that the characterization (typically presented as icc profile) that describes it remains accurate. If special device characteristic are required, set of color measurements is conducted for deriving correction functions to ensure that the device support desired color response. Tone reproduction curves are generally used functions for each device signal for achieving desired color characteristics. So first captured device signal is processed through a calibration function(linearization).

The characterization process derives the relationships between device-dependent (RGB, CMYK and others) and device-independent(CIEL*a*b*, CIEXYZ) color representations for a calibrated device ([11], 273). Simplified schema of device characterization and color transfer between two devices is presented on figure 3. Characterization is often presented as building device profiles that reflect their current behavior ([12], 114).

For many devices (according to [13]) the process characterization can be considered to consist of two stages:

- 1 stage performs linearization (sometimes termed for some devices as gamma correction);
- 2 stage performs linearized values into the CIE XYZ or CIEL*a*b*;

Practical device characterization will almost certainly require if non-linear transform is used performing the linearization process and then use approximately linear values as input to non-linear transform.
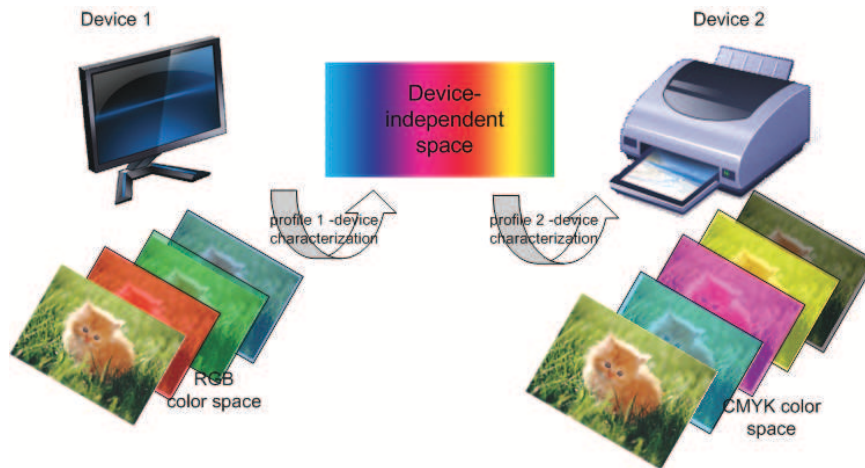
Figure 3: Device-independent color management

2.1.1 Input and output device characterization

There are two direction of device characterization according to ([11], 274):

1. the forward characterization (defines a response of the device to a known input);

2. the inverse characterization process (defines input characteristics to the device that is required to obtain a desired response).

The characterization process is different for input and output devices. The digital input color devices are presented by 2 main types: scanners (captures light reflected or transmitted through a medium) and digital cameras (directly capture light from scene). The captured light passes through color filters (commonly, red, green, blue) and then catches by system of charge-coupled devices (CCDs)([11],281).

Output devices are generally categorized into emissive display devices and devices that produce reflective prints or transparencies (different printers' types). Such devices as CRT (cathode ray tube) displays, liquid crystal displays LCDs, organic light emitting diodes (OLEDs), plasma displays, projection displays are emissive devices which based on additive mixing of red, green and blue (RGB) lights for producing colors.

For these devices some assumptions are usually made for simplification of characterization (according to ([11], 281)):

- channel independence (each of R,G,B channels to the display operates independently of the others);

- chromaticity constancy (the spectral radiance due to a given channel has the same basic shape and is only scaled as a function of the device signal).
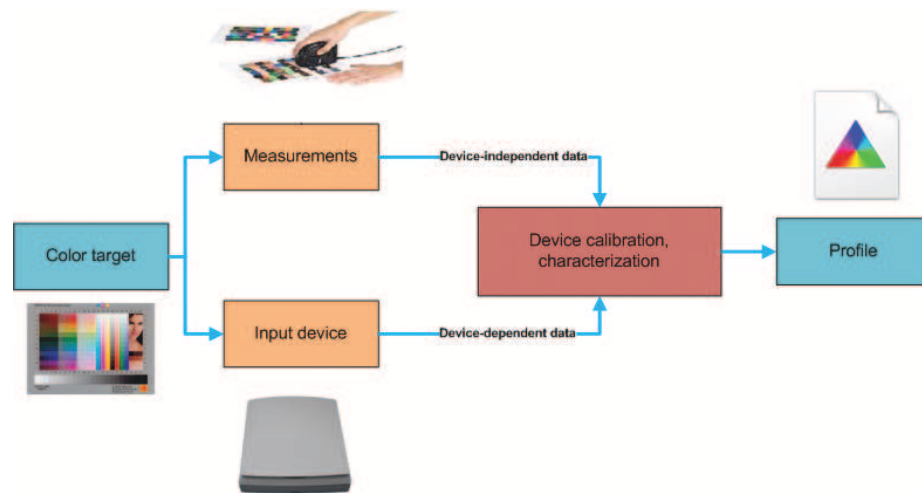
Figure 4: Input characterization workflow

Printing devices color reproduction is based on subtractive color mixing. Subtractive color mixing system uses medium for the colorants (usually paper or transparency) reflection or transmission of the light at all visible spectrum. The different spectral distributions (or colors) can be produced by combining cyan, magenta and yellow(C,M,Y) colorants and respectively removing spectral energy from the red, green, blue portions of electromagnetic spectrum. Black colorant (is designated as K) is applied for reducing costs of color inks and for increasing the capability to produce dark colors.

Printers could be classified according to ([11],283):

- Continuous-tone process (generates uniform colorant layers and changing the concentration of each colorant to produce different intercity);
- Halftoning process (generates dots at a small fixed number of concentration levels and modulates the size, shape, and frequency of the dots to produces different intensity levels).

For the input devices, the forward function is a mapping from device-independent color stimulus to the resulting color stimulus to the resulting device signals. For the output devices, this is mapping from device-dependent colors driving the device to the resulting rendered color in device-independent coordinates.

The general workflow for input and output device characterization are presented on figures 4 and 5 (according [11]).

For input device characterization, first, the device is calibrated, usually by ensuring various internal settings which should be fixed in nominal state. Then characterization is implemented using a target presenting set of color patches that spans the gamut of input
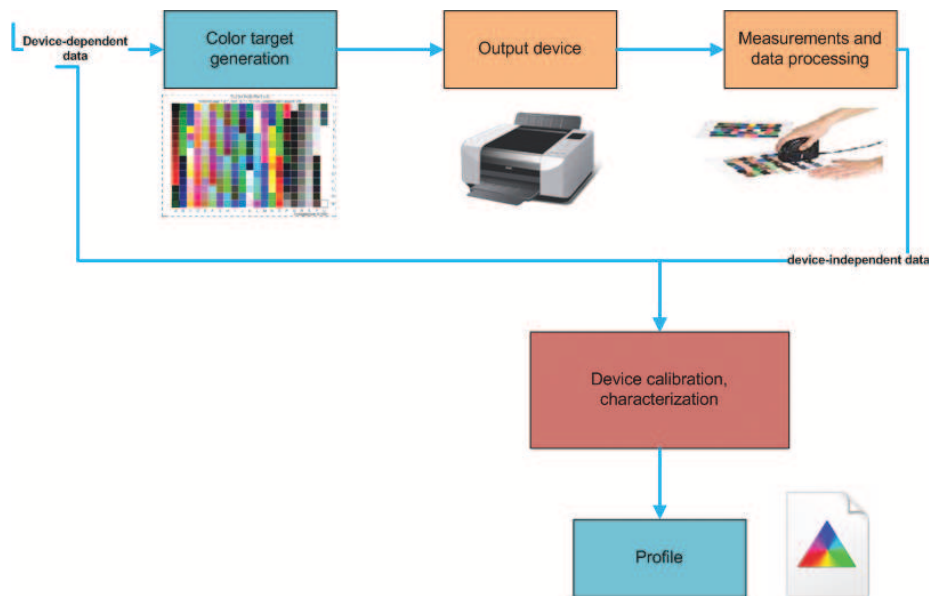
Figure 5: Output characterization workflow

device. Industry standard targets designed for input devices (scanners) are the Q60 and IT8 (IT8-7.1 is transmissive target, IT8-7.2 is reflective target). Device-independent color measurements are made of each patch in the target using a spectroradiometer, spectrophotometer, or colorimeter. The data obtained after measurements should be stored in new data file or using a data reference file supplied by the manufacturer for the target. Then input device records an image of the target (in example with scanner characterization, scanning image of the target). The captured by device image should be processed through calibration functions derived in the previous step. The device-dependent values (typically in RGB color space) for each patch should be extracted from image by using color management program. Extracted device-dependent values are correlated with the corresponding device-independent values to obtain characterization of device. This data is recorded in profile for input device.

The common output characterization workflow could be presented as on figure 5. A digital target of color patches with known device values is sent to device. Then these displayed or printed color target could be measured in device-independent (colorimetric) color coordinates. Then relationships between device-dependent and device-independent color coordinates should be found. These data should be stored in device profile.

2.1.2 Methods of device characterization

There are 2 main methods of device characterization [11],[14]:

- Physical models;
- Empirical models.

Model-based approach or physical models are based on knowledge of physical properties or behavior of the device, such as absorbance, scattering and reflectance of colorant and substrates. Physical models describe how the device captures and rendering color.

Empirical models is models which do not require prior knowledge about of the physical properties of a device, and they rely on measurement of large number of color samples, used either to optimize a set of linear equations based on regression algorithms or to build look-up tables for 3D interpolation.

The model-based approach may require fewer measurements and thus less time consuming than empirical methods. The physical model can be generalized for different image capture or rendering conditions. Empirical technique is employed for a restrictive set of conditions and has to be re-derived when conditions are changed.

Model-based approaches generate relatively smooth characterization functions when empirical technique could have additional noise from measurements and often require additional smoothing of data. But certain types of devices are not readily amenable to tractable physical models so empirical approach in this case should be implemented.

P. Green argues that there are 3 methods for device characterization [15]:

- Physical models;
- Numerical models;
- Look up tables.

As numerical models Green considered models in which series of coefficients is defined usually by regression from set of known samples, with no prior assumptions about physical behavior of the device or associated media. Look up tables defines conversion between a device space and CIE color space at a series of coordinates within the color space, and interpolate the values for intermediate coordinates [15]. They could be defined by using physical models or by direct measurements.

In this project first division on 2 main methods of device characterization is considered in this project as mostly presented in literature. Empirical approach of printer and display characterization are in focus of attention in this thesis.

It is worth to notice that several physics-based models have been developed to predict the colorimetric response of a printer: Beer-Bouguer model, Kubelka-Munk model, Naugebauer model, Yule-Nielsen model and etc ([11],338). They are based on physical and mathematical modeling interaction between light, colorants, and medium at macroscopic level.

GOG(Gamma Offset Gain model) and GOGO (Gamma Offset Gain Offset model extended model) are model-based approaches for characterizing CRT(Cathode Ray Tube) displays ([15], 143),([13],112). These models are based on power-law response of display to voltage. Poynton formulated [16] it is as: the luminance produced at the faceplate of the display is approximately proportional to the applied voltage raised to a power in the range 2.35-2.55. The value of exponent of this power function is called the gamma of CRT display. This relationship can be expressed as:

$$L = V^\gamma \tag{2.1}$$

where L is the luminance of the display, V is the applied voltage, γ is the gamma.

Berns and Katoh (2002) et al. studied non-linear relationships between the digital display values (sometimes referred to as digital-to-analogue converter values) and the displayed luminance for various typical CRT devices, and investigated complex equation based also on the system gain and offset (it is considered in next subsection). These equations are known as GOG model.

Liquid crystal displays (LCD) displays use backlit active-matrix LCD (AMLCD) employing twisted nematic technology. The characterization of LCD often exhibit an electro-optic response which is better modeled as a sigmoid or S-shaped function [17]. But many LCD manufactures build their correction tables into the video card that results in the LCD response mimicking that of a CRT with a power law of about 1.8 – 2.0 ([11], 330). So same assumptions as for CRTs displays are implemented for LCD displays but measurements should be taken of light emanating perpendicular to the plane of the screen. Because the property of AMLCD is that the radiance of the emanating light can be strong function of viewing angle.

2.1.3 Display characterization by GOG model

So in this subsection overview of display characterization by Gamma Offset Gain model is presented because it was applied in this project.

The typical CRT display system is presented on figure 6 according to ([4], 342). A display interface card connects the computer and monitor. This card includes three main components: bus interface, display memory and digital-to-analog converters (DAC). The memory stores 24 bits per pixel (8 bits per color) for providing 16.8 million colors. But human cannot distinguish all these colors. So LUTs are used between the screen memory and the DACs for mapping colors into a smaller palette of colors. The DACS provides voltages to the video amplifies that drive RGB guns. The guns strike red, green and blue phosphors with electrons. The phosphors emit an additive mixture of red, green and blue lights.

Process of displays calibration involves setting contrast (gamma) and brightness. Considering simplified assumptions formula of the relationship between R, G and B input digital values from the tree gun voltages and the resulting displayed luminance
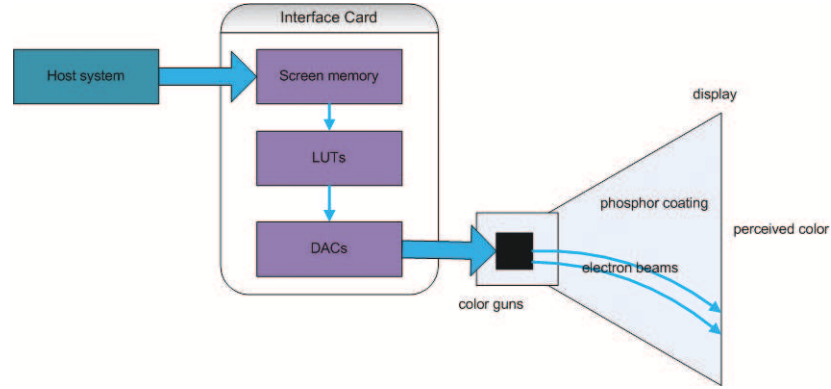
Figure 6: Schema of a typical CRT display system

([11],325) can be presented as:

$$\frac{L_R}{L_{Rmax}} = \left(\frac{D_R}{D_{max}}\right)^{\gamma_R} \tag{2.2}$$

where L_R is resulting luminance from the red channel; L_{Rmax} is luminance of the red channel in full intensity; D_R is input digital value for red gun; D_{max} is maximum digital count (in a 8 bit system equal 255); γ_R is nonlinear power law factor. The analogical expressions could be obtained for green and blue channels. According to ([11],325) values of γ_R , γ_G, γ_B for typical CRTs lie between 1.8 and 2.4.

Correction function for gamma that is applied for each digital signal R, G, B inputs which could be implemented in CRT calibration programs with specified by user system γ_{system}. The formula is presented for digital signal R(analogical for G and B):

$$D_R = D_{max} \cdot \left(\frac{D_R'}{D_{max}}\right)^{\gamma_{system}/\gamma_R} \tag{2.3}$$

D_R' is linear in luminance; D_R is the raw signal that drive the gun voltage.

The idea of applying non-linear preprocessing functions (gamma correction) allows to reduce the visual perceptibility of quantization errors ([11],325). Gamma is a way of quantitatively specifying display contrast. Another setting which necessary consider in device calibration is a color balance of actual light source (specified in Kelvin). CIE determined mathematical description of this illuminant. Illuminant D50 performs natural day light, and is expressed in terms of color temperature equals 5000K. The mid-day sun daylight illuminant D65 has color temperature 6500K. The selection of monitor white point can be highly individual choice. D50 and D65 are commonly used illuminants. D50 agrees with the ANSI standard of viewing conditions for the graphic arts. The standardized RGB color space was proposed by Hewlett-Packard and Microsoft. sRGB involves standard monitor phosphor colors, a white point of 5000K, and the gamma 2.20.

Berns et al. have studied the relationship between the digital monitor values (sometimes referred to DAS digital-to-analogue converter) and the displayed luminance for a

range of typical CRT devices. Following equation describes relationships between digital and spectral data. For red channel it could be presented as ([15], 144) :

$$L_{\lambda,r} = \begin{cases} k_{\lambda,r} \left[a_r \left[(v_{max} - v_{min}) \left(\frac{LUT_r(d_r)}{2^N - 1} \right) + v_{min} \right] + b_r - v_{c,r} \right]^{\gamma_r} \\ v_{c,r} \leq a_r \left[(v_{max} - v_{min}) \left(\frac{LUT_r(d_r)}{2^N - 1} \right) + v_{min} \right] + b_r \\ 0; \, v_{c,r} > a_r \left[(v_{max} - v_{min}) \left(\frac{LUT_r(d_r)}{2^N - 1} \right) + v_{min} \right] + b_r \end{cases} \quad (2.4)$$

where LUT is the video look up table; N is the number of bits in the digital-to-analog converter DAC; v_{max} and v_{min} are voltages dependent on the computer video signal generator; a_r and b_r are the CRT amplifier gain and offset; $v_{c,r}$ is the cut-off voltage defining zero beam current; γ_r is an exponent accounting for the nonlinearity between amplified video voltages and beam currents; $k_{\lambda,r}$ is a spectral constant accounting for the particular CRT phosphors and faceplate combination. This equation describes also components such as DAS, video LUTs, video signal generator, and video signal amplifier.

An complex accurate physical model of monitor behavior is not suitable for purposes of characterization. The relationships between luminance L and DAC $d/(2^N - 1)$ is generated as ([13],113):

$$L = \left[\left(\frac{ad}{2^N - 1} \right) + b \right]^{\gamma} \quad (2.5)$$

where a and b is the system gain and offset respectively. This formula describes generally gain-offset-gamma model(Berns and Katoh, 2002). The effective gamma of a system will dependent upon the offset and gain controls are set.

This equation could be used for mapping the normalized DAC values $(d_r/(2^N - 1)); (d_g/(2^N - 1)); (d_b/(2^N - 1))$ to the linearized normalized DAC values (R,G,B). So expression for red channel can be presented as:

$$R = \begin{cases} \left[a \left(\frac{d_r}{2^N - 1} \right) + (1 - a) \right]^{\gamma_r}; \, \left[a \left(\frac{d_r}{2^N - 1} \right) + (1 - a) \right] \geq 0; \\ 0; \, \left[a \left(\frac{d_r}{2^N - 1} \right) + (1 - a) \right] < 0; \end{cases} \quad (2.6)$$

The normalization procedure requires that the system gain and offset are equal to unity. Because CRT based on additive mixing last equation the relationship between tristimulus values and RGB as linear transformation:

$$\begin{bmatrix} X_{pixel} \\ Y_{pixel} \\ Z_{pixel} \end{bmatrix} = \begin{bmatrix} X_{r,max} & X_{g,max} & X_{b,max} \\ Y_{r,max} & Y_{g,max} & Y_{b,max} \\ Z_{r,max} & Z_{g,max} & Z_{b,max} \end{bmatrix} \times \begin{bmatrix} R \\ G \\ B \end{bmatrix} \quad (2.7)$$

R,G,B is lineralized and normalized DAC values.

The display could be characterized in two ways:

1. without color management software;

2. using color management's software.

Process of monitor characterization without using software was described by Berns et al([18]).They determined 3 main characteristics which are important in considering

process of display characterization ([18],175):

- system gamma Γ which represents the entire non-linear relationship (this gamma could change be changed by video-look-up table values, contrast and brightness);
- invariance of cathode ray tube's γ describes by gamma γ;
- gun amplifier's offset (contrast control) adjusted with slight negative bias for obtaining zero spectral radiance as response on DAC values

The typical display calibration and characterization steps are described bellow according to original Berns at al. paper[18] and strandards ISO 12646[19] and ISO3664[20]:

1. **Warming up display (takes 2 hour) and preliminar preparations.** A measurement instrument (colorimeter) should be calibrated as well and set to mode (Y,x,y). It should be temporally stable and always leaving turned on. Display should be located in room with neutral, preferable, gray or back surrounding to minimize flare. If it is not possible avoid illumination in the room with display than level of ambient illumination and illumination source might be regulated according to standard (ISO 3664).

   The faceplate of monitor might be degaussed and cleaned. Colorimeter should be contacted with faceplate of monitor.

2. **Determining colorimetry of each channel.** The tristimulus values in matrix (equation 2.7) should be derived that was described before.

   There are 2 methods to derive it:

   - Use published data of each channel's chromaticities and measurements of each channel's luminance. Chromaticities are usually published for a given class of CRT. But this method is not recommended.

   $$\begin{bmatrix} X_{r,max} & X_{g,max} & X_{b,max} \\ Y_{r,max} & Y_{g,max} & Y_{b,max} \\ Z_{r,max} & Z_{g,max} & Z_{b,max} \end{bmatrix} = \begin{bmatrix} \frac{x_r}{y_r} & \frac{x_g}{y_g} & \frac{x_b}{y_b} \\ 1 & 1 & 1 \\ \frac{z_r}{y_r} & \frac{z_g}{y_g} & \frac{z_b}{y_b} \end{bmatrix} \times \begin{bmatrix} L_{r,max} & 0 & 0 \\ 0 & L_{g,max} & 0 \\ 0 & 0 & L_{b,max} \end{bmatrix}$$
   (2.8)

   - Use colorimeter or spectroradiometer and measure each channel's peak output. Spectroradiometer should have good photometric linearity and wavelength accuracy $\pm 0.5 nm$.

3. **Rough calibration of display system.** It is better use firmware monitor's software for this goal. Purchase a monitor with its peak white chromaticities close to monitor specifications. If there are no specifications the chromaticities might be selected near D65. The gun amplifier's gains and offsets of the three channels should be set for achieving color temperature, peak luminance and black level. So it requires rewriting the video LUTs to smooth values. A image could be used for regulating contrast and brightness until image's tone reproduction will not pleasant. There is another way

by displaying black image in dark room and adjust gun amplifier offset to just above setting when light become perceptual. Then text might be displayed, and gun amplifier gain should be adjusted to maximize luminance without loss of image sharpness. The luminance of the white monitor shall be at least $80\mathrm{cd/m^2}$ for CRT displays and $100\mathrm{cd/m^2}$ for LCD displays([19],5).

4. **Channel independence test.** (output from one channel does not affect another channel): The background is set with a luminance 20% of the peak white (approx. L=50). It might be neutral grey. The central colored square should be larger than aperture of measure instrument. The values of each channel's maximum output and the system's peak white should be displayed and measured. The samples for channel-independence test are presented in Appendix A(figure 47).
For confirmation of channel independency, the sum of three channels should be equal the measured peak white. The luck of channel independence is due to overdriving the gun amplifiers and it could be corrected by decreasing each channel's gain. The channel offset in this case might be close to zero or little bit negative(between -0.01 and -0.03). The peak white and calculated should be compared and satisfy to condition ≤ 1. Using a mathematic or statistical package, gain, offset and gamma could be preliminary calculated by solving equations with 3 unknowns and three data points.

5. **Spatial independence.**(output from one spatial location does not affect another spatial location) test. The central stimulus is set to the peak white. The background is first set to black RGB=[0,0,0]. The central stimulus should be measured.
The background is next set also to the peak white and central stimulus should be remeasured. Difference between the two measurements indicates lack of spatial independency. The samples for spatial-independence test are presented in Appendix A(figure 48).

6. **Spatial uniformity.** The reason of spatial uniformity lies in construction of display: the spectral radiance reduces from the centre to the edges of most displays due to an increased path length of the electron beam. This was not considered in details in Berns et al. paper [18]. Because spatial non-uniformity is reason of perceptual artifacts which are depend on monitor construction, and it is better to choose monitor with reasonable uniformity. For measuring spatial uniformity the lighting on a white image separated into 9 areas of equal size ([19],9). The each area stimulus is measured by instrument. The samples for spatial-independence test are presented in Appendix A(figure 49). Image was separated on 25 areas because of the display's size was large in project experimental setup.

7. **Determining flare.** Using background which set in neutral gray the darkest neutral or black should be displayed in square and measured. Then it could be evaluated if reflection flare is presented in the system. The background is contributed for optical flare of about $0.10\mathrm{cd/m^2}$.

8. **Determining the system gamma.** There are 2 approaches for determining the system data depending on characterization methods which have chosen: physical model (GOG model) or empirical method (LUTs).
For a first approach a minimum 2 measurements are required to calculate the three model parameters (gamma, gain and offset) for a given channel because the gain and

16

offset values must sum in unity. The parameters of video LUT should be known. Normally 5 patches are recommended to use for estimating GOG parameters (Luo,2003). Berns et al. in ([18],178) used following digital counts for these patches: 32, 64, 112, 176, 255. Tristimulus values of these patches were measured using spectrophotometer, and then are inverted to predict the linearized normalized DAC values (formula 2.9). In this project 17 patches were used for estimating GOG parameters (Appendix A, table 24).

$$
\begin{bmatrix} \hat{R} \\ \hat{B} \\ \hat{G} \end{bmatrix} = \begin{bmatrix} X_{r,max} & X_{g,max} & X_{b,max} \\ Y_{r,max} & Y_{g,max} & Y_{b,max} \\ Z_{r,max} & Z_{g,max} & Z_{b,max} \end{bmatrix}^{-1} \times \begin{bmatrix} \begin{bmatrix} X \\ Y \\ Z \end{bmatrix}_{meas.} - \begin{bmatrix} X \\ Y \\ Z \end{bmatrix}_{am.fl} - \begin{bmatrix} X \\ Y \\ Z \end{bmatrix}_{int.fl} \end{bmatrix}
$$
(2.9)

where meas. is abbreviation of measured; am.fl is abbreviation of ambient flare; inter.fl is abbreviation of interreflection flare.

Then GOG parameters was determined using multidimensional optimization technique such as simplex method in any statistics software package(MS Excel Solver function was used in this project).

For second approach determining the non-linear relationships by directly measurements (for LUTs based approach). For 8 bit DAC 256 measurements are required. But the relationship is monotonic, so number of required measurements could be reduced by subsampling, and 17 measurements should be used for this task: 0, 16, 32, 48, 64, 80, 96, 112, 125,144, 160, 276, 192, 208, 224, 240, 255([18],178). Other colors might be obtained by interpolation technique. For measuring samples each channel should be ramped separately where colors range from black to either red, green or blue. Tristimulus values of these patches were measured using spectrophotometer and then are inverted to predict the linearized normalized DAC values, and then using statistic package for determining gamma.

The display characterization using software package will be described in next section (ICC profiling).

2.1.4   3D LUTs and interpolation

The three-dimensional (3D) look up table (LUT) is conversion matrix between device-dependent and device-independent color spaces. The 3DLUTs can be considered as 3D grid (for one color space) with values in nodes of another color space. So element of grid with coordinates RGB(0,0,0) contains corresponding to it measured values in CIELAB space (2.0031,1.8430,-0.6785). More widely 3D LUT are implemented in ICC profiles (as three dimensional CLUT). In this project 3D LUTs are used for mapping from device RGB color space to the 3D CIELAB color space and visa versa (this coversion will be considered in next chapters).

3D RGBLAB LUT is based on the color cube representation of RGB color space. The
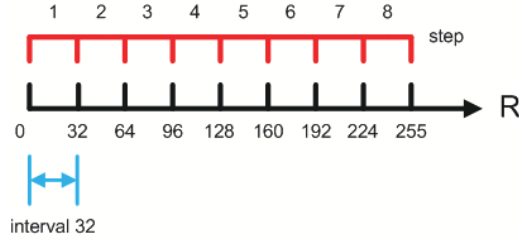
Figure 7: LUT's interval and step

R	G	B	L*	a*	b*
0	0	0	2.0031	1.8430	-0.6785
0	0	32	2.5341	4.7361	-9.6141
0	0	64	4.7529	16.7500	-29.8944
0	0	96	9.1433	28.9652	-45.7321
...	...	...	...	...	...
0	32	0	7.6906	-10.2314	7.5726
0	32	32	8.2197	-7.3298	-1.2984

Table 1: Fragment of 3D LUT (mapping RGB to Lab)

RGB color cube is divided on equal or non-equal subcubes with particular size which is determinate by interval or 3D LUT's step (figure 7). LAB grid points LAB subcubes correspond to RGB subcubes. This process is called color quantization (because number of distinct colors will be reduced to numbers of subcubes). As example, true color images with 8 bit per channel can display up to 16 777 216 colors. If this number of distinct color were included as entries to 3D LUT then size of 3D LUT would be big, and it would take more computational time. So color quantization is an unavoidable process. But larger LUT will raise smaller error at the transformation stage. The precision of final color conversion depends on interval between entries of each color component.

In case of true color image (24 bit for pixel), the interval could be defined as 255/(step-1) where step determines number of divisions in each dimension of 3D LUT. As example, 3D LUT with step 9 contains 9x9x9 entries, and interval between entries values is 32 (255/8). This 3D LUT is presented in table 1.

The values of colors which are not in the 3D LUT or non-lattice points are interpolated by using the nearest lattice points. The purpose of an interpolation algorithm is to estimate the output value of a coordinate whose input value is known, given two or more coordinates for which both input and output values are known. The relative distances of the point to be found from the known points are used as weights in determining the value of the unknown point ([15],135).

There are some geometrical methods of interpolation. Trilinear, prism and tetrahedral interpolation methods are implemented in this project. As example, linear interpolation for determining the y coordinate of a point x,y from two points x1, y1 and x2, y2 where x is known is given by:

$$y = y_1 + (y_2 - y_1)\frac{x - x_1}{x_2 - x_1} \tag{2.10}$$

The color spaces have three or more dimensions, and require the extension of the linear interpolation to a trilinear interpolation from eight vertices of a three-dimensional cube. For non-lattice points subcubes icluded these points in 3D LUT should be found for interpolation. Non-lattice point is performed as P on figure 50, Appendix B.

It is important to define correct to which subcube point belongs to. The 3D LUTs entries have limited set of values which have distance from each other equals to interval. If interval of 3DLUT equals to 32 then R, G, B values could take following values: 0, 32, 64, 96, 128, 160, 192, 224, 255. The value 256 is exchanged on 255 because R, G, B values could be values from interval 0-255. So RGB values of image pixel could be presented between following boundaries:

$$R_{intMin} < p(R) \leq R_{intMax}$$
$$G_{intMin} < p(G) \leq G_{intMax}$$
$$B_{intMin} < p(B) \leq B_{intMax}$$

$$\tag{2.11}$$

As example, the image pixel p(R,G,B)=p(254,3,2) has: $224 < 254 \leq 255; 0 < 3 \leq 32; 0 < 2 \leq 32$. The subcube could be defined by 2 main points: p000 and p111, others points could be obtained as combination of coordinates of these points (figure 50 – right picture). So for example with point p(R,G,B)= p(254,3,2) points p000 and p111 are equal p000(224,0,0) and p(255,32,32).

In this way color subcube for mapping point P could be determined. For each point of RGB subcube there is corresponding $L^*a^*b^*$ point. Thus, CIE $L^*a^*b^*$ subcube for interpolation could be easily defined. The trilinear equation is obtained by applying the linear interpolation seven times in 3 dimensions. The main trilinear equation implemented in project was proposed by H.R King ([4],67):

$$\Delta x = x - x_0;$$
$$\Delta y = y - y_0;$$
$$\Delta z = z - z_0;$$
$$p(x, y, z) = c_0 + c_1\Delta x + c_2\Delta y + c_3\Delta z + c_4\Delta x\Delta y + c_5\Delta x\Delta z +$$
$$+ c_6\Delta y\Delta z + c_7\Delta x\Delta y\Delta z;$$
$$c_0 = p_{000}; \ c_1 = \frac{p_{100} - p_{000}}{x_1 - x_0}; \ c_2 = \frac{p_{010} - p_{000}}{y_1 - y_0}; \ c_3 = \frac{p_{010} - p_{000}}{y_1 - y_0};$$
$$c_4 = \frac{p_{110} - p_{010} - p_{100} + p_{000}}{[(x_1 - x_0)(y_1 - y_0)]};$$
$$c_5 = \frac{p_{101} - p_{001} - p_{100} + p_{000}}{[(x_1 - x_0)(z_1 - z_0)]};$$
$$c_6 = \frac{p_{011} - p_{001} - p_{010} + p_{000}}{[(y_1 - y_0)(z_1 - z_0)]};$$

$$c_7 = \frac{p_{111} - p_{011} - p_{110} - p_{101} + p_{100} + p_{001} + p_{010} - p_{000}}{[(x_1 - x_0)(y_1 - y_0)(z_1 - z_0)]}$$

(2.12)

So in this project work these equations were used to interpolate point P within RGB sub-cube to point P' within CIE $L^*a^*b^*$ subcube when location of P in particular subcube was determined.

Prism interpolation is similar to the trilinear. For prism interpolation subcube is cut into two halves. Each part has shape of prism as shown on figure 51, Appendix B. The location of point P could be defined according to symmetric structure of subcube. So for determining the location of point in one of prisms point' coordinates are checked on identifying that this point lies above or under middle (diagonal) plane (which divides cube on two prisms) : if $\Delta x > \Delta y$ then the point is in Prism 1; otherwise the point is in Prism 2. There are some situations when point P could be laid on middle plane ($\Delta x = \Delta y$). Then one of prism could be used for interpolation. Equations for prism interpolation are presented ([4],69): as:

First prism,

$$\Delta x > \Delta y;$$
$$p(x, y, z) = p_{000} + (p_{100} - p_{000})\Delta x/(x_1 - x_0) +$$
$$+ (p_{110} - p_{100})\Delta y/(y_1 - y_0) + (p_{001} - p_{000})\Delta z/(z_1 - z_0) +$$
$$+ (p_{101} - p_{001} - p_{100} + p_{100})\Delta x \Delta z/[(x_1 - x_0)(z_1 - z_0)] +$$
$$+ (p_{111} - p_{101} - p_{110} + p_{100})\Delta y \Delta z/[(y_1 - y_0)(z_1 - z_0)]$$

(2.13)

Second prism,

$$\Delta x < \Delta y;$$
$$p(x, y, z) = p_{000} + (p_{110} - p_{010})\Delta x/(x_1 - x_0) +$$
$$+ (p_{010} - p_{000})\Delta y/(y_1 - y_0) + (p_{001} - p_{000})\Delta z/(z_1 - z_0) +$$
$$+ (p_{111} - p_{011} - p_{110} + p_{010})\Delta x \Delta z/[(x_1 - x_0)(z_1 - z_0)] +$$
$$+ (p_{011} - p_{001} - p_{010} + p_{000})\Delta y \Delta z/[(y_1 - y_0)(z_1 - z_0)]$$

(2.14)

Each prism equation is obtained by applying the linear interpolation 5 times in 3 dimensions. So prism interpolation requires smaller number of computational operations.

Tetrahedral interpolation divides cub into six tetrahedrons. Each of tetrahedron is triangle based. So first task in this case to define in which tetrahedron point P is located. The main equation of tetrahedral interpolation is proposed in as ([4],70):

$$p(x, y, z) = p_{000} + (c_1 \Delta x)/(x_1 - x_0) + (c_2 \Delta y)/(y_1 - y_0) + (c_3 \Delta z)/(z_1 - z_0) \quad (2.15)$$

The coefficients c_1, c_2 and c_3 depend on to which tetrahedron point P belongs to. The relationships for planes which divide and the coefficients for tetrahedral interpolation

Tetrahedron	Test	c1	c2	c3
T1	$\Delta x > \Delta y > \Delta z$	$p_{100} - p_{000}$	$p_{110} - p_{100}$	$p_{111} - p_{110}$
T2	$\Delta x > \Delta z > \Delta y$	$p_{100} - p_{000}$	$p_{111} - p_{101}$	$p_{101} - p_{100}$
T3	$\Delta z > \Delta x > \Delta y$	$p_{101} - p_{001}$	$p_{111} - p_{101}$	$p_{001} - p_{000}$
T4	$\Delta y > \Delta x > \Delta z$	$p_{110} - p_{010}$	$p_{010} - p_{000}$	$p_{111} - p_{110}$
T5	$\Delta y > \Delta z > \Delta x$	$p_{111} - p_{011}$	$p_{010} - p_{000}$	$p_{011} - p_{010}$
T6	$\Delta z > \Delta y > \Delta x$	$p_{111} - p_{011}$	$p_{011} - p_{001}$	$p_{001} - p_{000}$

Table 2: The relationships and the coefficients for tetrahedral interpolation

are presented in ([4],72) and in table 2.Except procedure of comparison where point P is located (which tetrahedron) tetrahedral equation is simpler than trilinear interpolation, and it is obtained by applying the linear interpolation 3 times in 3 dimensions.

Kasson and others [21] tested interpolation methods and concluded that tetrahedral interpolation provides similar accuracy to trilinear interpolation but with less computational effort. So the tetrahedral interpolation is faster in implementation than trilinear interpolation [22].

In this project work three interpolation methods were examined. They were implemented using environment of Matlab R2008b. Interpolation methods were implemented without using standard Matlab functions for interpolation, and absolutely were designed according formulas which were presented bellow.

2.2   ICC profiling

2.2.1   ICC profiles

Rapid development of different types of color reproduction devices requires achieving consistent way of managing and communicating color throughout different devices(on figure 8, a). This objective was basic for building color management systems. This system allows processing color images or mean adjusting several types of devices to achieve near identical image representation results. Color management systems provide calibration and characterization of input and output devices, so that data can be converted in colorimetric reference space, efficient way of processing images between input and output color devices.

The ICC color management architecture consists from 4 main components: framework, profile, color management module, application (figure 9).

ICC profiles standard [23] was designed more than 70 companies including HP, Adobe, Microsoft, Kodak, Fuji and other technical representatives from manufactures and software developers, which collaborate within the ICC (International Color Consortium group).The main aim of ICC profiles to manage color from one device to another for obtaining consistent and predictable result from very first try. The idea of ICC profile is based on color communication of devices throughout a reference color space to which

a) Devices' communication (according to [24]);

b) Device-independent solution (according to [24]).
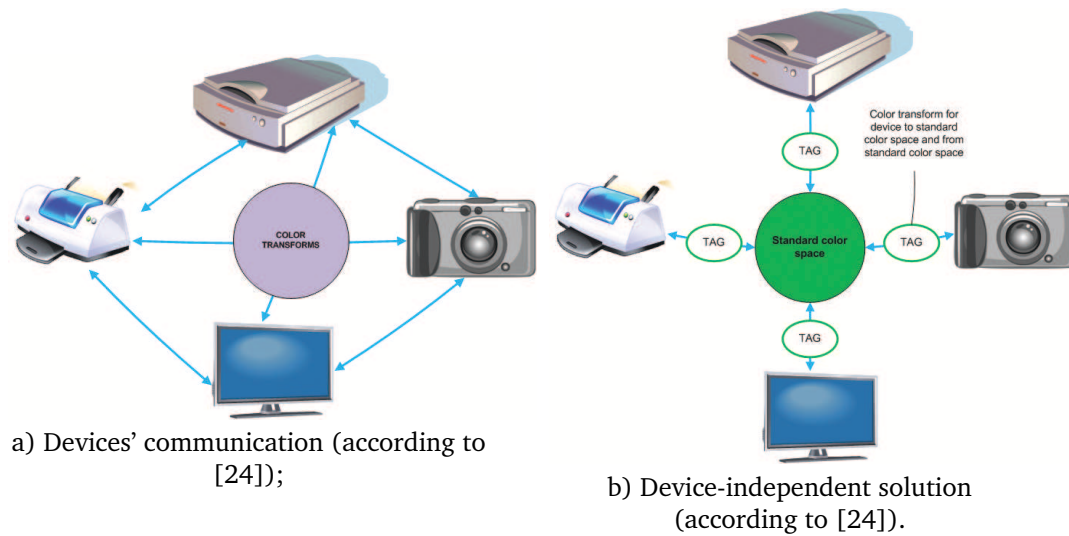
Figure 8: Color transformation jungles
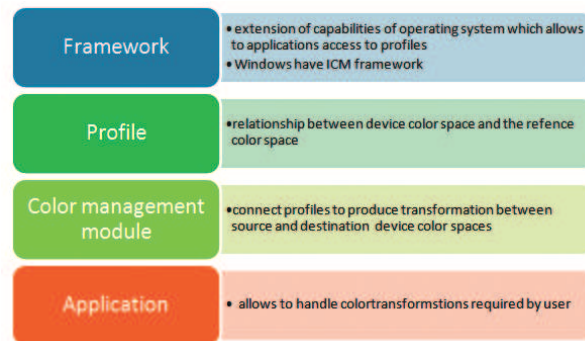
Figure 9: ICC color management architecture

every input and output device can be related (8, b). Such color space must define colorimetry of both the reference medium and its assumed viewing conditions. This color space is called profile connection space (PCS) and is defined as CIE colorimetry . PCS can be either 16-bit CIEXYZ or 8-bit or 16-bit CIELAB using the measurement conditions defined in ISO 13655.

The main function of ICC profile is to provide data and processing way to transforms color of an image from the color characteristic of one device to those of another (on figure 3). Profile includes data which allows identification of out-of gamut colors, additional information for conversion color data from the PCS back to device color space.

2.2.2 ICC profiles structure and color transformations models

ICC profile is file containing following information ([15],253):

- The company/software that created the profile;

22

- The device and its settings /media for which the profile was created;

- The color characteristics of the device;

- The data for conversion the color out of the device color space and settings into a PCS;

- The data to convert from the PCS back to device's color space;

- Additional information for printing, viewing or reproducing the image with desired color.

Tag Name	Description
mediaWhitePointTag	media XYZ white point
namedColor2Tag	named color profile type
redgreenblueTRCTag	1D tonal response curves
grayTRCTag	1D tonal response curves for grayscale data
redgreenblueColorantTag	3x3 color conversion matrix
preview#Tag	PCS to device space and back for previewing data
gamutTag	PCS to 1D output representing an out-of-gamut indicator

Table 3: Required processing tags in ICC profile

ICC profile has tag-based structure which allows to include different types of data in ordered way. The profile file contains the header, tag keywords, their byte offsets from the beginning of profile and their length. There are primary tags which are necessary for processing the color. Few of these tags are presented in table 3, and full description of ICC profiles' tags can be found in ICC specification [23]. Following tags contain 3DLUTs (CLUTs) and other data and elements for color conversion from device color space to PCS and vice-versa for some output devices:

- AToB#Tag multi-dimensional information structure(from device color space to PCS);

- BToA#Tag multi-dimensional information structure(from PCS to device color space);

where # is rendering intent(0 is perceptual, 1 is colorimetric, 2 is saturation).

The rendering intents are related to gamut compression techniques. In this case different intents allow achieve different desired quality. The ICC supports three styles of controlled compression: perceptual, saturation and colorimetric(clips abruptly gamut boundary or minimizing wide gamut to small gamut). So there are 3 different rendering intents that ICC profiles may have for resolving color differences:

- Perceptual intent tries to preserve the overall color appearance by changing colors of source image to fit into destination space for producing more visually pleasing image(when source has wide gamut and destination has a small gamut);

- Saturation intent tries to produce the most vivid colors of the source image as much as possible in destination color space(for business graphics);

- Colorimetric intent tries achieving color accuracy by changing color from one device to another. Absolute colorimetric intent(relative to illuminant) is usually used for

23
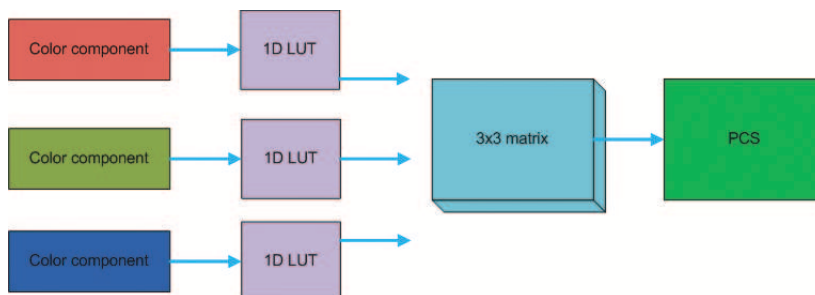
Figure 10: Shapermatrix processing model for the device-to-PCS direction

proofing (simulating one device on another). For relative colorimetric intent measurement (relative to paper) of output color should match that of input. It works very well when the source and distination profiles have similar gamut.

The mapping from device color space to PCS and back for some devices can have simple color transform model and complicated for others. There are some basic color transform elements which can be used for this conversion depending on type of profile:

- 1D-LUTs (they are also called as curves and applied only when CLUT is used);

- parametric curves (parameters defining one of the standard set of functions in profile, TRC curves, they are used only when matrix is used);

- matrix (3x3 matrix of coefficients stored in profile);

- matrix with offset (3x4 matrix of coefficients icluding offset stored in profile);

- multidimensional LUT (CLUT).

According to ([15],255) and ([25], 150-158) main two color conversion models are defined for ICC profiles using basic color elements.

Shaper-Matrix model (on figure 10 according to [15], [25]) is based on using three 1D tone reproduction curves(TRC) tables and the 3x3 matrix of colorants described by the ICC profile format. Three components of input data are processed through the devices' tonal response curves, and then through 3x3 matrix of the colorant primaries tristimulus values(red, blue, green colorants). This model is simple, provides small profile size and fast processing. This model is typically applied for monitors and for some input devices.

Matrix-tabulated model is more complex and involves also color LUTs. The input and output 1DLUTs and CLUT are one- and multi-dimensional functions which maps an input value in the domain of the function to an output value in the range of the function ([23],45). On figure (11) the multidimensional CLUT(BToA#Tag) and 1DLUTs are presented. First values from PCS are processed trough matrix and then by interpolation converted to device color space using 1DLUTs and CLUT. This type of model must be used for output devices such as printers and some types of input devices.
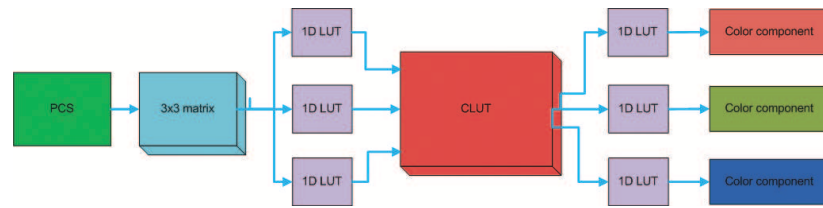
Figure 11: Matrix-tabulated function processing model for the PCS-to-device direction

E.Tapp and other authors considered several types of profiles depending from device which should be characterized by profile: output profiles, monitor(or display) profiles, input profiles (analogical with processes of device characterization).The color transformation elements of profile for each profiles' class are presented in table 4 according ([23],22-25).

Class of profiles	Color transform elements
Input (camera, scanner)	3-component matrices and TRCs, n-component LUTs for monochrome profile - gray curve (TRC)
Display	3-component matrices and TRCs, N-component LUTs, for monochrome profile - gray curve (TRC)
Output(printer, printing press)	n-component LUTs for monochrome profile - gray curve (TRC)

Table 4: Color transformations for different classes of profiles

Output profiles are a characterization of the range of colors that a specific printing device and paper type reproduces ([26], 12). The color patches should be printed and measured by spectrophotometer, and then enter data from the patches into software-profiling application to create ICC profile. Output ICC profiles contain AToB#tags' and BToA#tags' tables typically with 1DLUTs(A,B curves) and CLUT for color conversion. It can include also matrix with parametric curves (M curves).

Display profiles are created during the calibration process with a colorimeter, which compares the values and colors that it reads to known set of values and colors. The display profile or system monitor profile is used as a viewing filter allowing to see data more accurately. This profile contain TRCs(B curves) for each channel and matrix with coefficients for color conversion.

Input profiles of digital cameras and scanners are different because scanners and cameras do not have fixed gamut. Input profiling for digital cameras is limited to the target which is used for characterization. A digital camera captures colors in the real world much better than any target. The camera – profiling software extrapolate the colors that are outside target's gamut. Input profiles contain AToB#tags' and BToA#tags' tables with same elements as output profile.

2.2.3   Printer profiling

Xerox 7760/GX color laser printer (using Xerox toner cartridges 1 – cyan, 2 – magenta, 3- yellow, 4 - black) driving in RGB mode was used in this project. So characterization for this type of printers will be considered in this subsection. RGB printers require RGB signals as their input, and characterization applied to them is similar to characterization of RGB devices. In real life there is no RGB printer because all printers use cyan, magenta, and yellow inks, and also most use black.

Calibration typically involves configuring some settings for density, tone value and gray balance ([1],75):

- density is the light-absorbing property of a material, expressed as the logarithm of the reflectance factor (higher density shows that more light was absorbed);

- tone value increase (TVI) or dot gain is a measure (on scale of 0-99%) of net increase in apparent dot area from digital file or printed reproduction;

- gray balance is tone value amounts of cyan, magenta, and yellow required to produce a neutral gray.

Many modern types of printers have self-calibration function which specified by manufacturer and require less interference from user. Most all printers have special software or utilities from printers' manufactures maintaining process of calibration. For new generation of printers calibration includes automatic cleaning heads, nozzles of toners or cartridges, checking on color consistency by printing special page with samples.Printing presses are very complex devices, and it is difficult to keep it calibrated. These printers used a lot of different test targets for measuring devices to keep press in control. Calibration is important for obtaining consistent colors on reproduced image. There are many different conditions which influence on colors during printing process: temperature, humidity changes and so on.

There are also printing specifications such as SWOP, SNAP, PROP and GRACoL which specified substrates, inks, ink densities, tone values, and other variables.

So characterization process of printers contains following steps using color measurement software (according to ([1],76-81), ([12],194-197),([26], 70-73)):

- Printing of color chart. Printer's setup is managed by printer display menu: ensure that there is no color management or color adjustment implemented, choose media type (paper), print quality (resolution) depending from type of media. These setting affects on reproduction of the color. The size of patches might be kept proper. There are many different color targets for printers but standard target for characterization CMYK printing processes and devices according to ISO 12642 is IT8.7/3. In this project color target TC 9.18 –RGB i1-iO was used for characterization printer Xerox 7760/GX driving in RGB mode and for measurements instrument Eye-One iO. Color

target should be printed on calibrated printer.

- Checking for any problems on printed reproduction of target: marks, lines, scratches.

- Printed target should be dried before starting measurements. For ink-jet printers it requires approximately 2-3 hours because surface needs to become resistant and dried as well as pigmented inks (typically requires 15 minutes)([26], 79). Some printers allow automatically dry copy during printing process.

- Conducting color measurements of printed chart using colorimeter or spectrophotometer (straightforward patch-by-patch, strip-by-strip mode). Software connected with measurement instrument allow directly recording measurements results to file. It is important that measurements are conducted under illuminant D50 (according to ISO 3664) with luminance 250 reccomended ([27],55). After finishing reading colors on target by instrument software will combine measured data with known data.

- Choosing black generation strategy for building profile: Unser Color Removal or Gray Component Replacement. UCR separations use black only in the neutral and near neutral areas. GCR replaces the amount of CMY that would produce neutral with K, even in colors that are quite a long way from neutral. Total ink covering, maximum black and other settings should be set up.

- Generation of profile and saving it.

Color laser printers (type of printer which was used in project) are electrostatic devices. So this is a reason of variability which comes from 2 sources:

- Paper cannot be completely dry and needs some humidity to hold static charge;

- When eager toner particles are finishing toner is leaving less particles on the paper. So it decreases the density which can be achieved by colorants.

These peculiarities lead to frequent calibration and characterization of color laser printers. These printers are an example of moving target. There are some recommendations for characterization of color laser printers. First, the printer should be calibrated, and the profiling target is immediately printed. Second, the printer should be calibrated, then series of targets are printed (for each printed reproduction of target the printer should be recalibrated through interval) and results are averaged for targets.

2.2.4 Display profiling

Display calibration by software includes several steps(recommended in ([26], 68)):

- choose software with adjusted or supplied with display;

- adjust display brightness and contrast;

27

- determine display's native luminance response curve;

- choose desired response curve gamma;

- choose desired white point (warmth or coolness of white).

First, monitor should be stabilize and warm up one hour before starting calibration. There should be no window light influencing view of monitor, as brightness levels, changing color temperatures, and lights can affect what observer see on monitor. But if there are no possibilities to avoid ambient lightning than But if there are no possibilities to avoid ambient lightning than ambient illumination should be less or equal to that of the monitor white point ([27],52). It should be less or more than 64 lux and, preferably, much lower at less than 32 lux ([27],52). Software should be choose as optimal for display model, and it is preferable to use supplied package for this monitor (as example, Eye-One Match 3 for Macintosh PC or firmware in OS calibration software). The surrounding area should be neutral or grey color for avoiding glare and interrelations.

Second, decide on the white point for monitor. According to ISO 3664 daylight source 5000K should be used as standard for photography and graphic arts. But for displays 6500K is recommended because it matches standardized 5000 K light source, and monitors natively have this color temperature or close to it . There are some possibilities for choosing color temperature: warm white 5000K, 5500K, 6000K, medium white (6500K), 7000K, Cool white(7500K).

Third, determine gamma setting. The typically gamma should be between 1.8 and 2.2. The gamma equals 2.2 is best for different platforms ([26], 69) . The luminance settings are recommended by ISO 3664 ([27],52) for CRT displays greater than 75 cd/m^2 and preferably greater than 100 cd/m^2. For LCD monitor the author of ([26], 69) recommended luminance 120 cd/m^2.

CRT displays usually need to be recalibrated 2 times a month because they tend to change over time. LCD monitors are much more stable and need to be recalibrated only about 1 a month([26], 70). For characterizing monitor software will sent few color patches to the display, and instrument attached to display flatbed will measure it. Software will combine profile from known values and measured values of color. The profile could be implemented as long as display will be kept calibrated.

2.3   Smoothness of color transforms

There is no common definition of visually perceived smoothness, but many authors gave their own definition for smoothness of images or color ramps.

T.Olson ([6]) gave definition of ramp, smooth ramp and considered causes of disruptive artifacts such as contours and banding, and established set of visual limits. A digital color ramp has endpoint colors that are quantized in the space they reside in, and the intervening colors are constructed as discrete steps. The visually smooth ramp contains no

discernible steps. T.Olson investigated that contours appear when step size is too large, and in this type of artifact depends mostly on luminance channel. The studies of [28] and [29] shows that high dynamic range image no fewer than 400 steps are required in order to guarantee visual smoothness. Olson found that luminance step size should be limited to $\Delta L^* <= 0.25$ for guarantee smooth grading of colors in ramp. Human visual system typically subtracts the signal (desired ramp) and study that remains (noise) analyzing smoothness of the color ramp. So observer is interested in higher frequency components. It works like spatial adaptation, not seeing the ramp but sensing deviation from it. Low frequency(banding) errors must be limited in both amplitude and gradient. Rapid changes in luminance are tolerable, provided they are limited to a short interval, and hence small maximum error.

According to these visual thresholds analysis of the numeric representation and processing of color data based on ICC profiles some requirements for device profiles and their usage were described. The smooth ramps cannot be generated using 8-bit precision ICC profiles. 16-bit precision is necessary, and Luts should have more than 256 entries. The grid densities of measurement set and the profile CLUT influence how printer noise results in bounding artifacts.

A few researches investigated visual thresholds and sensitivity to luminance step and sin wave gratings(presented in table 5).

Reference	$\Delta L/L$	Approx.ΔL^*
[30],525nm, luminous display	0.0025 bp	0.15
[31],reflection prints	0.0025 bp	0.15
[28],video display	$0.002 - 0.005$ rms	$0.2 - 0.15$
PC, steps in gratings	0.0075pp	0.25
[32], backlit film	$0.01 + 0.001\ln^2(L/L_0)$	0.25

Table 5: Human visual sensitivity to luminance steps and sin wave gratings

J.Morovic et al.[9] investigated method for smoothing LUTs preserving at the same time a significantly greater degree of accuracy. The existed methods for smoothing LUT are also considered in this research. These methods were based on idea that human visual system's sensitivity to luminance changes being greater than chrominance changes [33].

J.Morovic et al. gave definition of smooth transition. The smooth transition is transition where the slopes of piecewise linear function defined by the LUT vary monotonically (change keeps getting more or less steep across the entire trajectory). So it is easy to smooth LUT only making changes where non-smoothness is detected.

One of the simplest methods to smooth LUTs is to take each LUT entry and replace it content with the weighted sum of that entry's $(2 * n + 1)^3$ neighborhood, centered on the entry being smoothed. This method is effective for smoothing LUT but it reduces accuracy of resulting transformation (hue shift).

29
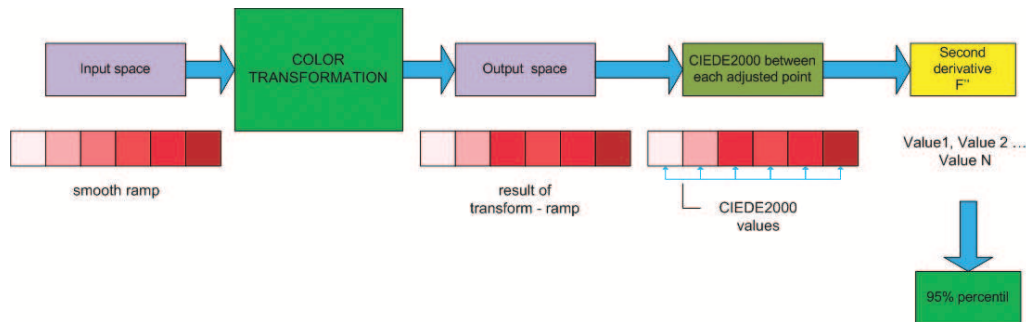
Figure 12: Schema of Phil Green proposed second derivative method

J.Morovic et al. proposed applying smoothing along 1D lightness path. So only $2*N+1$ 1D neighborhood of a LUT entry from which LUT entries will be used for replacing a given LUT node's content is considered. The performance of L-path smoothing using colorimetric and psychophysical tests was compared with 3D neighborhood weighted method for smoothing LUT and without smoothing LUT. These LUTs were presented in ICC profiles. Psychophysical evaluation, colorimetric accuracy and round-trip-test have shown that L-path has best representation than others variants of LUTs with higher accuracy.

Kitoh and Kang [34] (2005) proposed a way for quantitatively evaluating smoothness of color transforms using a characterized scanner-based measurement instrument. This method is based on generation of ideally smooth curve by averaging 20 smooth gradations generated by the spline interpolation between randomly chosen end-points, and finding difference between the ideal and given gradation. They used as test samples dark red, green, sky, sea and human skin colored hard-copies from 12 electrophotographic copies.

Some studies have considered methods for evaluating discontinuities in hard and soft copy prints [35], [36]. Brigg [35] considered banding problem, technique for quantifying the severity of the banding using automated measurement instrument, mechanical reasons of printing engines(misaligned cartridge rollers)which lead to appearing of banding effect.

Arslan et al. [36] developed a soft-copy environment for conducting various experiments for investigating the visibility of banding laser electrophotographic printers. In this environment they applied the methodology to duplicate print on the monitor and banding extracting technique which allows adjust the magnitude of banding of any printer.

P.J.Green [7] proposed 2 ways for evaluating smoothness of output color transform. One metric is based on taking a second derivative of the transform, and other method is based on computing series of smooth gradients and evaluates differences between these gradients and the derived output values. Green considered that observer perceives an unexpected jump in the difference between adjacent regions as luck of smoothness in color transform.
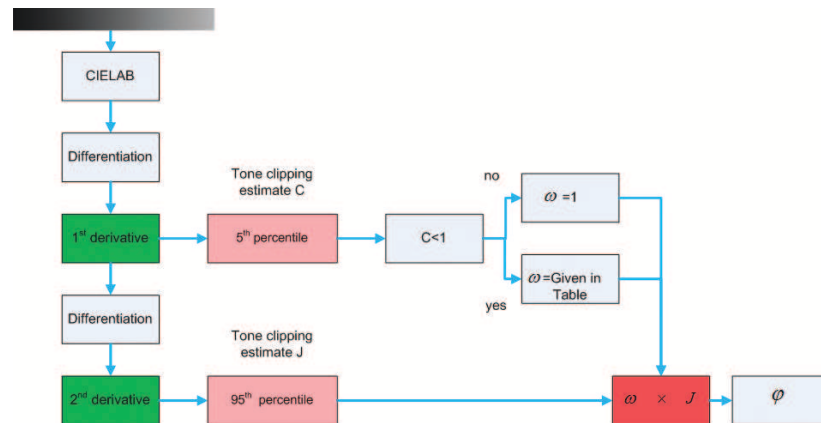
Figure 13: Framework of Kim et al. proposed model

The schematic representation of second derivative method for evaluating smoothness of color transforms is on figure 12. Uniformly-spaced points (uniform color ramp) within the input space are processed through color conversion. The color difference CIEDE2000 between adjusted points in output space is calculated. Then second derivative of this vector is computed to determining the degree of local changes from surrounding regions.

Difference from a smooth interpolating function method is based on suggestion that set of points which lie on a straight line or curve within the input space might to form smooth transition after transform in output space. So CIEDE2000 color difference between input curve points and output points are computed. The psychophysical experiment was conducted for comparing visual evaluation of smoothness by observers and values predicted by metric. 98 color ramps were generated. Each ramp was presented as set of 100 points in CIELAB color space which lies along gamut. The color ramps were converted to printer RGB using generated ICC(BToA table) profiles with different level of noise in LUTs. The soft and hard copies of these ramps were used for ramps' images assessment. Experimental results show high Pearson correlation between (above 0.97 for print and soft copies) visual judgments and predicted by metric values.

However, it is worth to notice that the color ramps set and experiment design are enough synthetic. It does not include real color images with gradations. The printer and monitor characterization processes were simulated by addition Gaussian random noise on the CIELAB dimensions.

A new study by Y.K.Kim, Y.Bang and H.-K.Choh [8] which was published in March of 2010 consists of tone-jump and tone-clipping estimators for predicting smoothness of color transforms.So this work was not known before the middle of this research work.

It is extension of Phil Green proposed method. They assumed that perceptually large variations of tone levels (tone-jumps) and sudden disappearance of tonal variations in the middle of transform (tone-clipping) are significant for human observers to appreciate the smoothness. The framework of this method is presented on figure 13. Green's second derivative method is used as component of this metric for predicting tone-jumps visible

to human subjects. CIELAB was used for calculating differences between adjusted points instead of CIEDE2000 because of simplicity and common usage in industry. In model J is 95th percentile of second derivative. Kim et al. also use 5th percentile of first derivative from transform -C for estimating tone-clipping effect. They have been used 5th percentile because it is smaller than the just-noticeable difference (JND) $\Delta E^* ab = 1.0$.

Then value of J is weighted by special weight factor ω if $C < 1$ (else $\omega = 1$). Magnitude of ω is used to increase metric output value if any tone clippings are visible. The values of weights were derived from optimization for best fitting the subjective data using least-square method to minimize errors between known subjective visual smoothness judgments and their corresponding model's predictions. These weights depend on variation in observer and application. The larger result ψ is the lower the percieved smoothness is. For perfectly smooth gradation scale, the model prediction should be equal to zero.

Kim et al. analyzed the statistics of natural object colors to design test stimuli for the purpose of quantifying the smoothness. According to [37] memory colors can be defined as the colors that are recalled in association with familiar objects in long-term memory. The familiar objects are usually natural scenes such as blue sky, green grass, foliage, skin, fruits. Based on previous works they conclude that Caucasian skin, green grass and blue sky regions should be used for generating image dataset.

The test stimulus were generated in CIELAB space 96 color-to-color gradations (using colors transitions corresponding to Caucasian skin, green grass and blue sky) and simply converted to sRGB. Then these samples were printed on 16 electrophotographic printers. Then colorimetric values of printed samples were measured using a spectrophotometer. The psychophysical experiment was conducted where 10 professional observers were asked to compare difference in smoothness between hard-copy reproduction and soft-copy original of gradation displayed on LCD display using categorical scale. Visual judgments results were compared with predicted by metric values using Pearson correlation. This method has shown best representation in comparison for all samples with Phil Green method and tone-jump model (without using weights). However, this method did not involve using ICC profile color transforms and real scenes images.

But as shows studies [5] and [38] there are many sources of errors during color transformation workflow(on figure 14). So then it is important to consider smoothness of color transform related to ICC profiles color conversions.

2.4   Image difference metrics

The short overview of few image difference metrics is presented in this section because they were implemented for comparison and analysis with proposed method [39].
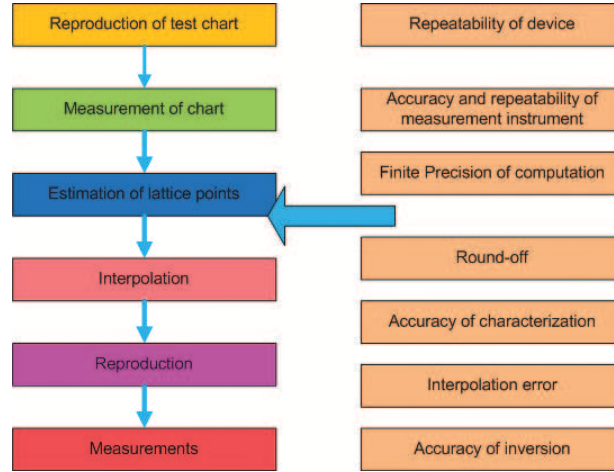
Figure 14: Errors during color transformation workflow

2.4.1 Color difference CIELAB

The International Commission on Illumination CIE (1986) [39] published the $CIEL^*a^*b^*$ color space specification. This color space is based on idea of creating perceptually uniform color space. The $CIEL^*a^*b^*$ metric is the Euclidian distance between two colors: sample and reference.

The distance between a color sample L_s^*, a_s^*, b_s^* and a reference color L_r^*, a_r^*, b_r^* is presented as:

$$\Delta E_{ab}^* = \sqrt{(\Delta L^*)^2 + (\Delta a^*)^2 + (\Delta b^*)^2},$$ (2.16)

where $\Delta L^* = L_s^* - L_r^*$, $\Delta a^* = a_s^* - a_r^*$, $\Delta b^* = b_s^* - b_r^*$.

For calculating color difference for images there is general formula. The color difference ΔE_{ab}^* is calculated for each pixel and then mean of these values is computed by formula:

$$\Delta E_{ab}^* = \frac{\sum_{i=0}^{M} \sum_{j=0}^{N} \Delta E a b_{i,j}^*}{M \cdot N},$$ (2.17)

where MxN is size of image (height and width). The CIELAB metric is widely used in image processing, photographic, art and print-press industry as simple and effective method for predicting color image difference.

The color difference metric is appropriate for measuring perceptual difference between uniform patches of color. But this metric does not good simulate human visual system and works fine only to large patches of colors. As example comparison two images a continuous-tone and halftone version of same image can be considered. A point-by-point computation of CIELAB will give large errors at most image points. But for the human eye images looks quite similar because halftone pattern are not obvious recognizable by eye. Some spatial metrics based on CIELAB 1976 were proposed for solving this problem.

The class of uniform color difference formula was developed. The common characteristic of these formulas is that Euclidian distance in CIELAB was presented as root from sum of differences in lightness, hue and chroma which was weighted differently for defining new color difference. This class include following formulas: CMC(1:c) distance function, the BFD(1:c) function, the CIE-94 color difference formula, and CIE-DE2000 color difference formula [40].

2.4.2 Color difference CIEDE2000

The CIEDE2000 ([11],35), [40] was proposed as improvements of CIEΔE_{94}.

$$\Delta E_{00} = \sqrt{\left(\frac{\Delta L'}{k_L S_L}\right)^2 + \left(\frac{\Delta C'_{ab}}{k_C S_C}\right)^2 + \left(\frac{\Delta H'_{ab}}{k_H S_H}\right)^2 + R_T \left(\frac{\Delta C'_{ab}}{k_C S_C}\right)\left(\frac{\Delta H'_{ab}}{k_H S_H}\right)} \quad (2.18)$$

where k_L, k_C, k_H are scaling parameters, S_L, S_C, S_H are lightness, chroma and hue scalling functions. $\Delta L'$, $\Delta C'$ and $\Delta H'$ ([11],35) are lightness, chroma and hue differences. R_T is an additional scallling function depending on chroma and hue.

2.4.3 Structural simularity measure

The human visual system is able to extracting structural information from images: structure of the objects in the visual scene. In [41] and [42] new approach for design image quality metric was performed. It was based on assumption that human eye will strongly perceive changes of structural information from the image. So measure of changes in image structural content can be used as metric for estimation image quality distortion. A images with same mean square error (MSE) can be perceived as images with different quality (contrast-stretched image could look better than same blurred image). The problem of suprathreshold, cognitive interaction and natural image complexity of visibility error's approach are avoided or reduced in new approach([42], 603).

Z. Wang, A.C.Bovik et al. [42] in 2004 constructed new SSIM quality measure based on structural information approach. They supposed that structural information on image is the attributes of the objects structure in the scene, independent of the average luminance and contrast. The x and y are two nonnegative image signals (spatial patches extracted from each image). If one of the signals has perfect quality then similarity measure performs quantitative measurement of the quality of the second signal.

There are three measurement tasks in the system:

1. Luminance measurement and comparison

$$l(x,y) = \frac{2\mu_x \mu_y + C_1}{\mu_x^2 + \mu_y^2 + C_2} \quad (2.19)$$

2. Contrast measurement and comparison

$$c(x,y) = \frac{2\sigma_x \sigma_y + C_2}{\sigma_x^2 + \sigma_y^2 + C_2} \quad (2.20)$$

3. Structure measurement and comparison

$$s(x,y) = \frac{2\sigma_{xy} + C_3}{\sigma_x \sigma_y + C_3} \tag{2.21}$$

μ_x and μ_y are the local sample means of x and y; σ_x and σ_y the local sample standard deviations of x and y, σ_{xy} is the local sample correlation coefficient between x and y. The local sample statistics are computed within overlapping windows, and weighted within each window. The constants C_1, C_2 and C_3 are used to compensate denominators when it become small or closely to zero.

The general expression of the SSIM index can be derived combining three comparison functions of $l(x,y)$, $c(x,y)$, $s(x,y)$:

$$SSIM(x,y) = [l(x,y)]^\alpha [c(x,y)]^\beta [s(x,y)]^\gamma \tag{2.22}$$

where α, β and γ are parameters that determines importance of components(typically $\alpha = \beta = \gamma = 1$, $C_2 = C_3$). Then SSIM is yelded as:

$$SSIM(x,y) = \frac{(2\mu_x \mu_y + C_1)(2\sigma_{xy} + C_2)}{(\mu_x^2 + \mu_y^2 + C_1)(\sigma_x^2 + \sigma_y^2 + C_2)} \tag{2.23}$$

In [42] sliding window over entire image space has size 11x11. The general formula for whole image is mean for all these local windows(number of them):

$$MSSIM(x,y) = \frac{1}{M} \sum_{j=1}^{M} SSIM(x_j, y_j) \tag{2.24}$$

For evaluating SSIM approach researchers ([42]) compared the cross-distortion and cross-image performances of different quality metrics including proposed SSIM on image database of JPEG and JPEG2000 compressed images.

2.4.4 Gradient Structural simularity measure GSSIM

SSIM does not show good results on blurred images[43]. For eliminating this problem new gradient-based variant of SSIM was proposed Chen at al.[43] which compares edges between original image and distored image. A sobel filter in horizontal and vertical directions is implemented in this metric. So both contrast $c_g(x,y)$ and structure comparison $s_g(x,y)$ are based on the Sobel filtered images.

If X' and Y' are denoted as the gradient maps of the original and distored images then x' and y' are window (or block) vectors from X' and Y'. So contrast and structure functions:

$$c_g(x,y) = \frac{2\sigma_{x'}\sigma_{y'} + C_2}{\sigma_{x'}^2 + \sigma_{y'}^2 + C_2} \tag{2.25}$$

$$s_g(x,y) = \frac{2\sigma_{x'y'} + C_3}{\sigma_{x'}\sigma_{y'}^2 + C_3} \tag{2.26}$$
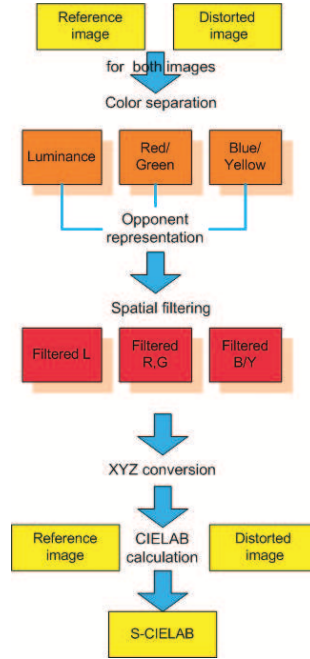
Figure 15: sCIELAB workflow

where the sample statistics have same description as for SSIM metric but applied on the gradient images.

So the formula for calculating G-SSIM (1 window or block) is presented [44]:

$$\text{GSSIM}(x, y) = \frac{(2\mu_x\mu_y + C_1)(2\sigma_{x'y'} + C_2)}{(\mu_x^2 + \mu_y^2 + C_1)(\sigma_{x'}^2 + \sigma_{y'}^2 + C_2)} \tag{2.27}$$

So for finding total GSSIM for image the mean for all windows should be found. GSSIM was evaluated on LIVE database and preforms better results than SSIM on an overall basis and blurred images.

2.4.5 Spatial CIELAB

Xuemei Zhang and Brian A.Wandell in [45] proposed a spatial extension of CIELAB known as sCIELAB. For designing the sCIELAB error measure spatial filtering operations were applied firstly for simulating the spatial blurring by the human visual system and then obtained uniform large areas will be as input for the basic CIELAB 1976 calculation.

The sCIELAB is presented on figure 15(according to [45]). The images (reference and distored) are processed through color separation and converted into opponent-color space. Then each of these opponent-space component is convolved with a kernel. Then filtered image is converted into CIEXYZ and CIELAB color space. The spatial processing stage is implemented as a pre-processor to existing CIELAB. The final value of sCIELAB computes using standard CIELAB color difference formula(measure error of the reproduction).

For testing sCIELAB images set contained JPEG-DCT compressed images, halftone images and simple pattern images.So sCIELAB difference metric reflects both spatial and color sensitivity, and can be considered as extension of CIELAB.

2.4.6 Adaptive bilateral filter

Adaptive bilateral filter was proposed by Z.Wang [46] for predicting color image difference. This metric is attempt to simulate human visual system when human eye is able to blur information on image (like on halftone images as example) and sense edges at the same time. The adaptive bilateral filter is based on bilateral filter (proposed by Tomasi and Manduchi [47]) which extended the concept of Gaussian smoothing by weighting the filter coefficients with their corresponding relative pixel neighborhood. Two Gaussian filters in the spatial(domain filter) and intensity domain (range filter)are combined and applied at localized pixel neighborhood. Wang considered method to optimize parameters which are designed to be adaptive and the quantity and homogeneity of information contained in an image.

2.4.7 Structural content and other metrics

There are many image quality measures. Peak Mean Square Error, Mean Square Error, Average difference and others are well-known and were evaluated in many different studies.

Structural content is simple simularity measure which can be found using this formula:

$$SC = \frac{\sum_{i=1}^{M} \sum_{j=1}^{N} [F(i,j)]^2}{\sum_{i=1}^{M} \sum_{j=1}^{N} [F'(i,j)]^2} \tag{2.28}$$

where F and F' are reference and source images of MxN size. The original equation and information about this metric were mentioned in many sources as [39],[48],[49]. In this project this metric was used as alternative candidate for evaluating smoothness of color transforms and computed for luminance channel.

Minkowski distance is a metric on Euclidian space but can be considered as a generalization of both the Euclidean distance and the Manhattan distance [50].

$$MINK(x,y) = (|x_1 - y_1|^k + |x_2 - y_2|^k + |x_3 - y_3|^k)^{\frac{1}{k}} \tag{2.29}$$

where x and y are pixel of two compared images, $x_1 - y_1$, $x_2 - y_1$, $x_3 - y_1$ are differences between values for each channel of images, k is degree of freedom.

Edge similarity metric is metric which were derived in this project. It is based on extracting edge information from two compared images and calculating Minkowski distance between them. The edge information is extracted using Prewitt operator.This metric allows to predict how different structural information on two images.

3   Methodology and solution plan

For linking color quality of reproduced images, algorithms for evaluating smoothness of these images and visual human experience **psychophysical methods** were mainly used in this project. Psychophysics is branch of experimental psychology concerned with developing experimental methods for objectively measuring our subjective perceptual experiences [51]. It allows quantify relationships between the dimensions of the external world of physical simulation and internal world of perceptual appearances.

The psychophysics proposed two fundamental quantities that psychophysical methods allow to measure: **thresholds** and   **scales**. Thresholds describe limits of perception. There are two types of thresholds: absolute/detection threshold (measure absolute limits of perception) and difference/discrimination theshold (measures ability to discriminate between similar physical stimuli) [51]. In **scaling** interest is in quantifying the suprathreshold appearances of things, and in measuring how appearance changes with changes in physical properties. Scaling studies are widely used in engineering application for solving task related to evaluation image quality by metrics and algorithms. So scaling psychophysics quantity was used in this project for psychophysical experiments.

There are wide variety of methods have been developed to derive psychophysical scales. They are divided on two main categories: **indirect** and **direct**. In indirect methods subjects are asked to make simple judgments about object properties (grouping, sorting, and ordering). Numerical scale values are derived using statistics on these judgments. In direct method subjects directly assign numerical values to their perceptions, or adjust stimuli to stand in some mathematical relation. In case of this project it is possible design interval scale which allows categorizing images according to their smoothness using indirect method. It is reasonable because there is no previous knowledge about magnitude of smoothness, but human visual system distinguishes difference in smoothness between original and reproduced image as, for example, perfect smooth or worst smoothness.

For achieving goal of project set of experiments was conducted because problem is complex and require consideration of few attendant problems. The entire project work was divided on 4 stages 16:

- **1 stage Analysis of limitations of 3DLUT-based color transforms.** On this stage limitations of 3DLUT-based color transformation in device characterization were studied and analyzed for defining reason of appearing image quality problems and smoothness problems. Based on previous studies 3DLUTs of different size with various level of noise and interpolation methods for mapping from RGB to $CIEL^*a^*b^*$ were considered as factors affecting on color transformations. Empirical printer characterization process was simulated in a way that it would be possible control color

transformations and reproduce results on display. Putting it in simple words, printer was modeled on display. It means that forward and inverse display characterization model was used for conversion between RGB and $L^*a^*b^*$ color spaces and vice versa. Gaussian random noise was added to $L^*a^*b^*$ values for simulating noise in color measurements during printer profiling. The 3DLUT with noise was considered as simulation of empirical printer (driving in RGB mode) characterization. The experimental set of images were processed (converted from RGB to $L^*a^*b^*$) using designed 3DLUTs and such interpolation methods as trilinear, prism and tetrahedral. Then set of images were converted to display RGB color space (using inverse monitor characterization model) for performing processed images'. Psychophysical experiment with 4 observers was conducted for evaluating difference in smoothness between original and processed images using category scale. The experiment environment and viewing conditions were prepared according to ISO 3664 and ISO 12646 [20], [19] and [27]. The relationship between visual judgments of images and interpolation method, noise ratio and LUTs size were analyzed. As the result of analysis the unavoidable noise in measurements is considered as main factor which affect on smoothness of color transformations.

- **2 stage Printer' profiles generation.** This stage is based on analyzed results of first stage. On this stage real noisy printer characterization data is received by empirical printer characterization or profiling. It was designed with purpose to approximate common printer profiling for average user in daily life. Printer profiling was conducted using color targets printed on color laser RGB printer using standard printer' mode and measured with different repeatability by spectrophotometer Eye-One i1-iO (strip mode) and software. Few color targets were printed on different substrates of same paper type. The measurements of particular repeatability and on different substrates were conducted for achieving variability of measured data and confirming assumption about random noise distribution in color measurements. The set of profiles was generated using l software. The measurements and data of different profiles were analyzed. The set of profiles have been chosen for preparing experimental set of images for obtaining images with different smoothness.

- **3 stage Psychophysical experiment** Image set was prepared and converted to profiles by Adobe Photoshop CS3 Version 10.0.1. This software is commonly-used by average user for working with profiles. The psychophysical experiment is aimed to provide visual evaluation of smoothness of image color transformation obtained by converting to particular profile. This is way to identify which color transformation (profile) allows to obtain better smoothness performance on image by human eye perception. Psychophysical experiment involved 20 observers. They were asked to judge about difference in smoothness between original and processed images using category scale from perfect match in smoothness to worse match in smoothness.

- **4 stage Experimental results and analysis.** For the visual judgments z-scores were computed according to Torgerson's Law of Categorical Judgment. Several image difference metrics-candidates for evaluating smoothness: SSIM, GSSIM, Edge similarity, Structural content, and CIELAB, SCIELAB and Adaptive bilateral filter were calculated between original and processed images in experimental set. Phil Green metric, Kim-Bang-Chon metric were calculated for each profile using color ramp. In conside-
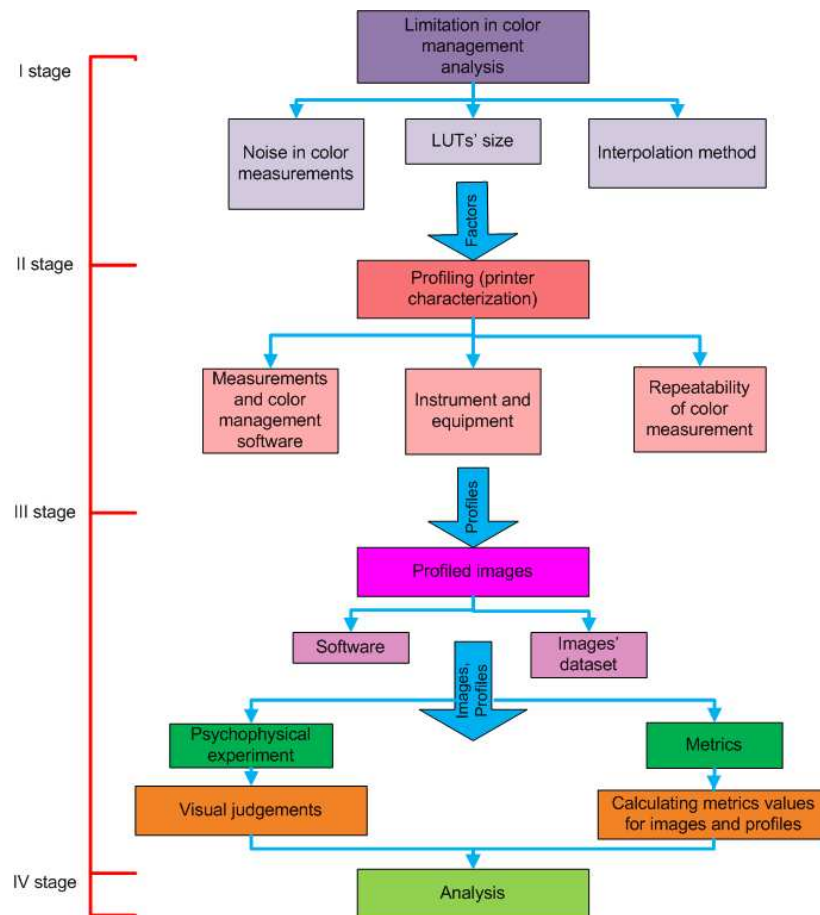
Figure 16: Main stages of project

ration of drawbacks of these methods new way for evaluating smoothness of color transformation was proposed. The idea of proposed method for evaluating is based on considering L*a*b* color planes in grid of 3DLUTs extracted from profile (AToB0 tag). These color planes contain 33x33 vertical and horizontal color transitions or ramps. ΔL^* , Δa^* and Δb^* and second derivative is computed for each horizontal and vertical ramp on the plain. 95 % percentile for each ramp esteems variation color between adjusted points in ramp. The maximum of 95 % percentile between 3 channels should be chosen as highest variation of component magnitude in ramp. The mean percentiles for horizontal and vertical ramps are derived, and these values are multiplied for obtaining value of metric for each color plane. The proposed method of color planes for evaluating smoothness were computed for each profile. The performances of proposed metric and existed metrics were compared with visual judgments data (z-scores), and results were analyzed using statistical methods and packages.

MatlabR2009b was used for implementing 3DLUT-based color conversion, metric algorithms, designing experimental GUI for displaying images and statistical analysis of data. The results dedicated to analysis of limitation of 3DLUT-based color transformation (Stage 2) and printer profiling (Stage 3), obtained during this project work, were also presented and accepted for a conferences [52] and [53].

4 Analysis of limitations of 3DLUT-based color transformations

4.1 Experimental setup

4.1.1 LUTs' size and interpolation

So factors inherited from the 3D LUTs transformation including size of LUT, interpolation method and noise from profiling appeared in LUTs were investigated. Three interpolation methods were designed according to formulas presented in 2.1.4 using MatLab R2008b environment (without applying standard functions): **trilinear**, **prism** and **tetrahedral** interpolation.

3DLUT were generated by sampling RGB values from 0-255 (8 bit) in different interval, and these RGB values were converted to CIELAB color space using DELL LCD display forward characterization model. For goals of experiment following intervals were chosen:

- 32 (256/8) for building 9x9x9 3DLUTs;

- 16 (256/16) for building 17x17x17 3DLUTs.

3DLUTs with these intervals are used for performing small and medium size 3LUTs which can be included in ICC profiles. 3DLUT with 33x33x33 size were not used in this experiment through computational cost of applied interpolation in Matlab. It worth to notice that 16-bit precision of the LUTs' encoding is preferable if requirements to quality are high ([15],138).

4.1.2 Display characterization

21-inch DELL LCD display were calibrated and characterized according steps detaily described in 2.1.3 based on ISO3664 standard. The forward and inverse GOG(Gamma-Offset-Gain) characterization model was applied for providing more accurate and reliable
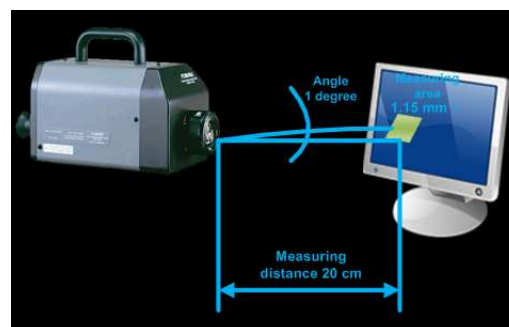
Figure 17: CS1000 setup for display characterization

conversion from RGB to CIEL*a*b* and building accurate LUTs. The reason why GOG model was used for LCD display characterization mentioned in 2.1.2.

Spectroradiometer CS-1000 was used for characterization purposes. This instrument allows to measure spectral power distribution, luminance, chromaticity and correlated color temperature for display devices with high-accuracy (for chrominance x:±0.0015, y:±0.001; luminance range 30 to 80 cd/m^2 with macro lens) [54].

The derived from measurements gamma, gain, offset, ambient flare and maximal tristimulus values for R,G,B channels were used for designing color conversion functions in Matlab according to original equations 2.6 - 2.9.

4.1.3 LUTs' transformations and color conversion

The main assumption was accepted in this experiment that noise from the color measurements could be presented as Gaussian random noise in LUTs. This assumption is based on idea that evaluation of repeatability and reproducibility of color measurements by instrument according ([55], 95) mostly relied on the central-limit theorem in which a series of events form a normal(Gaussian) distribution. In this case standard deviation represents precision. It means that for set of consecutive measurements with short-term interval repeatability by same instrument the variation of values will occur. So for the same color patch these color measurements will be slightly different. These noise depends on mostly environment conditions, instrument which related to measurement uncertainty.

For experiment different random noise ratios **0,1,5,10** and **20** were applied to the L*a*b* channels in LUT. These noise was generated by Matlab function **wgn**. Function makes matrix of specified size containing linear white Gaussian noise values. The noise ratio and corresponding to it noise variation are presented in table 6. The range values of noise was concidered from 0 to 20 where 0 means that there is no noise in LUT, and noise ratio 20 presents the largest noise applied to LUT. The noise ratios were chosen after small visual experiment for evaluation total images quality distored after color transformations involving 3DLUTs with noise. In this experiment two observers were participated.

As example, the noise ratio 1 means that noise values added to L*a*b* varied from -1 to 1. For original $L^* = 2.0031$ noise value is $n = 0.001$ then new distored by noise value of $L^* = 2.0041$.

Noise ratio	Noise variation
0	There is no noise in LUT
1	$-1\dots1$
5	$-5\dots5$
10	$-10\dots10$
20	$-20\dots20$

Table 6: Noise ratio

44
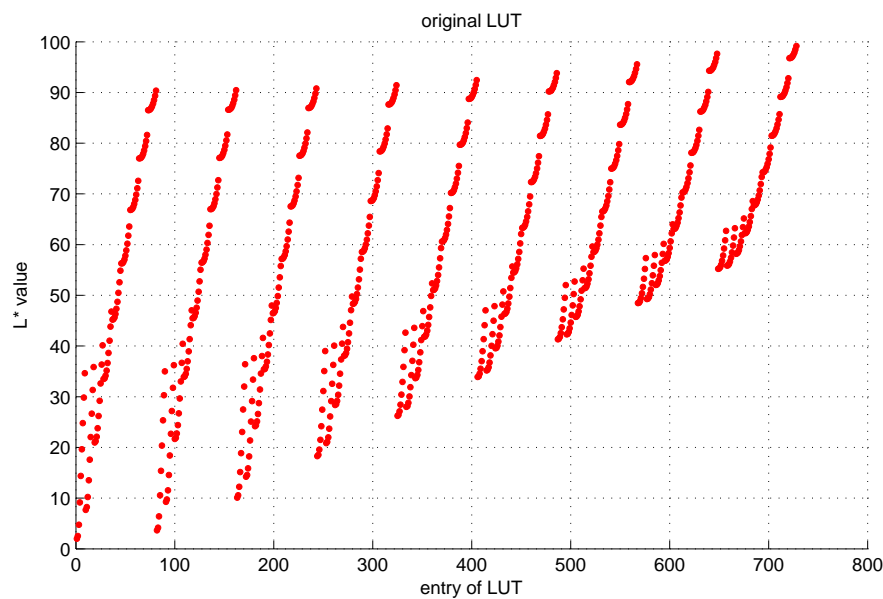
Figure 18: L* entries of LUT(9x9x9) with noise ratio 0

Original L* values without noise are presented on figure 18. The values distribution repeats trough interval. The one of these intervals(or segments) was chosen for presenting L* with added noise on the plots on figure 19. The original space from 82 to 162 L* values and noise of different ratio for entries in 3DLUT(9x9x9) are shown on figure. The noise deviation is marked by blue arrows and original values of L* are marked as red points. Direction of blue arrows shows how noise affect on particular L* value of LUT: if arrows direct to down then noise decreases original L* values, and vice versa when arrow direct to up.

The graph for LUT with noise ratio 1 on figure 19 a) shows that values of noise are too small. So LUT with noise approximates to original LUT, and difference between them is not perceptible. For noise ratio 5, 10 and 20 (19, b), c) and d)) original L* and distored L* values differ, and for some values distinctions are noticable, and for some values are significant(especial for noise ratio 20).

4.1.4 Image reproduction for experiment

The main workflow for image reproduction is performed on figure 20. The tool for applying all stages of workflow was implemented in Matlab.

I stage - Initialization and input parameters. Input parameters for reprodution workflow are input image for conversion, interval for generating 3DLUT, method of interpolation and noise ratio which defined noise for adding to LUT. Input image should be presented in RGB color space with 8 bit per channel. Three interpolation methods were considered in this project: trilinear, prism and tetrahedral. Two intervals were considered for building 3DLUT: 32 (9x9x9 LUT) and 16 (17x17x17 LUT). Noise ratio is one of these

a)noise ratio 1; b)noise ratio 5;

c)noise ratio 10; d)noise ratio 20;
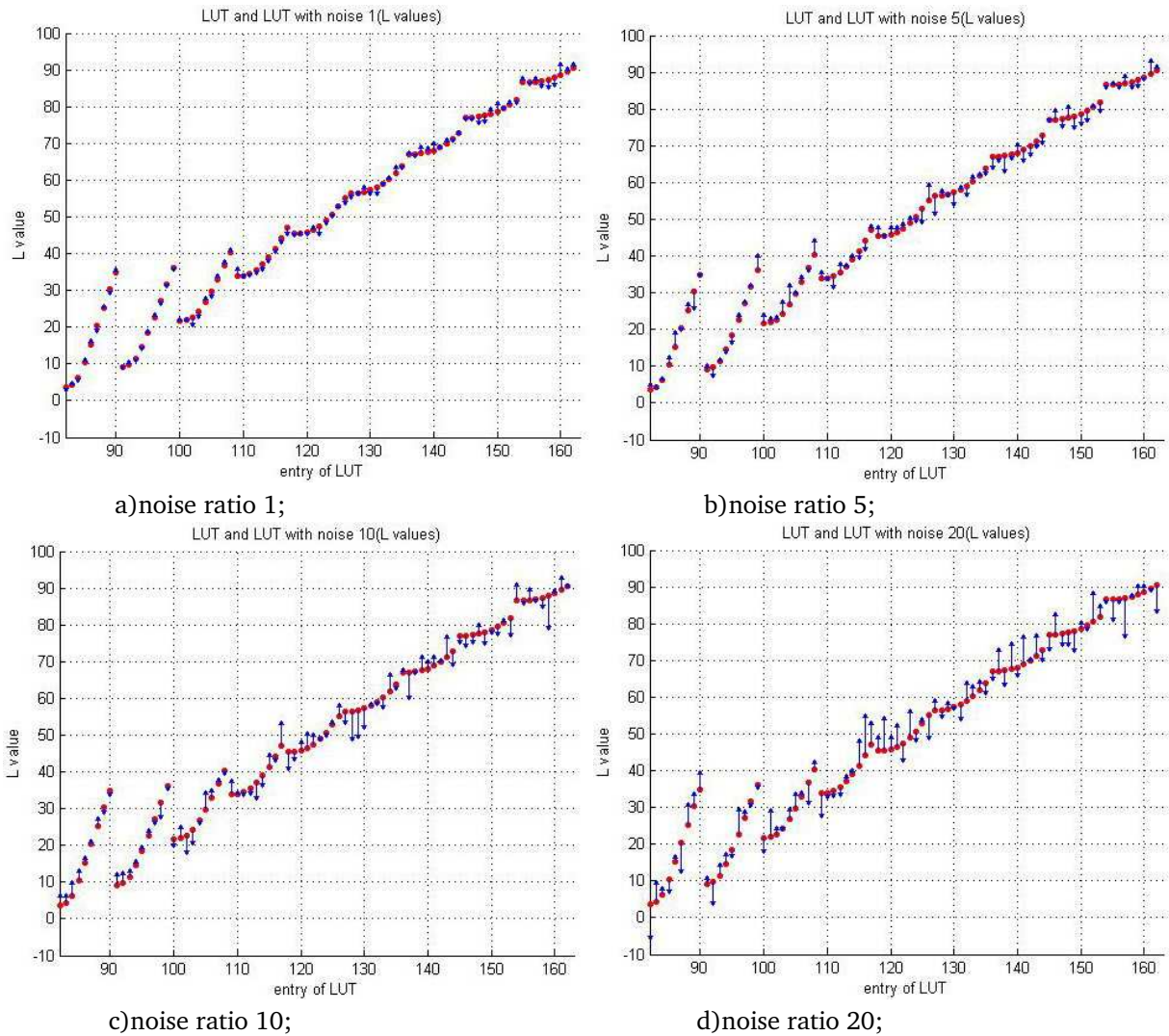
Figure 19: L values with added noise of different ratio

considered values: 0, 1, 5, 10 and 20.

II stage - LUTRGBLAB generation. The all possible combinations RGB values through interval were generated as explained in 2.1.4 and put to LUT matrix with RGB values (in same way as shown in table 1). Then these LUTRGB values were converted to CIEXYZ and from CIEXYZ to CIEL*a*b* using forward display characterization model implemented in Matlab(GOG model), and LUTRGBLAB was derived for color conversion. The standard Matlab function was used for generating Gaussian random noise with particular noise ratio. The noise values with particular ratio were only added to L* a* b* values from LUTRGBLAB.

III stage - Interpolation. For each image pixel RGB values were found corresponding RGB and CIEL*a*b* subcubes from 3DLUT with added noise. Then cubes can be devided on prisms or tetrahedrons for prism and tetrahedral interpolation method res-
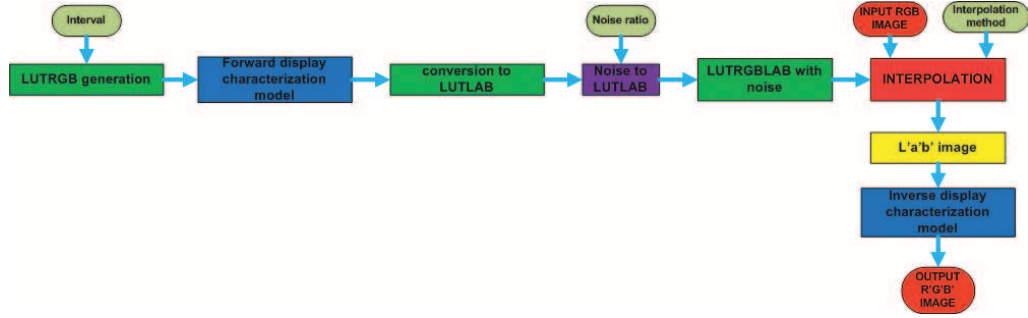
Figure 20: Workflow of image reproduction by 3DLUT-based transformation
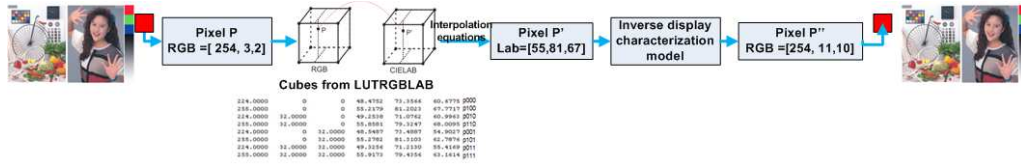
Figure 21: Red pixel 3DLUT-based conversion for display characterization

pectively. The tetrahedron or prism contains concidered point should be found. For tri-linear interpolation entire cube is used. For each pixels' R, G, B values corresponding CIEL*a*b* values are computed according to formulas 2.12, 2.13, 2.14 and 2.15 of chosen interpolation method (explained in details in 2.1.4).As example, pixel of red color with $p(R, G, B) = [254, 3, 2]$ will be interpolated in $p'(L^*, a^*, b^*) = [55, 81, 67]$ as shown on figure 21.

IV stage - Color conversion of image from CIEL*a*b* **to RGB and output result.** Interpolated image was obtained in CIEL*a*b* color space and then converted to RGB color space by inverse display characterization model by functions applied in Matlab. Processed image in RGB color space was used for experiment and analysis.

For project experiment LUTs with two different sizes, 3 interpolation methods and 5 random noise ratios (including noise ratio 0) were used for image transformations. Common number of generated transformed images were 30 for particular image (30 = 2x3x5). One image of business graphic and three pictorial images were selected for transformation (Appendix C). These images contain many color transitions and tones which are appropriate for evaluating smoothness . They were presented in RGB color space with size not exceeding 800x600 (96 pixel per inch) (in the table 7). For each image 30 transformed images were generated. So total number of images for experiment is **120**.

Name	Size
Balloon	800x600
Bows and threads	800x600
Picnic	794x595
RGB	797x598

Table 7: Images' set

Examples of images' reproductions are presented on figures 54 - 57 in Appendix C. Different noise in 3DLUT-based color transforms affects on images reproduction as it shows Balloon images obtained by 3DLUT with added noise of 0,1,5,10,20 ratios (figure 54). The interpolation methods perform quite similar results in combination with 3DLUT without noise(figure 55). On figure 56 RGB image reproductions obtained by 3DLUT-based color conversion with applied noise of 10 ratio have different smoothness distortions. For the 3DLUTs of different sizes reproductions of Bows and threads image slightly different (figure 55). The image reproduction produced by 3DLUT17x17x17 (figure 55, b)- based color conversion has more vivid colors. But objective evaluation of these image reproductions requires conducting psychophysical experiment involving few observers.

4.2 Psychophysical experiment

The psychophysical experiment have been taken place in dark room equipped by a DELL 21-inch LCD display which was calibrated and characterized according to ISO3664 and ISO 12646 [19],[20]. The sources of possible light, flare and glance were removed for avoiding influencies on visual judgements [27],[56].

As this experiment is concidered as short preliminary work for main part of project only four observers with normal vision were invited for participating in experiment.The following instruction have been given for observers before experiment: evaluate total image difference between two images(original and processed) using category scale from 0 (No difference in smoothness) to 7 (Extreme difference). Each category were explained as in table 8.

Image reproduction and original image were displayed by special experiment's tool designed in Matlab environment (on figure 58). The surrounding objects affects color perception, from light reflected off these objects and from adjacency when human percieves them in his field of view. The background for images have chosen as neutral gray ($L^* = 50, a^* = 0, b^* = 0$) as specified by viewing standard [56], [57]. Images were presented in white frames 20x20 pixels for limiting borders of images. The images' pairs were randomly mixed.

Category	Level of Difference	Description
0	No difference	There is no difference in quality between images
1	Slight difference	The quality of images gently different
2	Noticeable difference	There are few differences in quality between images
3	Moderate Difference	Medium difference in image quality
4	Acceptable Difference	Tolerable difference in image quality
5	Not Acceptable Difference	Essential difference in image quality
6	Very Large Difference	Considerable difference in image quality
7	Extreme Difference	The high difference in image quality

Table 8: Description of judgements' categories
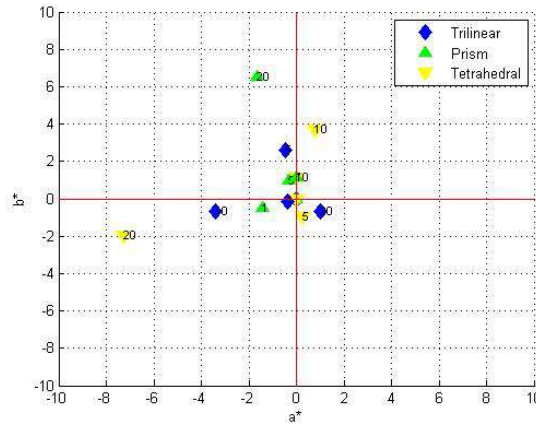
Figure 22: White shift according different random noise

4.3 Experimental results and discussions

The generated images by 3D-LUT color conversion with different added noise and intepolation methods have obvious artifacts (figure 59 in Appendix C from left side - original image, from right side - reproduced): stripes and grains in large uniform area, countours and the color shift which is more visible for the white background with a large noise ratio. The reason of appearing of color shift is a high random noise ratio. On few images white color is shifted in direction of blue tint (example on figure 59 in the middle).

This color shift is not constant due to noise is random. So various noise affects on color in distinct directions. White pixel was converted from RGB to $CIEL^*a^*b^*$ color space by 3DLUTs with added noise of different ratios and three interpolation methods: trilinear, prism and tetrahedral as shown on figure 22. White color with $RGB = [255, 255, 255]$ is supposed to map into $L^*a^*b^* = [50, 0, 0]$ in ideal case (consistent color transform and 3DLUT without noise). So for 3DLUT without added noise points gather in the center for all interpolation methods. But there is explicit shift from 0 in different directions for 3DLUTs with noise of different ratio. Then converted color is not pure white, and it can be bluish, yellowish white and etc. for large shift. It is not possible to predict how converted color will shift because of random noise.

For all observations of images' set mean opinion scores were found for each image reproduction according to formula using observers esteems:

$$MOS = \frac{\sum_{i=1}^{N} IS}{N}, \tag{4.1}$$

where N - number of observers, IS - individual esteem of particular observer. The individual judgements, mean opinion score and standard deviation from them is presented on table 25 in Appendix C.

The distribution of MOS for each images' reproductions is presented on figure 23.

Horizontal axis shows parameters for particular reproduction: 3DLUT size, noise ratio, interpolation method. For example, 90p means that for image reproduction 3DLUT 9x9x9 with noise ratio 0 and prism interpolation method were used. So first **9** or **17** are denoted 3DLUT 9x9x9 or 17x17x17; then **0,1,5,10,20** are noise ratios; **p** –prism, **tr** –trilinear, **tet** – tetrahedral interpolation methods. The plots explicitly shows approximately same MOSs for image reproductions with parameters 3LUTs 9x9x9 and 3DLUTs17x17x17 without noise for different interpolation methods overall images (90p, 90tet, 90tr and 170p, 170tet, 170tr areas on plot). So in this case interpolation methods show similar performance. The visual judgments are fluctuated from 0-2.5, and images' reproductions with parameter 3DLUT 17x17x17 for these areas on plot were estimated as more close to original because results are slightly lower than for 3DLUT 9x9x9. For all images' reproductions MOSs increase with increasing ratio of noise added to 3DLUT . It means that images' distortions increase, and reproductions more differ from reference image with growing magnitude of noise in 3DLUTs.
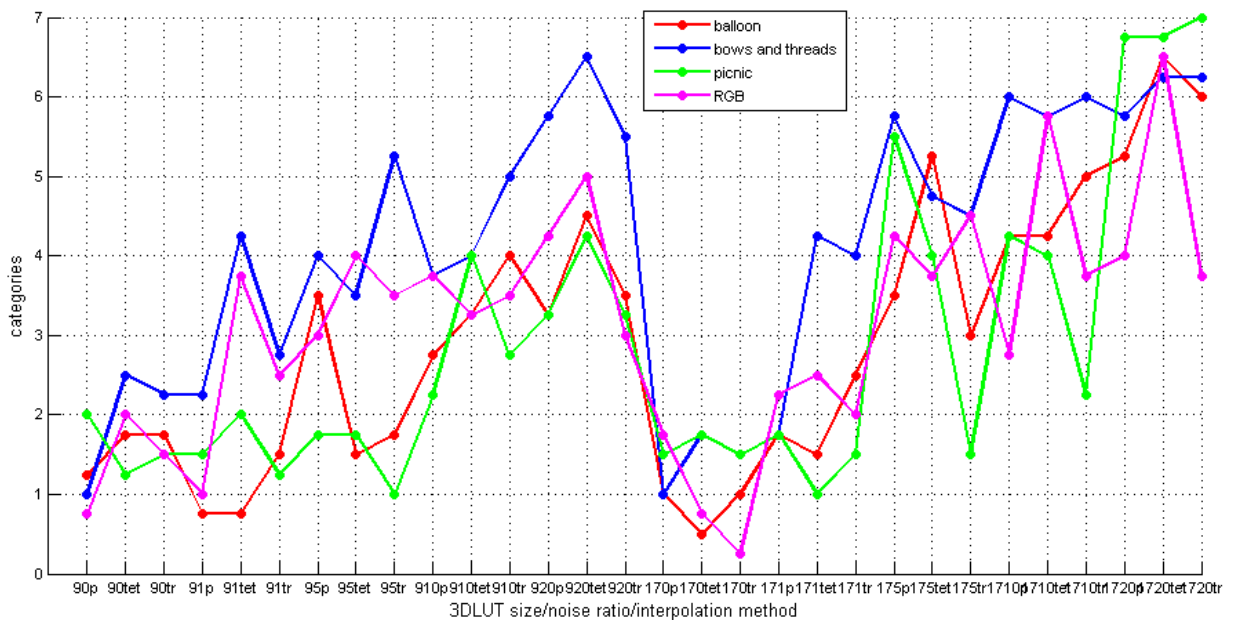
Figure 23: Mean opinion score for 4 observations

The level of accepted difference between original and reproduced image is category 4. From figure 23 it can be found that MOSs became significantly higher that this threshold for images' reproductions with parameters: 3DLUT size 9x9x9 and 3DLUT size 17x17x17 and noise ratio 5 (especially for reproductions of image Bows and threads). On interval with high noise ratio (10 and 20) MOSs for reproductions of image Bows and threads meaningfully exceeds level of accepted difference in comparison with original image. So image Bows and threads color content is more sensitive to noisy 3DLUTs-based color conversions than others images. It contains complex transitions of pink colors: from light rose color to saturated pink and white imitating glossy effect of satin.

On figure 60 in Appendix C MOSs distributions are presented with 95% confidence

interval among observations for each image reproduction. The 95% confidence intervals were calculated according formula ([58]):

$$\overline{X} \pm \frac{1.96 \cdot \sigma}{\sqrt{N}}, \qquad (4.2)$$

where $\overline{X}$ is the sample mean, 1.96 is the upper critical value of the standard normal distribution which is found in table for 95 % confidence, σ is known population standard deviation, $N = 4$ is number of samples. From MOS distribution plot with 95 % confidence interval broad variation in visual judgements is presented for Bows and Threads image and RGB image reproductions because of complexity of images' content. For Picnic and Balloon images reproductions observers judgments' variations are relatively small.

The images' reproductions quality with parameter 3DLUTs 17x17x17 with high noise magnitude were estimated as more lower than for images' reproductions obtained with same parameters but by 3DLUTs 9x9x9. But it contradicts to common practice where 3DLUTs of larger size provides more consistent color conversion because number of points in grid increases, and mapping is accomplished more accurate ([15], 138). In case of this project large 3DLUT 17x17x17 has more grid points, and consequently became noisier because noise is added for each point. In worse case generated random noise with ratio 10 affects on original $L^*a^*b^*$ with $\Delta L^* = 10, \Delta a^* = 10, \Delta b^* = 10$, and then $\Delta E_{ab}^* = 17.3$. The randomly generated noise values of high ratios significantly differ from each other. In real practice noise provides slight and relatively slight variations in 3DLUT, and only for several points' magnitude of noise is very high (it will be detaily considered in next chapter). The 3DLUTs with noise of 10 and 20 ratio can be seldom met in real practice but this is just simulation which allows to us consider how it affects on color reproduction in more simple way.

The relationships between noise ratio and average visual judgments are presented on figure 24 and table 9. The average visual judgments were found for each noise ratio. The standard deviations from average are presented as bars on the graph. From figure 24 it can be obviously found that the tolerance of acceptable difference for images' reproductions can be achieved by noise ratio smaller than 5. So noise in 3DLUT should not exceed ratio of 5 for acceptable results in image reproduction. For noise ratio 5 maximal magnitude of added noise to the $L^*a^*b^*$ values in 3LUT is 5, then $\Delta E_{ab}^* = 8.66$.

Noise ratio	Average category	Standard deviation
0	1.4063	0.3698
1	2.1250	0.9697
5	3.5313	1.0143
10	4.0104	0.8585
20	5.1146	0.8618

Table 9: Average MOSs for noise ratios

On figure 25 green plot performs MOSs for images' reproductions obatined by 3DLUTs 9x9x9- based color conversion (with different noise and interpolation methods), purple plot - MOSs for images' reproductions obtained by 3DLUTs 17x17x17- based color conver-
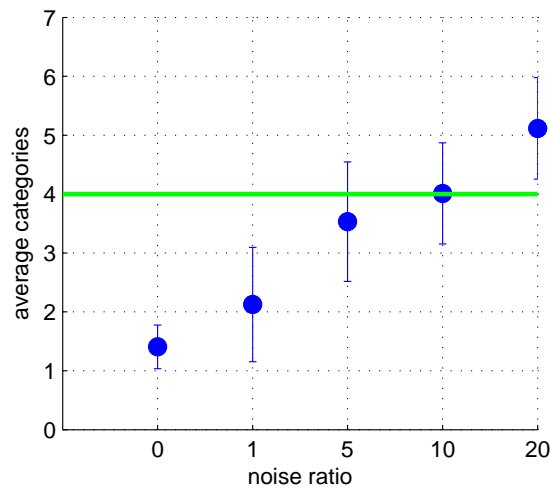
Figure 24: The relationships between noise ratio and average categories for visual judgements

sion (with different noise and interpolation methods). On area from 0p to 1tr (horizontal axis) color conversions with 3DLUTs of different size shows approximately similar performance. 3DLUTs 9x9x9 have slightly higher score for images' reproductions of Bows and threads and RGB than 3DLUT 17x17x17, for other images - MOSs distributions for different 3DLUTs are almost same (on area from 0p to 1tr). It means that 3DLUT of large size allows to obtain better color conversion with low noise ratio than 3DLUT of small size. Starting from 5 noise ratio 3DLUTs of large size have more higher MOSs, and in this case 3LUT with small size shows better representation.

Figure 26 illustrates MOSs distribution for images' reproductions depending on interpolation method which was used in color conversion. The horizontal axis defines parameters which were used for color conversion: 3DLUT size and noise ratio. For example, **90** means that 3DLUT 9x9x9 without noise was applied for image reproduction. In total three interpolation methods shows approximately same representation for different images reproductions. But there are some cases where MOSs of images reproductions differs for interpolation methods. MOSs of Picnic image reproductions for 3DLUT 17x17x17 with noise of ratios 5 and 10 are lower for tetrahedral interpolation than for prism and trilinear interpolation. Returning to figure 60 in Appendix Cwith 95% confidence interval it can be noticed that on area from 175p to 175tr and from 1710p to 1710tr the visual judgments are quite various, and differences between MOSs for interpolation methods on these area can be caused of these variations. Analogous, trilinear interpolation for Bows and threads image reproductions which were obtained by color conversion with 3DLUT 17x17x17 and added noise of ratio 1 performs lower results than other interpolation methods. On figure 60 in Appendix C 95 % confidence intervals for MOSs of Bows and threads image' reproduction (on area from 171p to 171tr along horizontal axis) show that variations in visual judgments are high. This is can be a reason of appearing differences between interpolations methods representations for this area.

The results clearly shows that one of main factors which affected on 3DLUT-based co-

lor transformation and quality of reproduced image is random noise. Larger 3DLUT size with low level of noise improves color conversion in comparison with smaller 3DLUTs. The evaluation of complex and natural images is not easy task because observers gave various esteems for some images' reproductions, as example Bows and threads and RGB images. An images can contain color transitions more sensitive to combination of noise and 3DLUT size parameters of color conversion.It depends on which part of LUT values was affected by noise more, and it coincidences with color in transition part. But this is subject for another research which is not in scope of this project.
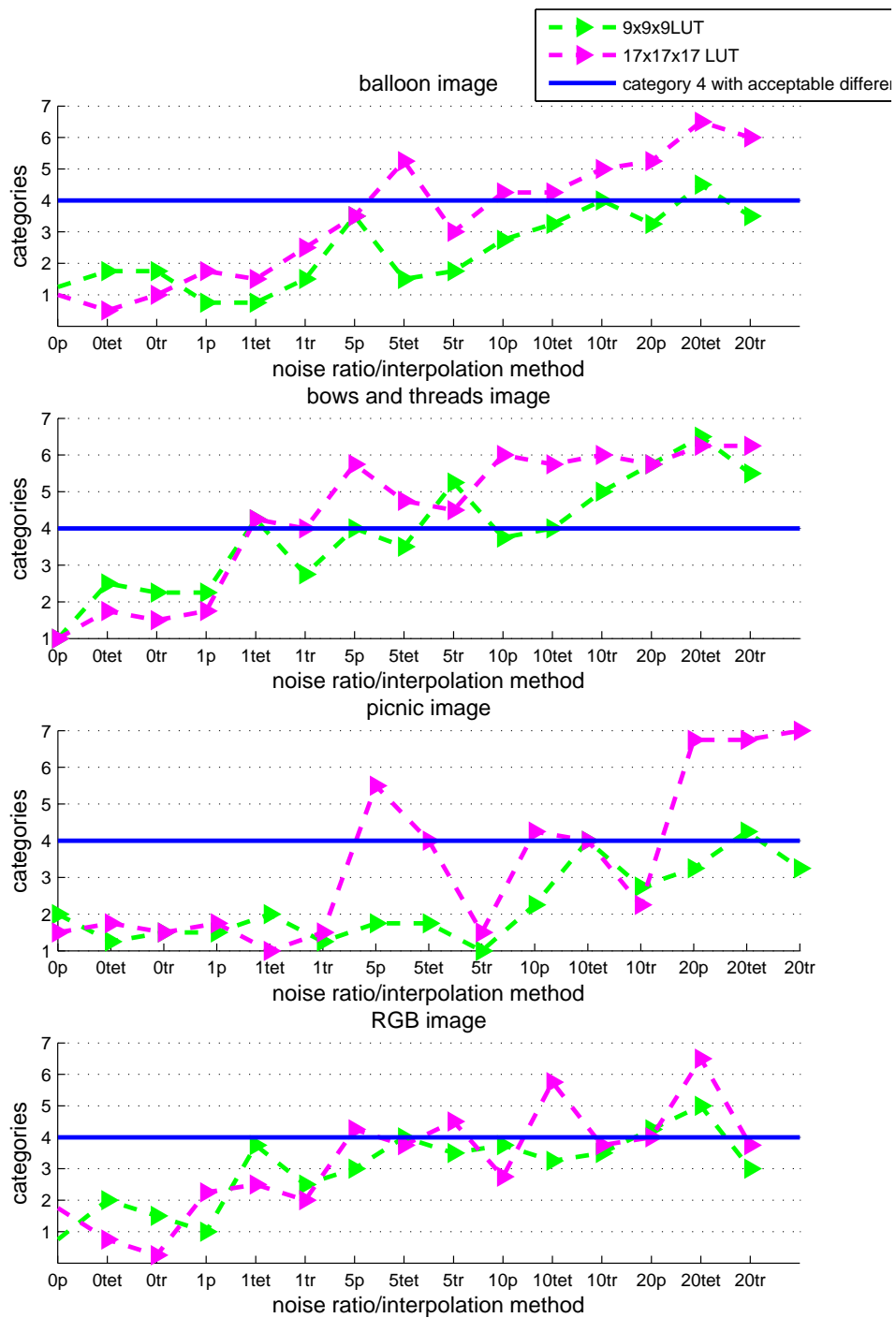
Figure 25: The difference between MOS for images' reproductions (3DLUTs size)
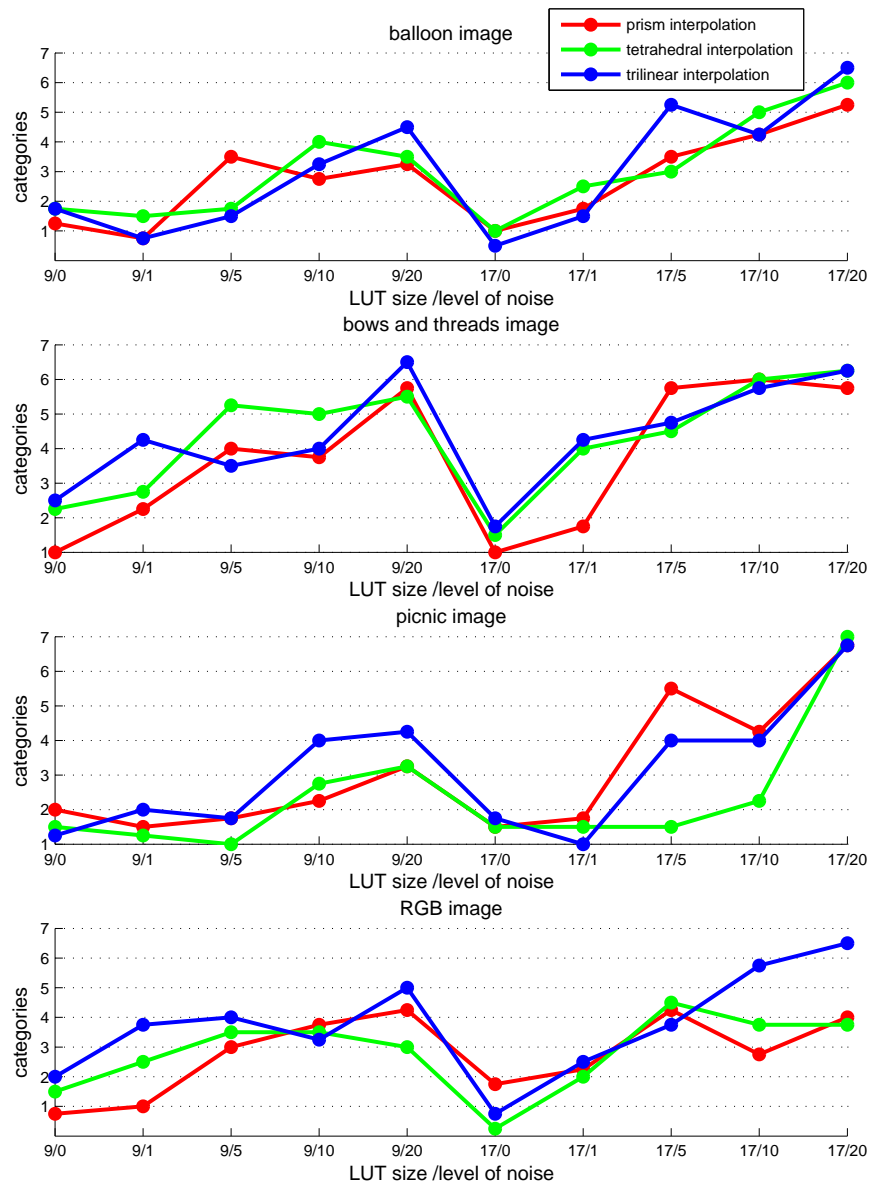
Figure 26: The difference between MOS for images' reproductions (interpolation methods)

5   Printer profiles generation

5.1   Equipment and applied settings

Detailed description of profiling process was concidered in 2.2.3. Printer profiling were conducted according to sequence of actions described. Equipment and software have been chosen for approximating to printer profiling by average user.

The GretagMacbeth **Eye-one Pro i1-iO** spectrophotometer with robotic automatic chart reading system was used for color measurements (figure 27, left side from XRite official web-site). Eye-one Pro i1 is popular instrument for different categories of user: photographers, designers and press-industry companies' staff. This spectrophotometer has connection with GretagMacbeth software system.The Eye-one Pro is supplied by i1iO scan table with arm and base plate which is designed to work with i1Pro devices. These robotic arm imitates movements of human hand during measurements.

The UV(ultra-violet) cutoff filter at 400 nm have been used for removing UV part of spectrum of light reflected from paper and preventing it from distributing measurement in visible spectrum part. For profiling UV filter was built-in Eye-one Pro for providing high precision in printer profiling. These settings for Eye-One i1-iO and Xerox Phaser 7760-GX have applied for simulating standard printer profiling by average user.

Option	Parameter
Software	Measure Tool 5.0.10
Measure mode	Stripe
Additional facilities	Scan table with arm and base plate
UV cut-filter	Yes
Color target	TC9 18 RGB i1 iO

Table 10: Parameters for measurements by Eye-One i1-iO

GretagMacbeth ProfileMaker Pro 5.0.10 solution includes **Measure Tool** subsystem for automatic color measurements including instrument configuration and controlling process of measuring. MeasureTool provides special color charts designed for spectrophotometer Eye-one Pro i1-iO. For printer driving in RGB mode **TC9.18 RGB i1 iO** color

Figure 27: EyeOne i1iO Pro spectrofotometer and Xerox Phaser 7760GX color laser printer

chart have been chosen. This color chart is presented on figure 61.TC9.18 RGB i1 iO color chart contains 27 color ramps (9-step in each) covering the color spectrum and 7 narrow gamut(17-step in each) and grayscale color ramps for linearising. Each of color ramps is repeated three times used to be averaged in profiling sofware. The total number of color patches is 936. The chart has original size 27.9x18.4 cm.

Measure Tool has two modes of measuring colors charts:

- strip measurement mode;

- single patch measurement mode.

In strip mode the Eye-one Pro i1-iO moves robotic system with along line with color patches and makes approximately 100 measurements per second. Each colored patch will have multiple measurements which are averaged by the software. So measuring of whole color target does not require long time. The Eye-One spectrophotometer can also be configured to make single patch measurements. This mode provides higher accuracy but takes more time for measuring. Strip mode have chosen for goals of experiment because average user mostly prefer faster way for measuring color charts. The parameters for Eye-One i1-iO are presented in table 10. Short-term repeatability for Eye-One i1-iO Pro is described as deviation error (DE) $\Delta E_{94}^* \leq 0.1(D50,2°)$ with respect to the mean CIELAB value of 10 measurements every 3 seconds [59]. Inter-instrument agreement is described as average DE $\Delta E_{94}^* \leq 0.4$, Max DE $\Delta E_{94}^* \leq 1$ [59].

The color printer **Xerox Phaser 7760-GX** was used for profiling. The printer allows achieve relatively Detail specification for this model of printer is presented [59]. Xerox Phaser 7760-GX (figure 27, on right side from Xeros official web-site) has maximal resolution 1200x1200 dpi and speed in color mode is up to 35 pages/min. It allows print in 3 modes:

- standard;

- photo;

- enhanced.

The standard mode is intended for general-purpose of printing (crisp, bright color prints at high speed). This mode is recommended for most office use and quick prints. Enhanced mode is high-quality mode for fine lines and sharp text. It is recommended for detailed prints. The photo mode provide highest-quality reproduction for very smooth color shades recommended for printing photographs or when using graphic arts applications and press matches (according to [60]).

There are additional options for three these modes: color correction, color sRGB neutral grays. Color correction options provide simulations of different color devices. Xerox Phaser 7760 options which in detail described in [60]:

- automatic;

- office color;

- press match;

- none;

- black and white;

- use printer control panel settings.

Automatic color correction applies the best color correction to each graphic element: text, artwork, and photographs. An average user of printer applies this option for printing.

The Color sRGB neutral gray is option available only for Macintosh OS version 10.2, 10.3. It allows determine way of reproducing black color. It can be achieved by mixing colorants' inks CMY or using single colorant inks K(pure black). The parameters for printing color chart applied in this project are presented in table 11.

Option	Parameter
Printer quality mode	Standard
Color correction	Automatic
Color sRGB neutral grays	Pure black
Resolution	600x1200dpi
Paper	Multicopy office paper
Format of paper	A4
Target size	27.9x18.4cm
Patch size	0.65x0.65cm
Software	Adobe Photoshop CS3 Version 10.0.1
Color management	No color management

Table 11: Parameters for printing color chart TC9.18 RGB i1 iO on Xerox Phaser 7760-GX

Xerox Phaser 7760-GX has options for automatic calibration such as cleaning heads, nozzles of toners, checking on color consistency by printing special page with samples. It was warmed up and automatic calibrated. Printer has driven in RGB mode and simulated RGB printer. Test pages with different color samples were printed, and results were visually estimated for achieving consistent and productive printer work. The printed color charts were checked on presence of scratch and defects.

Before starting measurements Eye-One i1-iO has been connected to Measure Tool software and warmed up by conducting 10 measurements on target.

5.2   Color measurements

The color measurements were conducted according specification [61] developed by ICC. This specification was designed following to ISO 13655 standard for color measurements and successful experience of members of ICC group.

The Eye One i1-iO Pro is designed according to requirements of ISO 13655 for spectral measuring instruments. The geometry of Eye One is $45°/0°$. The all calculations of tristimulus values were achieved using the CIE 1931 standard colorimetric observer, which

assumes a 2 degree field of view by Measure Tool software. ISO also calls for using the CIE D50 illuminant and defines spectral weighting functions derived from this observer and illuminant, which should be used when measurement is made with a spectrophotometer or spectroradiometer in which the spectral sampling interval is coarser than that specified by CIE, namely 1 or 5 nm ([61],1-2).

UV cutoff filter also reccommended for using in experiment because of UV excitation is different from one device to another, and for most printed media the strong fluorescence is found in the substrate.

Printer consistency and uniformity and error during measurements are important for building profiles. Despite on careful printer calibration, variations in printing can be met very often. Some errors arise during measurements because of operator error or poor instrument repeatability. So ICC reccomendations in this case to use several measurements of prints made during a reasonable time period which reflects mean of printer and operator variations.

It was concidered in previous chapter that noise in color measurements is main factor affected on output result of 3DLUT-based color transformations. So for obtaining images with different smoothness and quality and achieving the variation of noise in LUTs the various measurements were conducted with different repeatability and substrates(table 12).

Interval	Number	Paper-Target
consecutive ≤ 1 min	20	Same paper-target
30 min	20	Same paper-target
1 hour	10	Same paper-target
consecutive ≤ 1 min	20	Several copies of target on same paper type

Table 12: Measurements for printer profiling

First, color chart reproduction were consecutive (interval approximately more less than 1 min) measured 20 times, then each 30 min - measured 20 times and each 1 hour - measured 10 times. These measurements shows variability of instrument and operator in LUTs data of profiles by short-time repeatability. **Second**, same color target were consecutive printed on 20 substrates of same paper type. It gives us idea about printer variability. They were printed in 1 day after color target for first test was printed. The spectral and CILAB data for all measurements were gathered, computed and stored in .∗.txt files by Measure Tool 5.0.10.

5.3   Building of printer profiles

Printer profiles were generated using Profile Maker Pro 5.0.10 software. The color chart and corresponding to it file with measured data (spectral or CIELAB data) are required for this purpose. For generating profile following paparameters should be setted up before:

- Profile size;

- Perceptual rendering intent;

- Gamut mapping;

- Viewing light source.

Profile size can be defined as Large and Default. Default size option allows generate profiles of relatively small size which can be used, for instance, for posting on a web-site. Large profile size is appropriate for producing more smoother profile (according to [62]).

There are three options for gamut mapping: LOGO Colorful Gamut Mapping, LOGO Classic and LOGO Chroma Plus. The following explanation comes from ProfileMaker's [62] documentation:

- LOGO Colorful Gamut Mapping Method is notable for maximum color saturations and particularly clean primary colors;

- LOGO Classic variant incorporates the Gamut Mapping method placed heavy emphasis on lightness reproduction and thus on preserving detail reproduction in the entire color space;

- LOGO Chroma Plus variant is on higher Chroma in color reproduction, while keeping detail losses to a minimum.

Some studies argues about which gamut mapping algorithm allows achieve better result in smooth transitions of colors. It mostly depends on images data [63]. In this case LOGO Colorful gamut mapping method have been chosen for best peceptual representation of colors.

The Perceptual (or Photographic) Rendering Intent reproduces an image considering the paper, dynamic, and color characteristics of the output system in such a way as to ensure that the human eye will perceive the image in the target color system as the most faithful reproduction of the original [62]. For Perceptual Rendering Intent two option are available Neutral Gray and Paper-colored gray. The Neutral Gray intent is appropriate for most purposes. This attempts to neutralize any color cast in the paper where ther is sufficient dot area to do so. As an example, Paper-colored Gray could be used to retain a buff-colored cast in the media for an artsitic effect.

Profile generation settings are presented in table 13:

Option	Parameter
Profile size	Large
Perceptual rendering intent	Neutral Gray
Gamut mapping	LOGO Colorful
Viewing Light Source	D50
Correct for Optical Brightener	Yes
ICC profile version	ICCProfileVersion 2.4

Table 13: Printer profile generation parameters for Profile Maker Pro 5.0.10

Viewing Light Source (available option for spectral data) is used ot make the profile match color under the specified lighting condition. D50 have been choosen as standard light source defined by CIE specification.

The Correction Optical Brightener function offers a solution for the yellowcast problem caused by papers with optical brighteners. ProfileMaker allows to detect whether there is an optical brightener in the measured file. The correction always corresponds to the level of the optical brightener[62].

70 profiles were generated based on obtained measurement data. After analysis of measurements results, spectral data 45 profiles were prepared for converting images set and evaluating the smoothness of LUTs-based color transformations. 20 successive measurements, 20 substrates measurements and 5 measurements for 1 hour and 30 min repeatability are used for generating these 45 profiles.

5.4 Analysis of profile generation results and discussions

The ICC reccomendation [61] is based on optimization of random noise in several consecutive measurements using the average of these measurements. So for each group of measurements (20 successive, 20 substrates, 30 minutes repeatability measurements, 1 hour repeatability), average of these measurements were found using function **Averaging** of Measure Tool Pro. Then the color difference between averaged data and each single measurement were calculated by function **Comparing** of Measure Tool Pro, and average of overall color patches were found. The Measure Tool Pro measuring data in two forms: spectral data for each color patch on target or computed by software $L^*a^*b^*$ values for each color chart.
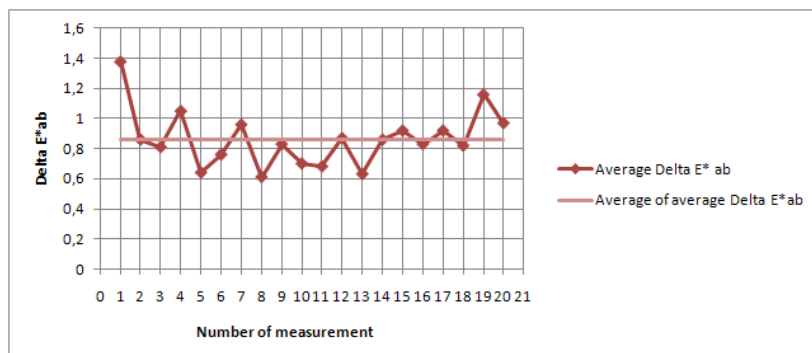
Figure 28: Average ΔE_{ab}^* for 20 successive measurements

On figure 28 average ΔE_{ab}^* between particular chart measurement and averaged data for 20 concecutive measurements overall patchesis presented (on table 26) . The plot shows that measurements slightly different from each other. It means that profiles based on these color measurements will provide similar color transformation results and respectively output image quality. Average ΔE_{ab}^* is general indicator for identifying dif-

ference between color measurements. The maximal ΔE_{ab}^* for 15th item of 20 successive measurements higher than for others (in table 26). The measurements for 2 color patches were considered in details. Color patch J1 RGB = [255, 0, 0] and T4 RGB = [255, 0, 96] (J1 and T4 are notations of color patch on color target in MeasureTool software) present patches of red and purple respectively. The meanΔE_{ab}^* between averaged measurements for these patches and particular mesurement were found (tables 27 - 28 Appendix D) and plotted on figures 62 and 64. On these plots **1th** and **15th** items of successive measurements have higher deviation from others. Spectral reflectancies of this patches for each successive measurement were drawn on spectral plots (figures 63 and 65 Appendix D). On figure 63 graphs show 15th item spectral reflectance on area from 400nm to 600nm (horizonatal axis) differs from others successive measurements. On figure 65 graphs perform 1st item spectral reflectance on area from 640nm to 730nm (horisontal axis) deviates from others successive measurements.
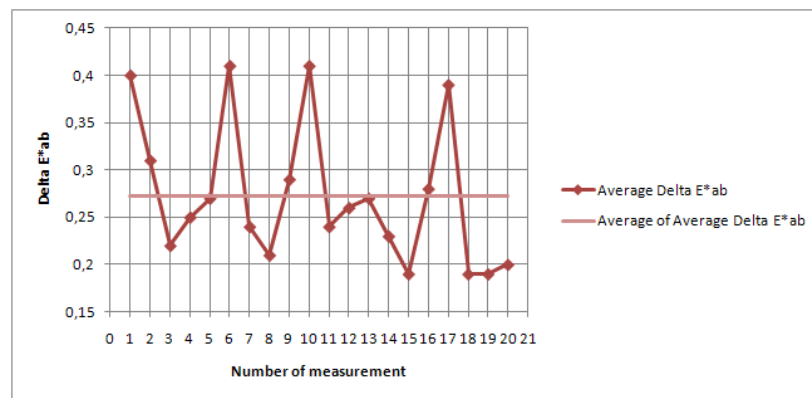
Figure 29: Average ΔE_{ab}^* for 20 measurements with 30 minutes repeatability

The reason of appeared difference for 1st and 15th can be explained as unpredictable small motions of target during measurements by spectrophotometer using strip-mode. Each new time when color chart is measured the robot arm with spectrophotometer moves, and software asked operator to identify corners of chart. Then operator launches process of measuring of chart from software, and robot arm moves instrument strip by strip on scan table. The statically charged scan table holds color target. So micro-displacements of paper take a place during measurements: they happen eventually.

So averaging results of these successive measurements reduces difference between measurements and the variations in 3DLUT transformation which effect on the appearance of reproduced images. But combination slightly different measurements with highly noisy data (as 1th and 15th items of successive measurements) can influence on color conversion rather negative than positive, and artifacts appear.

Measurements with repeatability 30 minutes also slightly differ from each other according to figure 29 except **1st** item of measurement (from figure 70 and 71). Spectral distributions of measurements with repeatability 30 min for J1 color patch almost repeat each other. So this difference is not significant in comparison with previous case.

63
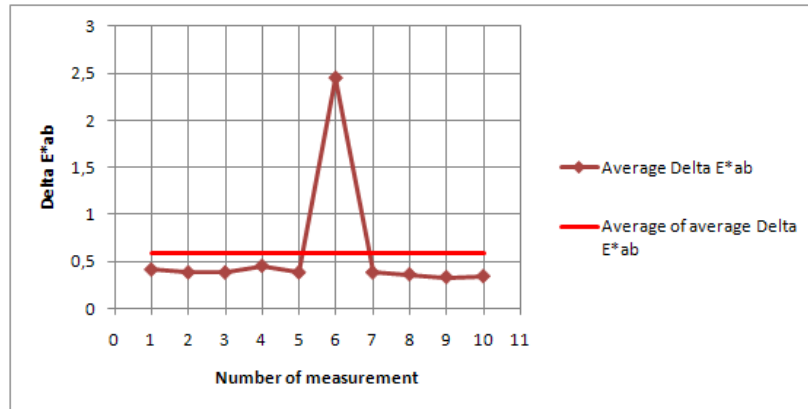
Figure 30: Average ΔE_{ab}^* for 10 measurements with 1 hour repeatability

Maximal ΔE_{ab}^* between averaged of measurements and particular measurement with repeatability 30 minutes higher for **6th** and **17th** items of measurements than for others. Thus measurements for concrete patches were obtained with high level of noise. This is reason for appearing artifacts on particular colors after color conversion.

Similary, measurements of color target with repeatability 1 hour are insignificantly various. Figure 30 shows mean ΔE_{ab}^* between averaged of measurements with repeatability 1 hour and each single measurement. **6th** item of measurements obviously differs from others (on figures 68 and 69 from Appendix D).
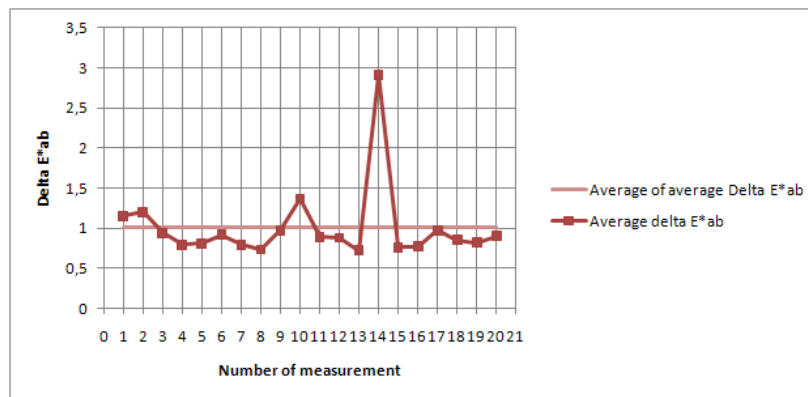
Figure 31: Average ΔE_{ab}^* for 20 substrates measurements

20 substrates measurements were obtained by using color charts consecutively printed on substrates of same paper type. The same analysis as for previous cases were applied for these measurements. As expected measurements should have high variation between each other because every time new printed color chart is measured. An operator has to exchange copies during measurements which also leads to noise appearing. In ideal case printed color charts are supposed to be almost same but limitations of printed process account for appearing distinctions. Average ΔE_{ab}^* and maximal ΔE_{ab}^* between averaged of 20 measurements on different substrates and measurement for particular substrate are presented on figure 31 and in table 29 respectively. **10th** and **14th** items
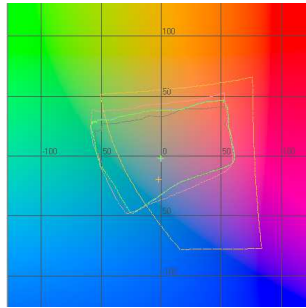
Figure 32: The gamut differences between display and printer profiles, L = 50

are significantly distinct from others measurements. For color patch J1 figures 30 and 67(on area from 400nm - 590nm) show deviation of 10th item from measurements in the set.

For each group of measurements values of mean value of average ΔE^*_{ab} were computed and presented in tables26, 29, 31, 33. Average of average $AvAv\Delta E^*_{ab}$ shows that variation inside set of measurements higher for 20 substrates ($AvAv\Delta E^*_{ab} = 1.007$)and 20 successive ($AvAv\Delta E^*_{ab} = 0.863$) groups and lower for measurements 30 min ($AvAv\Delta E^*_{ab} = 0.2725$) and 1 hour ($AvAv\Delta E^*_{ab} = 0.586$) repeatability groups. For goals of experiment images with different smoothness should be obtained. So profiles with different level of noise in 3DLUTs can be used. The mesurements from groups of repeatability 30 min. and 1 hour are not various very much from each other, and only few of them were used for generating profiles and converting images. So only 45 profiles have been chosen based on: 20 successive measurements, 20 substrates measurements, 6th, 7th, 9th items of measurements with 1 hour repeatability and 16th and 17th items of measurements with 30 min repeatability. These measurements represent variability of printer and operator(noise in measurements). The 'problem' profiles based on 6th item of measurements with 1 hour repeatability, 17th item of measurements with 30 min repeatability, 10th and 14th items of measurements for 20 substrates, and 1st and 15th items of 20 succesive measurements were included. These profiles can provide distortions of colors and respectively smoothness problem on images. So it was decided to include them for estimating effect and getting worst cases of smoothness distortions.

The last important notification is color conversion of images to chosen profiles. For evaluation of smothness processed images will be reproduced on display. For calculating image difference metric and aims of perceptual experiment all reproduced images should be converted from printer RGB back to sRGB because of difference in gamut between printer and display. On figure 32 gamut of representative each group of profiles are presented: blue contour is 16th item of measurement with 30 minutes repeatability profile, orange contour is sRGB display profile, green contour is 7th item of measurements with repeatability 1 hour, yellow contour is 1st item of 20 substrates measurements, and gray countour is 1st item of 20 successive measurements.

6 Evaluation of smoothness of color transformations

6.1 Set of images

The images' set have been designed (on figure 72) based on algorithm proposed by Eric Garcia (implemented in Matlab) and described in paper [10]. The images contain smooth transitions between different colors and appropriate for testing the variations in smoothness.

These images were processed with 45 printer profiles using **Adobe Photoshop CS3 10.0.1** (table 14). Adobe Photoshop function **Convert to profile** converts image from image color space(its embedded profile or current working space in case of untagged image) to any other profile' color space. The images were converted from **sRGB color space** to profiles **printer RGB space**. Perceptual rendering intent have been chosen for preserving the overall image appearance. The Color Management module for mapping the gamut of one color space to the gamut of another is Adobe ACE engine. This CCM provides all necessary conversions needs [64].

Conversion Option	Parameter
Engine	Adobe ACE
Intent	Perceptual

Table 14: Conversion to printer profile parameters

So total number of reproduced experimental test images is 180 = 45x4. Examples of image **Six color balls** converted to different profiles is presented on 73. Thus profiles obtained by various group of measurements affect on quality of this image with different strength. Converted images have different level of smoothness caused by different level of noise in 3DLUTs of profiles. The images samples converted to 7th profile of 20 successive measurements are presented on 74. This figure illustrates that conversion to the same color profile affects on images quality approximately with same magnitude of changes but type of artifacts depend on particular image content.

Name	Size
Four color cubes	800x500
Six color balls	800x533
Six color stripes	512x511
Red and green ball	800x800

Table 15: Experimental images(in format ∗.tif)

67

6.2   Psychophysical experiment

Perceptual experiment were conducted in similar way as in 4.2. Perceptual experiment were conducted in a dark room. So sources of possible light, flare and glance were eliminated using black tablecloth, paper and black screen baffler. The recommended viewing distance by Bhattacharya et al.[65] and [66] is between 50 and 75 cm.

The LCD display DELL 21-inch was used for viewing test images. The display was calibrated and characterized according to ISO3664 [20] which gave a predictive error with a median $\Delta E_{ab} = 0.43$ for the forward characterization and a median $\Delta E_{ab} = 0.97$ for the inverse characterization.

For participating in experiment 20 observers with normal color vision and age from 22 to 37 years were invited. The color-defective (color blind) observers could not correctly perceive colors so they should be eliminated from participating in color visual judgements. Before beginng of experimental session each observer passed Ishihara test on color blindness [67].

The experiment has 3 session, and each session contains 60 test samples comparison. Each observer was asked compare difference in smoothness between original and reproduced images using category scale from 1(perfect match in smoothness) to 5(worse match in smoothness) corresponding to the smoothness level. In instruction it was mention that observer should not look at difference in color, the focus of attention has to be putted to smoothness changes. The meaning of each category are presented in table 16.

Category	Name	Description
1	Perfect match in smoothness	There is no difference in smoothness
2	Slightly different in smoothness	Noticeable difference in smoothness
3	Acceptable match in smoothness	Tolerable differences in smoothness
4	Moderate match in smoothness	Quite essential difference in smoothness
5	Worse match in smoothness	Large differences in smoothness

Table 16: Description of judgements categories

For demonstrating images to observers experiment's tool was designed in MatlabR2009b (on figure 75). The background for images have chosen as neutral gray. Neutral background was shown between each pair of images for removing eye memory effect. The pairs of different images were randomly mixed.

6.3   Visual judgements analysis

Observers evaluated smoothneess using category scale from perfect match in smoothness(1) to worse match in smoothness(5). Category scaling is related to indirect scaling were observers are asked to make simple judgements about objects properties (grouping, sorting and ordering). Then numerical scale can be derived using statistics on these judgements.

68

There are few notations of profiles and images which used for convenience and simplicity of data presentation. The ICC profiles obtained from 20 successive measurements are called **20 succesive profiles**, from measurements of 20 substrates - **20 substrates profiles** , from measurements with repeatability 30 min and 1 hour - **30 min and 1 hour profiles**. For convinience each reproduction got number (table 17). Each original image has 45 reproductions: 1-20 obtained by conversion to 20 successive profiles, 21-40 - by conversion to 20 substrates profiles, 41-45 - by conversion to 5 profiles presented 30 min and 1 hour repeatability measuremets.

Image	Abbreviation	Number
Four color cubes	Image 1	1-45
Six color balls	Image 2	46-90
Six color stripes	Image 3	90-135
Red and green ball	Image 4	136-180

Table 17: Description of images' abbrevations

MOSs presents average categories for each image derived from 20 observations (figure 33). Figure 76 (Appendix F) shows that MOSs of each image are higher for images converted 20 successive profiles and 30 min and 1 hour profiles, and lower scores for images converted to 20 substrates profiles. It means that for reprodutions obtained by 20 substrates profiles perform better results in smoothness than image reproductions obtained by 20 successive profiles and 30 min and 1 hour repeatability. On this figure it can be noticed that for Image 1 and Image 2 difference in judgements between groups of profiles significant, but for Image 3 and Image 4 difference between groups of profiles is not large. 95 % confidence intervals of visual judgements show that judgements for Image 3 and Image 4 vary greatly than for Image 1 and Image 2. It can be found that for 30th, 34th items (10th and 14th) in 20 substrates group MOSs and 43th item from 30 min and 1 hour group are higher than for others profiles in these groups. In this case visual judgements detect 'problem' profiles.

In project experiment numbers from 1 to 5 associated with level of smoothness difference. The categories assumed to be linearly and equally spaced. The Torgerson's law of categorical judgement is applied to find the true shape and spacing of the scale ([51],[68]). For determining categories' boundaries by Torgerson's law follwoing steps can be considered according to [51]:

1. Calculating frequencies how many times image were placed into each category for all observervations;

2. Calculating cumulative frequencies and proportions for each image;

3. Calculating z-score using inverse of the cumulative standard normal distribution function (cumulative proportions have to be between 0 and 1);

4. Estimation boundaries between categories using the z-scores and the law of categorical judgement.
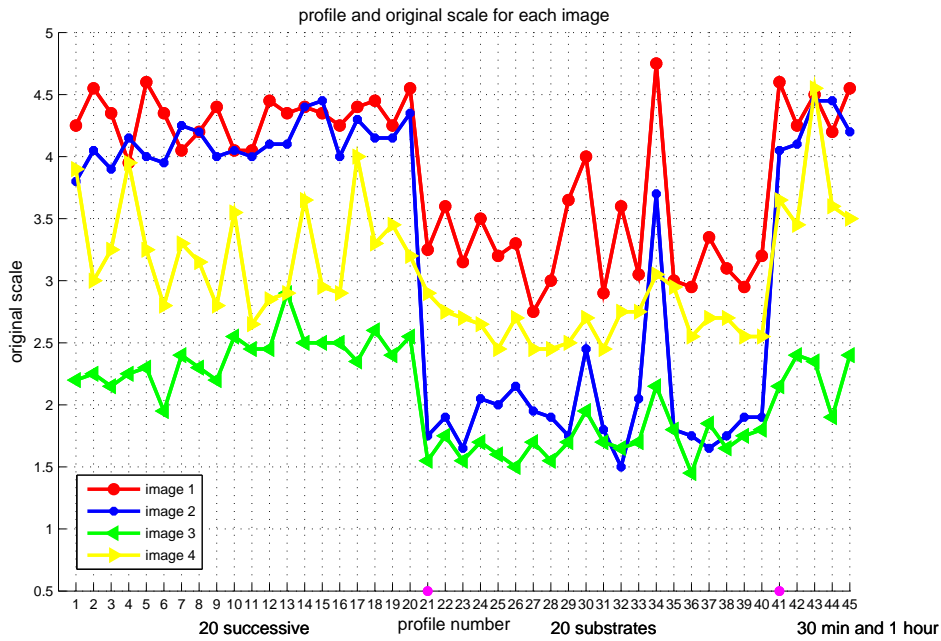
Figure 33: MOSs of four images

On the table 35 (Appendix F) frequencies of estimation images into categories by observers were computed.Then final z-scores for all images were found following to described algorithm. Each concreate evaluated image reproduction was obtained by convertion to profile. So summary statistic can be found for each profile. In the same way frequencies(how many times profile were placed into category by observers) and z-scores for profiles were calculated (table 36, Appendix F).

W/M	M/A	A/S	S/P
Images			
-1.20206	-0.3848	0.2620	1.2070
Profiles			
-0.8509	-0.2230	0.2035	0.7974

Table 18: New scales for images and profiles

New scales allow to identify real bourders between categories and classify each image or profile to particular category of predicted smoothness.The abbreviation W/M,M/A,A/S,S/P in table 18 and means that category boundary between worse match in smoothness(W) and moderate difference in smoothness(M), moderate match in smoothness(M) and acceptable match in smoothness(A), acceptable match in smoothness(A) and slightly different(S), slightly different(S) and perfect match(P). Smaller z-score tells that image reproduction have worst match with original image smoothness.

Figure 33 shows mean opinion score for each image, and figure 34 shows z-score distribution for each image. From these figures it can be seen explicitly that z-scores
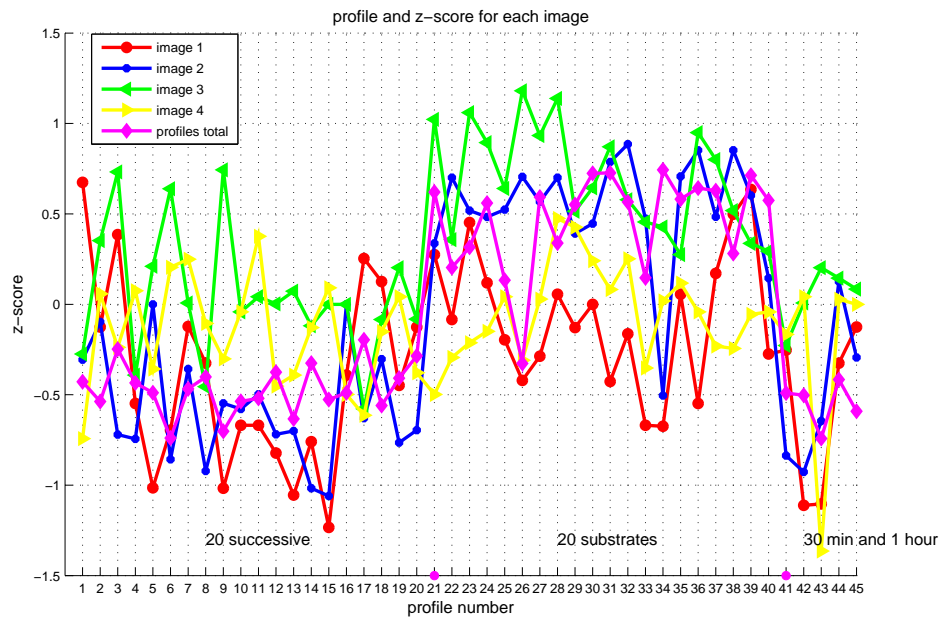
Figure 34: Z-score score for each image related to profile

and mean opinion scores distributions are inversely proportional. On figure 34 z-scores curves of different images for same set of profiles are quiet similar. Image 3 and Image 4 have diffused curve because of noisy visual judgement. Image 2 and Image 1 are almost similar with z-scores curve corresponding to particular profile. So there is dependence between profile and image reproduction visual assessment by observer. For checking and confirming this statement Chi-square test were performed.

Image reproduction	Profile	Obser 1 judgements	. . .	Obser20 judgements
Img1	1 profile	4	. . .	4
Img2	2 profile	5	. . .	4
Img3	3 profile	4	. . .	4
Img4	4 profile	4	. . .	5
. . .	. . .	. . .	. . .	. . .
Img45	45 profile	5	. . .	4
Img46	1 profile	3	. . .	2
Img47	2 profile	4	. . .	4
Img48	3 profile	4	. . .	3
Img49	4 profile	4	. . .	3
. . .	. . .	. . .	. . .	. . .
Img90	45 profile	4	. . .	3
. . .	. . .	. . .	. . .	. . .

Table 19: Grouping images according to profile

Chi-square Pearson criterion is common test for significance of the relationships between categorical variables. In this case observers judgements for image reproductions can be grouped according to profile which was used for obtaining this reproduction

71

(example in table 19). But each image belongs to particular smoothness difference category chosen by observer then frequency of hit each profile to categories can be determined. So two grouping variables are defined: **profile** and **category**(example in table 20). Null hypothesis H0 tells that there is no relationship between profile and chosen by observer category for evaluating smoothness difference. If there is no dependency between these variables, then approximately an equal number of choises of categories for particular by observer should be expected. So Chi-square test becomes increasingly significant as the numbers deviate from this expected pattern.

Profile	Obser1				
	Category 1	Category 2	Category 3	Category 4	Category 5
1 profile	0	1	1	1	1
2 profile	1	0	1	1	1
3 profile	0	0	1	2	1
4 profile	0	0	1	3	0
. . .	. . .	. . .	. . .	. . .	. . .
45 profile	0	1	0	2	1
All groups	28	55	37	48	12

Table 20: Crosstabulation example for 1st observer

Chi-square Pearson criterion were defined for each observer using statistical package STATISTICA 7.0. For small frequencies Yates' correction for continuity is reccomended for computing Chi-squre. Following formula presents Chi-square criterion for crosstable 2x2 (formula 6.1). Statistical packages have fucntions for defining Chi-square criterion for tables of large sizes. Results for each crosstable is presented in table 37(Appendix F) . For 90% of observers H0 was rejected. So it means that there is dependence between profile and observer categorical judgement.

$$\chi^2 = \sum_{i}^{2} \sum_{j}^{2} \frac{(O_{ij} - E_{ij} - 0.5)^2}{E_{ij}} \qquad (6.1)$$

Figures 35 and 36 present z-scores distrubutions for each image (1-4 on axis Image) and total z-score distribution for all profiles (corresponding to 0 on axis Image) shows categories of each reproduction based on new scale for z-score. For 20 successive and 30 min and 1 hour profiles image reproductions mostly estimated as having moderate match in smoothness compare with original image. Image reproductions for 20 substrates profiles are slightly different from original in most cases. Total statistic about percentage of profiles associated with category presented on pie-plot 81, Appendix F. It can be noticed that image reproductions of 30th, 34th ('problem') profiles belong to category slightly different compare with original. In this case main role plays difference in visual judgements for image reproductions of these profiles. The reproductions of Image 2, Image 3 and Image 4 were estimated as obtained by profiles which provide relatively good smoothness compare with original reproductions. From another side, 30th and 34th profiles perform relatively higher MOSs in group of 20 substrates profiles for each particular image (from figure 33). During experiment many of observers told that reproductions of Image 3 and Image 4 are difficult for evaluating smoothness difference. Second reason is
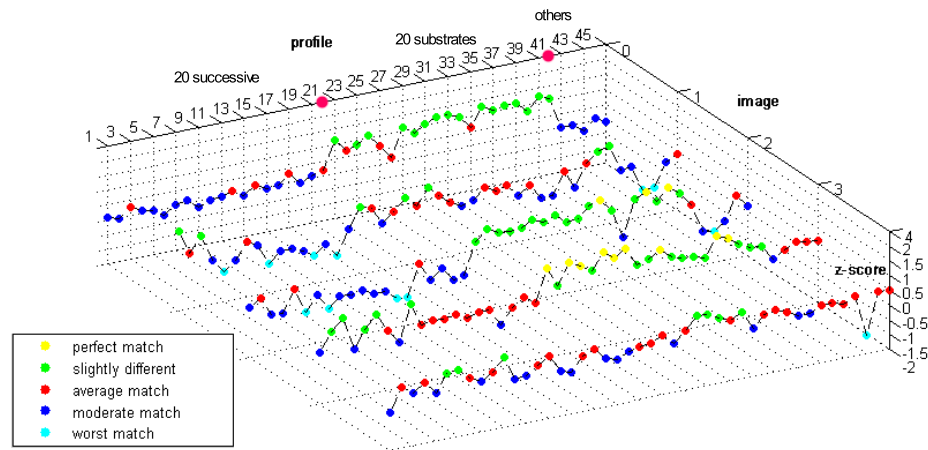
Figure 35: Images, z-scores, profiles diagramma

that profile can provide smooth color conversion for one color transition and unsmooth color transition for another. It depends on which grid points of 3LUT were affected by noise more. So color transformation by profile depends on content of image. In this case if profile provides worse color conversion for some images and smooth color conversion for others then this it can not be considered as profile provided really good smooth color transition.

Reproductions of images in caregories are presented detaily on figures 77, 78, 79 and 80 in Appendix F. Profiles categories are presented on the figure 36. The bourders between categories are presented by dashed purple lines. Bars lengths indicate z-scores magnitudes. Obviously, z-score higher for reproductions of Image 3 than for reproductions of other images applying same profiles 79. The reason hides in content of image. Image 3 includes 6 color stripes with very subtle color transitions on white background. Distortions (banding) on some reproductions are not easily detected on such background. Differences would be explicit if attention is more concentrated on reproductions. It happens very often that observer became tired during experement, and choses category at first sight. For reproductions of Image 1 opposite situation takes place: there are more image reproducions which were estimated as having worst and moderate match with original 77.This image is sensible to color conversions because it contains many complex color transitions.

On figure 77 reproductions of Image 2 are devided on 3 explicit groups depending on profiles applied for color conversion: 20 successive, 20 substrates and 30 min and 1 hour. The images in first group were estimated as moderate as having worse match in smoothness compare with original, 20 substrates - as slightly different from original, 30 min and 1 hour - as worst and moderate much in smoothness. But it can be noticed from figures 77 - 80 that image reproductions obtained by applied 20 successive profiles performs better results in smoothness compare with image reproductions obatined by applied 20 successive profiles and 30 min and 1 hour repeatability. Total z-scores overall
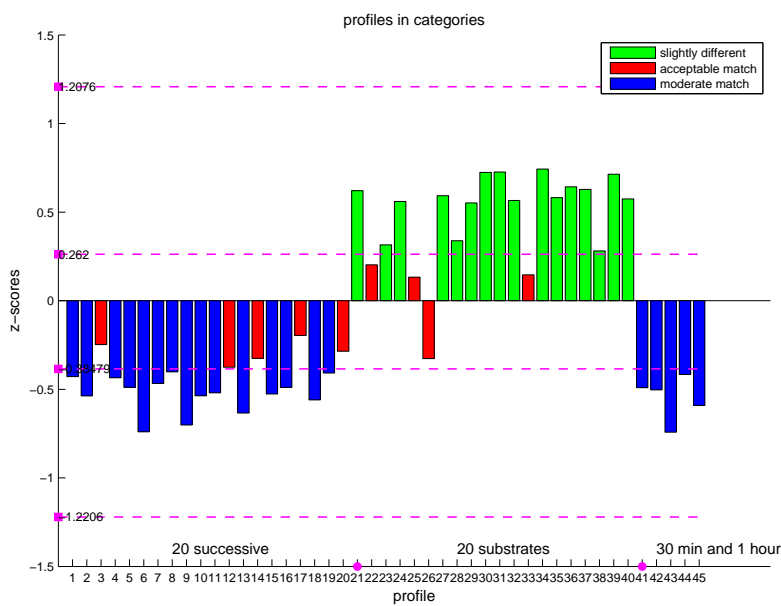
Figure 36: Profiles in categories

images (figure 36) show common categories for profiles.

6.4 Metrics and algorithms implementation

In this project two categoris of metrics were considered:

- smoothness metrics for color transforms (Phil Green metric (2008), Youn Kim et al.(2010) metric and proposed in this project method of color planes) which based on estimating 3DLUT-based transformation smoothness properties;

- image difference metrics (SSIM, GSSIM, pixel-wise color difference CIELAB, sCIELAB, Adaptive bilateral filter, Edge simularity, Structural content) which are full-reference metrics and predict difference between two images.

6.4.1 Proposed method for smoothness evaluation

The idea of proposed method is based on consideration smooth CLUT in ICC profile as main factor for achieving smooth color transitions. J.Morovic [9] determines smooth transition as one where the slopes of the piecewise linear function defined by LUT vary monotonically (change keeps getting more or less steep across the entire tranjectory).

Generated profiles contains large 3DLUTs which have more nodes in grid than number of patches in color chart. The additional nodes are yielded by interpolation color of patches in chart during ICC profile generation. In ICC profiles tables for conversion from device color space to PCS are packed as 4 dimensional: three dimensional device color space coordinates and corresponding to them three dimensional PCS coordinates.

74

As example, extracted from ICC profile (AToB# table) CLUT has size and dimensionality 33x33x33x3. First three coordinates means device RGB grid point coordinates which contains corresponding to it L^*, a^*, b^* values: CLUTdRGB(1,1,1,:) = [0, 0, 0] and corresponding to it CLUTLAB(1,1,1,:) = [0, 0.0020, −0.3770]. CLUTdRGB is not presented in AToB# table because its values can be generated trough interval. CLUTLAB extracted from 1st ICC profiles of group obtained by 20 successive measurements and generated CLUTdRGB are depicted on figure 82 (Appendix G) in three dimensional space as grids of points. In CLURdRGB grid points are equally spaced trough interval. Entire CLUTdRGB cube can devided on planes where values of two primaries are constant and value of another primary changes though interval. Total number of these plains equals to step. For CLUT 33x33x33x3 number of planes is 33. The devision of CLUT on planes is implemented in three dimensions: B changes, R and G are constant; G changes, R and B are constant; R changes, G and B are constant. CLUTLAB presents 'irregular parrallelepiped' of measured and interpolated points corresponding to device RGB uniformly-spaced CLUTdRGB 82.

a) RGB color planes;

b) Corresponding $L^*a^*b^*$ color planes.
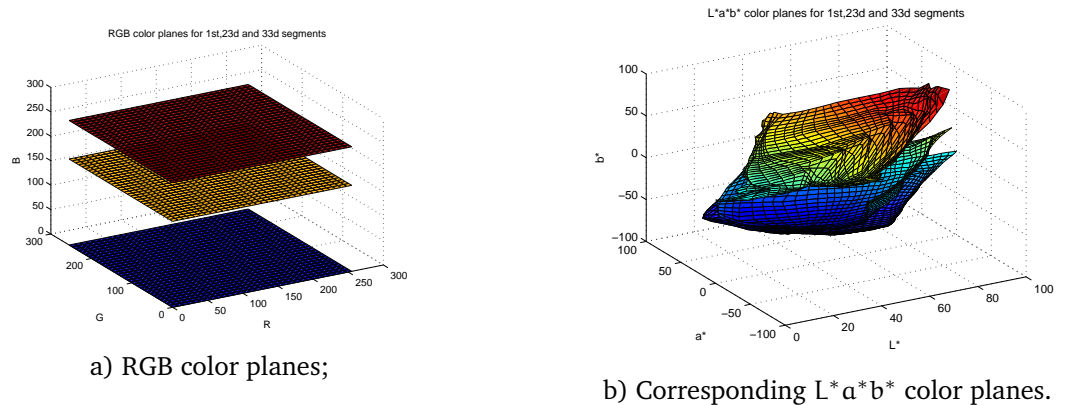
Figure 37: Color planes in 3DLUT (AToB# table) from ICC profile

Each grid point of CLUTdRGB' color plane has corresponding to it CLUTLAB' grid point. Thus every device RGB color plane has corressponding to it $L^*a^*b^*$ color plane (on figure 37). RGB color plane can be considered as set of horizontal and vertical uniform color ramps in device color space. T.Olson [6] gave definition to digital uniform ramp: an uniform ramp properly (linearly) interpolates its endpoints and contains equally spaced in the ramp's source color space. The ramp should be straight containing no bumps that take it to the side of its interpolating. $L^*a^*b^*$ color ramp corresponds for each horizontal and vertical RGB color ramp. The color conversion of this uniform ramp from RGB color space to PCS and from PCS back to RGB should have as ideal result uniform ramp in RGB space. RGB vertical and horizontal color ramps have corresponding to them values in $L^*a^*b^*$ color space. For simplicity they are called $L^*a^*b^*$ ramps. In ideal case $L^*a^*b^*$ values for RGB color ramp should monotonically changes approximately through same interval. The abrupt changes of $L^*a^*b^*$ values on areas of ramp tells about high noise appeared during measurements and affected on color conversion.

In this project RGB color planes are considered in 1 direction when R and G are
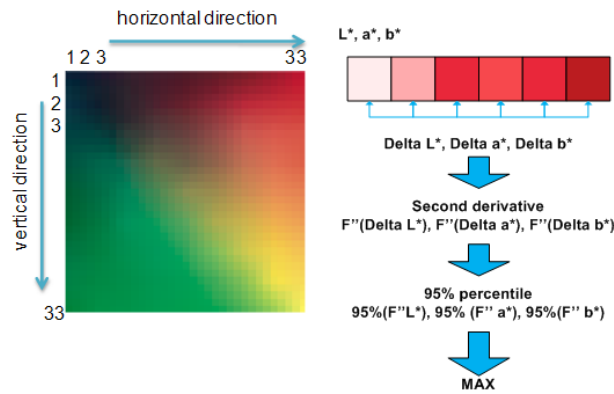
Figure 38: Schematic presentation of computation proposed algorithm

constant and B changes. On figure 38 example of device RGB color plane converted to $L^*a^*b^*$ color space and then again converted to sRGB for displaying it is presented. In this project ICC profiles with 3DLUTs 33x33x33 are generated, and thus each color plane has 33 horizontal and vertical ramps. Different color planes are presented on figures 84,86,88 and 90 (Appendix G). The L^*, a^*, b^* values (or CLUTLAB entries) of horizontal and vertical RGB ramps were plotted on figures 83,85,87 and 89 (Appendix G). Each ramp has 33 steps that equals to interval of CLUTLAB. L^*, a^* and b^* increases or decreases monotonically from step to step. In some parts distributions of L^*, a^* and b^* have abrupt changes.

Following to algorithm of P.Green, variations of L^*, a^* and b^* in each ramp can be estimated as differences between adjusted points in ramp (schematically shown on figure 38) and second derivatives from these differences. For presenting common statistic about variations on each ramp 95 % percentile was used. For instanse, 95 percentile from set of values $(9, 13, 7, 6, 9, 11)$ is 12.5 that shows 95% of values are smaller than 12.5. So 95% precentile shows how high variations of L^*, a^* and b^* of ramp and computed from second dervatives of $\Delta L^*, \Delta a^*, \Delta b^*$ between adjusted points. In this case two variants of method can be used computing only ΔL^* or computing $\Delta L^*, \Delta a^*, \Delta b^*$. According to previous studies [6], [9] reason of appearing unsmoothness underlies in abrupt changes in L^* luminance channel. Consideration of changes in chrominace can be disputed because then it is hard to distinct between estimation of color fidelity and smoothness itself. In this project $\Delta a^*, \Delta b^*$ are used for computing algorithm because of they are not constant in color ramps and changes. Another argument for accounting chrominance changes is that appearing inconsistent or wrong colors in color transition means smoothness distortions (as it shows perceptual experiment). On figures 83,85,87 and 89 (Appendix G) b) second derivative from ΔL^*, Δa^* and Δb^* for different vertical ramps of color planes are presented. Channel L^* presents high variation compare with others channels for 8th vertical ramp of 8th color plane. From figure 85 channel a^* significantly varies compare with other channels (16 th vertical ramp for 16th color plane). From figure 87 channel b^* changes much in comparison with L^* and a^* (23 th vertical ramp for 23th color plane).

Then higher varition among channels should be derived by finding maximum bet-
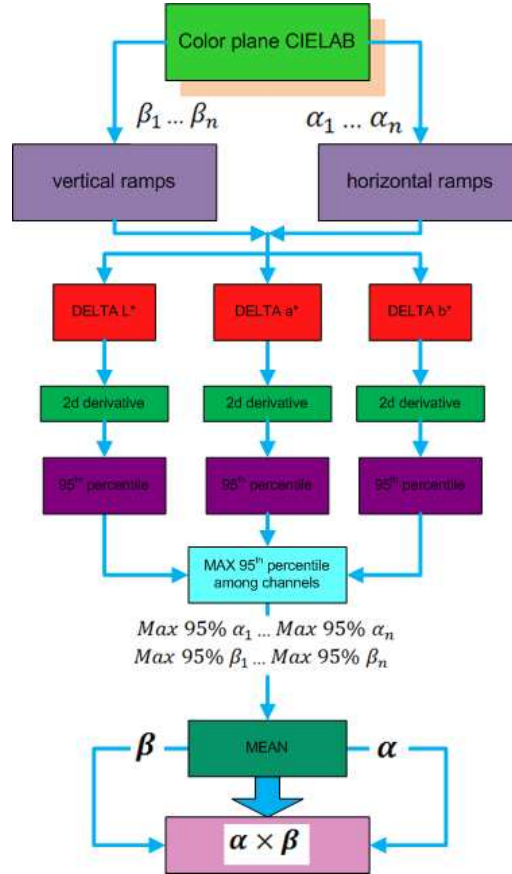
Figure 39: Workflow of proposed method

ween 95 % percentiles of each channel. Then simple statistic were applied for obtaining resulting value of algorithm for color plane. The average of maximal 95 % percentiles should be found between horizontal α and vertical β ramps. The horizontal and vertical components are multiplied for obtaining results: $\alpha x \beta$. For several planes algorithm value is computed as (N is number of concidered planes):

$$PM = \frac{\sum_{j=1}^{N} \alpha_j \cdot \beta_j}{N}. \tag{6.2}$$

So this values shows predicted by algorithm value of smoothness for particular profile. The larger value of this metric is the lower percieved smoothness is. The workflow of proposed algorithm is presented on figure 39. This algorithm was implemented in Mat-labR2009b environment and called as metric of color planes. For calculating metric of color planes 45 experimental ICC profiles (AToB0 tables -perceptual rendering intent) were used. The proposed algorithm does not require color ramps, and special optimization component. It tests many different RGB color ramps on smoothness and consequently provides more reliable prediction.

6.4.2   Phil Green and Youn Kim et al. metrics

Proposed by Youn Kim et al. metric can not be easily used for any color ramp because experiment includes optimization with visual judgement data and deriving weights for tone-clipping estimation of each particular ramp. So the decision was to compute this metric for Blue Sky ramp which described in paper [8]. This ramp contains 100 steps, and was generated with beginning from $LAB = [71, -6, -18]$ with fixed chrominance. The $L^*a^*b^*$ values of ramp have been taken in gamut.

Figure 40: Blue sky ramp

The ramps were printed and measured by spectrophotometer for computing Youn Kim et al. metric values. In this project Blue sky ramp($L^*a^*b^*$ values) was converted to profile using BToA0 conversion (perceptual rendering intent) for simulating printing process. Then for presenting color of ramps in device-independent space the Blue sky ramp were converted back to CIELAB color space using AToB0 profile conversion. Then metric were calculated for derived $L^*a^*b^*$ values of Blue sky ramp.

For computing Phil Green metric Blue sky ramp also was used, and same workflow of color conversion as for Youn Kim et al. metric was applied.

6.4.3   Image difference metrics

According to [39] nowadays, there are more than 100 full-reference image quality metrics. For evaluating smoothness differences between reference and reproduced image following metric-candidates have been chosen: **SSIM**, **GSSIM**, **color difference CIELAB**, **sCIELAB**, **Adaptive bilateral filter**, **Edge simularity**, **Structural content**. The reasons of chosing these metric are presented in table 21.

The metrics were computed between original images (before conversion to profile) and repoduced image (converted to profile). Analysis of printer measurements and profiles (subsection 5.4) shows that it is necessary to convert reproduced image back from printer RGB color space to sRGB workspace. The metrics were implemented according to original papers. Matlab codes of sCIELAB, SSIM and Adaptive bilateral filter were available on-line or given by authors of these metrics. Structural content, Edge simularity, SSIM and GSSIM were computed only for luminance channel of images because of requirements of algorithms.

6.5   Analysis and discussions of metrics performance

The metric of color planes was computed in two ways (as it was discussed before): only for luminance channel L^* (abbreviation **PM**L^*) and for three channels L^*, a^*, b^*(abbreviation

Metric	Reason
ΔE^*_{ab}	Euclidian distance between two colors in perceptual uniform color space. The common and widely used metric in industry and other areas.
SSIM (Z.Wang, A.C.Bovik)	Metric for evaluating structural changes. Smoothness distortions are often presented as changes in images structural information(contours, banding).
GSSIM (Chen et al.)	Extension of SSIM for gradients. Changes in smoothness are related to gradient changes.
sCIELAB (X.Zhang, B.A.Wandel)	Spatial extension of ΔE^*_{ab} simulating ability of HVS blurring images. Widely used metric for predicting image quality difference.
Adaptive bilateral filter (Z.Wang)	This metric is aimed to in good way simulate HSV(blurring image with preserving structural information).
Structural content (E.Silva,T.Kratochvil)	Predicting structural changes which are related to changes in smoothness.
Edge simularity metric	Contours and banding effects appear on image changed structure and edges of objects of this image.

Table 21: Full-reference metrics-candidates for evaluating smoothness

PM$L^*a^*b^*$). The Phil Green metric (**PG**), Youn Kim et al. metric (**KM**) and proposed algorithm were calculated for 45 profiles, and results are presented in table 39 Appendix G. The Pearson correlation between z-scores and values predicted by metrics were calculated. The Pearson correlation is defined on intervals [-1,0] or [0,1] where 0 means that there is no correlation between variables and 1 means absolut correlation. Results are presented in table 22 and on figure 41. 95 % confidence interval is computed $95\%CI = 1.96/\sqrt{2 \cdot N} = 1.96/\sqrt{2 \cdot 180 \cdot 20} = 0.02$ for 180 images reproductions and 20 observations. Blue sky ramp was used for computing value of metrics KM and PG. In this analysis total z-scores obtained from psychophysical experiments with images reproduction were used. Because authors of PG and KM metrics are asserted that these metrics can predict how smooth or unsmooth particular color transform(profile) using color ramp. Total z-scores of profiles reflects visual assesments of observers regarding to profiles. Thus PG and KM metrics values can be compared with total z-scores.

Metric	Pearson corr.	Oultliers	Pearson corr. without outliers
Phil Green PG	-0.50	2(20,41)	-0.57
Kim et al. KM	-0.46	-	-
Color planes PM L^*	-0.62	1(30)	-0.85
Color planes PM L^*, a^*, b^*	0.05	1(30)	-0.87

Table 22: Pearson correlation between PG,KM, PM L^* and PML^*, a^*, b^*

Outlier for metrics PM L^* and PM L^*, a^*, b^* are 'problem' profile - 30th profile (10th profile of 20 substrates profiles). The image reproductions of Image 2,Image 3 and Image 4 obtained by convertion to this profile were estimated as having slight and acceptable difference with original image among all observations. But reproduction of Image 4 converted to 30th profile was putted in category worse match in smoothness in compari-
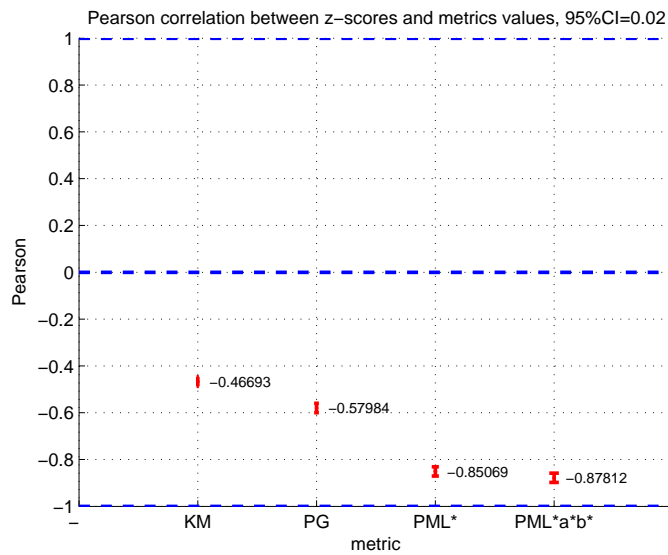
Figure 41: Pearson correlation between z-scores and metrics

son with original image overall observers. Total z-score for 30th profile reflects common statistic among observers that this profile provides color transformation with smooth output result. But profile is considered as profile providing smooth color transformations in case if for any image content it gave output reproduction which have acceptable visual difference in smoothness with original image. Profile 30th does not provide smooth color transitions for Image 1, thereby exclusion this profile and considering it as outlier is reasonable. For PG metric outliers are 20th and 41stprofiles. These profiles got meaningfully different values of PG metric than others. These profiles were not considered as 'problem' profiles. For computing PG metric Blue sky ramp was used. So smoothness of blue transition was only tested. Conversion to 20th and 41st profiles gave as output result not smooth color transitions of blue. Image 1 also contains blue color transitions, its reproductions obtained by 20th and 41st profiles were considered as moderate level of smoothness distortions. But these profiles provides better color conversion for other images (Image 3 and Image 4).

As shown figure 42 proposed metrics of color planes PM L^* and PM L^*, a^*, b^* performs best correlation with visual judgements. From scatterplots on figure 42 values of KM metric are highly dispersed, and have low correlation with z-scores. The reason of it is that algorithm was not repeated completely same as in original paper, because authors of metric applied optimization metric values with visual data. PG performs weak correlation with visual data because ICC profiles were not designed in case of this project, and visual data is real and raw. On scatterplots of PM L^* and L^*, a^*, b^* versus z-score profiles obtained by measuring 20 substrates have lower values of metric that profiles obtained from measuring 20 substrates z-score and PM values comparing with profiles obtained by 20 successive measurements. So these results are similar to previous analysis of MOSs for images (33). PM L^*, a^*, b^* performs slightly higher correlation than PM L^*.

Figure 43 presents distribution values of PM L* and PM L*, a*, b* metrics for each profile (red line). Distribution of z-score is inversely proportional to metrics distribution. It is obviously from plots that PM L* and PM L*, a*, b* metrics detect 'problem' profiles: 15th (20 successive profiles), 30th (10th for 20 substrates profiles), 34th (14th for 20 substrates profiles) and 43d(6th for 1 hour repeatability profiles). From figures it can be seen that distributions of z-score and PM L* and PM L*, a*, b* metrics are similar. 30th profile was not shown on plot of metric PM L*, a*, b* (dotted black line) because it has greatly high value compared with others (over 50). 30th 'problem' profile for some color provides totally wrong conversion. Thus PM L* and PM L*, a*, b* performs realtively good results for evaluating how smoothness of color transformation.

For evaluating percieved smoothness image difference and quality metrics can be used as effective instrument for predicting difference between reference and reproduced image. These metrics can be used in case when there is no information about profile or color conversion which processed image, and reference image is available. Metric-candidates have following abrevations color difference ΔE^*_{ab}, Adaptive bilateral filter **ABF**, Gradient Structural Similarity Index metric **GSSIM**, Structural Similarity Index metric **SSIM**, spatial CIELAB **sCIELAB**, EdgeSimularity **EdgeSim** and Structural content **SC**. The computed values of metrics are presented in table 38 Appendix G. Pearson correlations between values predicted by metrics and z-scores(visual judgements assessment) for each 45 reproductions of particular image were found. The results are presented in table 23.

Metric	Image 1	Image 2	Image 3	Image 4
ΔE^*_{ab}	-0.3854	-0.7324	-0.5822	-0.1542
Adaptive bilateral filter(ABF)	-0.3839	-0.6929	-0.5729	-0.1418
GSSIM	0.4561	0.7040	0.5346	0.2538
SSIM	0.4471	0.4918	0.2260	0.3538
sCIELAB	-0.3809	-0.7801	-0.6461	-0.1200
EdgeSim	-0.2925	-0.4518	-0.5437	-0.1503
SC	0.4056	0.7773	0.6477	0.3075

Table 23: Pearson correlation image difference metrics and z-scores

As shown on the plots of figure 44 all metric perform relatively low correlation for Image 1 and Image 4 because visual esteems higly vary for these images as it was discussed before. Images 2 and 3 has z-scores distributions very close to total z-scores for all profiles 35. So attention was focused on correlation z-scores for 45 reproduction of Image 2. Realtively high Pearson correlations are found between sCIELAB, SC and GSSIM metrics and z-scores for each image figure 44. ΔE^*_{ab} performs high correlation with visual data. It means that variation of color is also important in smoothness evaluation, and it is hard to separate changes in color and changes in smoothness on image. SC and sCIELAB presents approximatelly same correlation. Pearson correlation between GSSIM and z-score slightly lower for Image 1 than for SC and sCIELAB but relatively higher for Image 1 and Image 4.

a)z-scores versus PG metric;

b)z-scores versus PG metric without outliers;

c)z-scores versus PM L* metric;

d)z-scores versus PM L* without outliers;

e)z-scores versus PM L*, a*, b* without outliers;

f)z-scores versus KM metric.
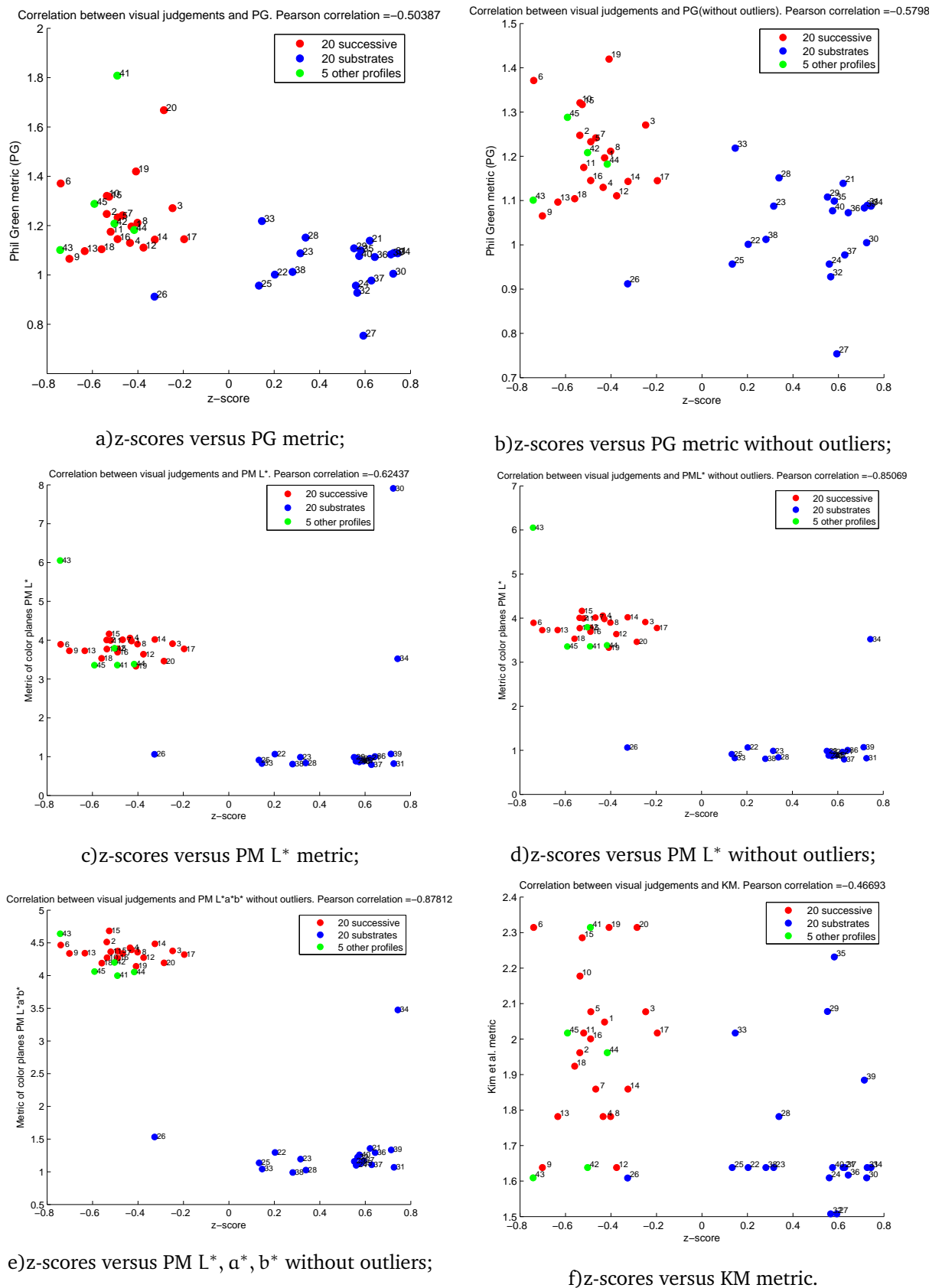
Figure 42: Correlation between z-score and metrics values
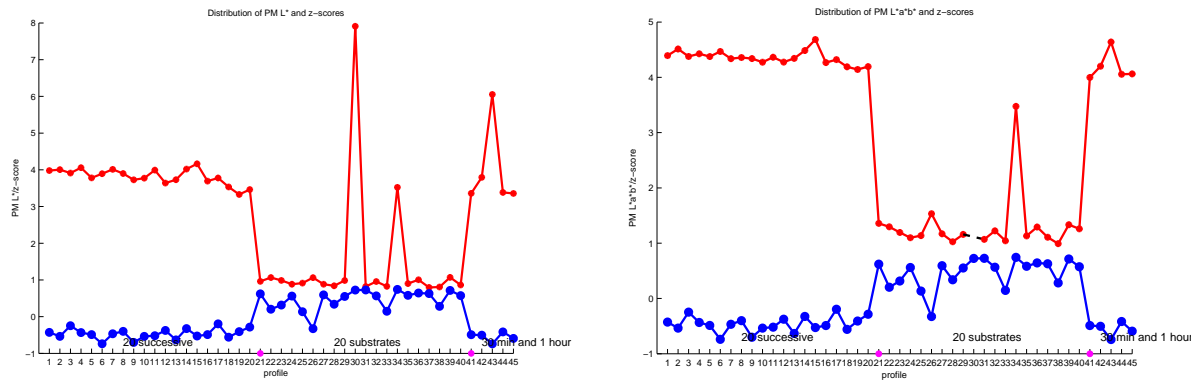
a)PM L* of profiles(red) and z-score(blue); b)PM L*, a*, b* of profiles(red) and z-scores(blue);

Figure 43: Distribution PM L* and PM L*, a*, b* functions in comparison with z-score
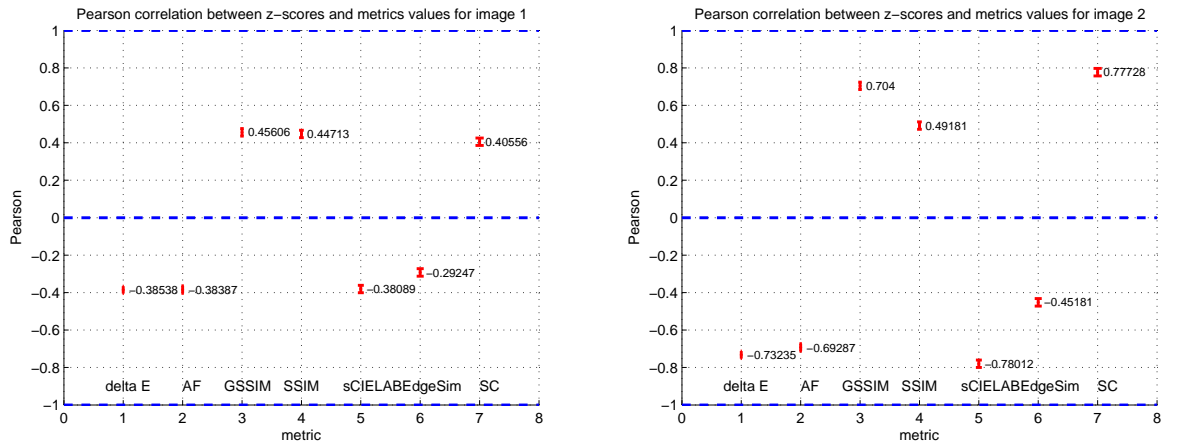
a)for 45 reproductions of image 1;

b)for 45 reproductions of image 2;
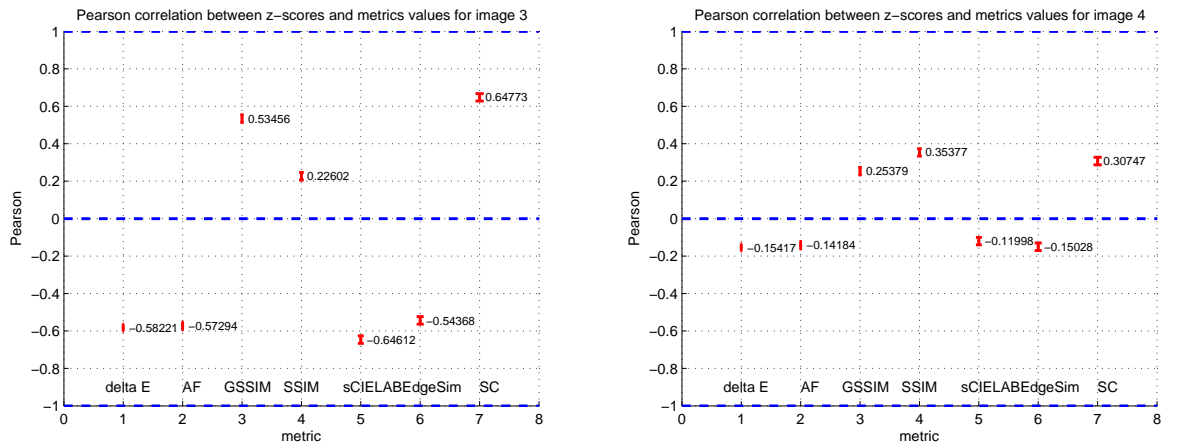
c)for 45 reproductions of image 3;

d)for 45 reproductions of image 4.

Figure 44: Pearson correlation between z-score and ΔE_{ab}^*,ABF,GSSIM,SSIM,sCIELAB,EdgeSim,SC 95%CI=0.02)

Scatterplots of metrics values versus z-score 92, 94, 96 Appendix G for Image 2 and Image 3 two groups of image reproductions can be defined: image reproductions of 20 successive profiles and 30 min and 1 hour profiles and image reproductions of 20 substrates profiles. Image 2 and 3 reproductions obtained by 20 substrates profiles and 30 min and 1 hour repeatability (SC and GSSIM are closely to 1, sCIELAB is lower) perform better results in smoothness than image reproductions obtained by 20 successive measurements. The distributions of metric values for 45 reproductions of each image in comparison with z-scores are presented on figures 93, 95 and 97 Appendix G. SC values are lower for reproductions of Image 1, Image 2, Image 3 comparing with other profiles in groups obtained by conversion of original images to 'problem' profiles (15th, 30th, 34th and 43th). 34th problem profile performs even better output conversion results compare with others for reproductions of Image 4 according to SC values and z-scores. In general SC distribution curve for reproductions of different images is similar to z-score. sCIELAB values of Image 1, Image 2 and Image 3 reproductions indicates 'problem' profiles: they got quite distinct value of sCIELAB compare with other profiles in groups. But Image 3 reproduction obtained by 34th profile got low sCIELAB and high z-score. Analogous, GSSIM detects 'problem' profile for Image 1, 2 and 3 reproductions and performs lower values for them inside each profiles' group. But it can be noticed that Image 4 reproduction obtained by 34th profile also got low GSSIM value. According to z-score for this image reproduction in comparison with original the difference in smoothness is not high. sCIELAB metric algorithm applies blurring of image for simulating HVS and gave results quite close to visual judgements. SC metric computes common statistic of structure changes overall image. GSSIM specially designed to predict changes in gradients of images. Image 3 reproduction by 34th profile has slight smoothness changes which are blurred by HVS, and observer is not able to detect or need more attention and time for adapting vision to detect them. So in this case GSSIM fair enough predicts that image reproduction have slight or acceptable differences in smoothness comparing with original.

The illustration for previous discussions is presented on figure 45 where reproductions of Image 2 obtained by converting to different proiles. SC and sCIELAB are higher for reproduction obtained by 34th profile (or 14th item of 20 subtsrates profiles on figure) in comparison with reproduction obtained by 30th profile (or 10th item of 20 substrates profiles). On first one it can be noticed appearing wrong colors in the middle of color transition gray), and reproduction by 34th profile have more smoothness distortions in comparison with reproduction by 30th profile at first sight. GSSIM value for reproduction by 34th profile is lower than for reproduction by 30th profile. In other case SC, sCIELAB and GSSIM provides quiet reasonable and consistent results for other reproductions. The image reproduction by 43d profile (or 6th item 1 hour repeatability) got worst match in smoothness comparing with original according to GSSIM,sCIELAB and SC.

Concidered image difference metrics can only evaluate result of color transformation applied to **concrete image** and define difference in smoothness comparing with reference image. But it is not correct to conclude that color transformation give smooth or unsmooth output result. Figure 46 shows same color transformation (30th profile or 10th item of 20 substraes profiles) gave distinct output results on images with different content. Reproduction of Image 2 and Image 4 are relatively smooth but reproductions

10th item 20 successive profile
PML*=3.7730;
PML*a*b*=4.2733;
GSSIM=0.9509;
sCIELAB=0.9352;
SC=0.9725

15th item 20 successive profile
PML*=4.1631;
PML*a*b*=4.6839;
GSSIM=0.9492;
sCIELAB=0.9774;
SC=0.9673

2d item 20 substrates profile
PML*=1.0654;
PML*a*b*=1.2960;
GSSIM=0.9789;
sCIELAB=0.6374;
SC=0.9853.

10th item 20 substrates profile
PML*=7.9096;
PML*a*b*=51.6103;
GSSIM=0.9483;
sCIELAB=1.0709;
SC=0.9666.

14th item 20 substrates profile
PML*=3.5226;
PML*a*b*=3.4747;
GSSIM=0.9404;
sCIELAB=0.9373;
SC=0.9695.

6th item 1 hour repeatability
PML*=6.0530;
PML*a*b*=4.6394;
GSSIM=0.8799;
sCIELAB=1.0609;
SC=0.9451.

Figure 45: Evaluating of smoothness of Image 2

Image 2
PML*=7.9096;
PML*a*b*=51.6103;
GSSIM=0.9483;
sCIELAB=1.0709;
SC=0.9666.

Image 3
PML*=7.9096;
PML*a*b*=51.6103;
GSSIM=0.9433;
sCIELAB=1.2967;
SC=0.9772

Image 1
PML*=7.9096;
PML*a*b*=51.6103;
GSSIM=0.9465;
sCIELAB=25.2024;
SC=0.7793

Image 4
PML*=7.9096;
PML*a*b*=51.6103;
GSSIM=0.9752;
sCIELAB=6.7576;
SC=0.9911
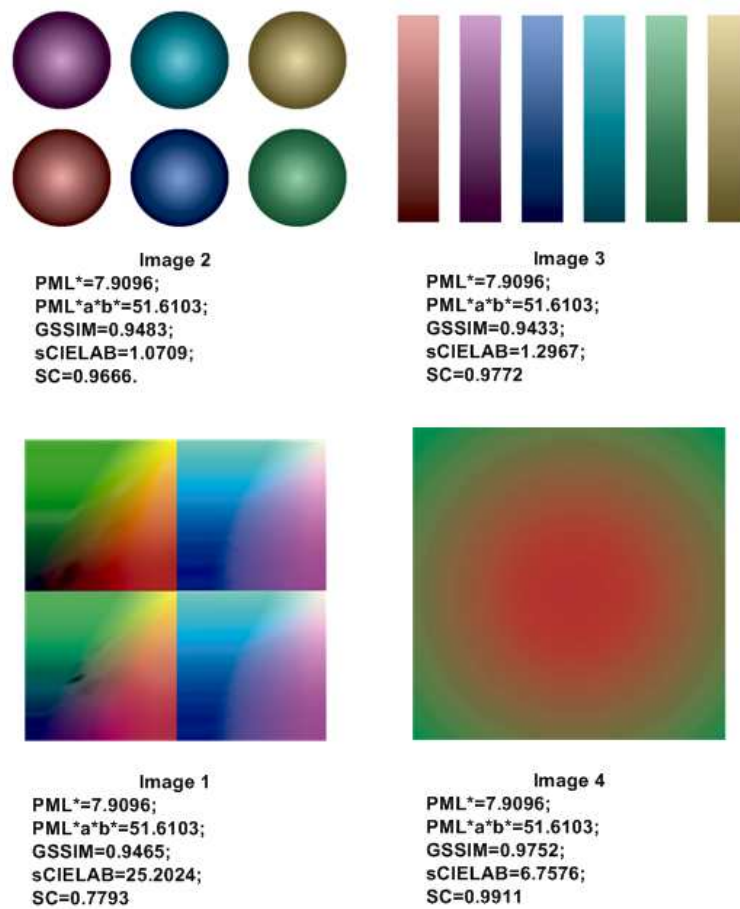
Figure 46: Evaluating of smoothness of images (10th item of 20 substrates profiles)

of Image 1 and Image 3 have great smoothness and color distortions. Thus metric PM L^* and PML*, a^*, b^* have advantage in this case because they allow to predict how smooth would be results of converting to profile in general. 30th profile gave smooth output results for some images. But the values of PM L^* and PML*, a^*, b^* is high enough because color conversion to this profile for few images provides totally wrong color and high smoothness distortions.

7 Conclusion and future work

Evaluation smoothness of color transformations is very complex task which requires integration of knowledge in different areas – from color management to psychophysics and image quality assessment. In this project this problem has been investigated in different aspects. The 3DLUT-based color transformations were considered in scope of attention in this project as widely-used empirical approach of device characterization and basis for ICC profiles.

Factors affected on smoothness of color transformation were analyzed. These factors inherited from the 3D LUTs transformation are size of LUT, interpolation method and noise from profiling appeared in LUTs. The process of printer characterization was modeled involving display inverse and forward characterization models. Analysis of experimental results shows that main factor influences on smoothness 3DLUT-based color transformation is unavoidable noise in 3DLUT appeared during color measurements. 3DLUTs of large size provides better color conversions in comparison with 3DLUTs of small sizes on conditions that noise in 3DLUT is not significant. If ratio of added noise to 3DLUTs is high, 3DLUT of smaller size provides better color conversion. The different interpolation methods perform similar results.

The existed methods for evaluating smoothness of color transformations were tested on designed 3DLUT-s and profiles (generated with added noise) and they were not evaluated on complex and natural images. In this project printer profiling was conducted involving instruments, equipment and tools with orientation on printer characterization by average operator in daily life. For obtaining essential variation of noise in 3DLUTs of profiles printed color target were printed and measured with different repeatability (20 successive measurements, measurements with 30 min and 1 hour reparability on same target) and on same and different substrates from one paper batch (20 substrates measurements). The color measurements were analyzed, and 45 of them were chosen for generating profiles and processing images. Complex images with different color transitions were converted to profiles, and images reproductions with different smoothness were obtained.

The implementation and analysis of two groups of algorithms for evaluating smoothness of color transformations were considered. First group includes smoothness metrics for color transforms: PG -Phil Green metric (2008), KM -Youn J.Kim et al. metric and proposed algorithm of color planes for one channel PML^* and three channels PML^*, a^*, b^* which are based on considering properties of color transform for providing smooth output. Second group includes image difference and quality metrics such as ΔE^*_{ab}, Adaptive bilateral filter, GSSIM, SSIM, sCIELAB, Edge Similarity, Structural content. These metric allow evaluating how smooth output result of color transforms comparing with reference image.

For elimination of drawbacks of existed algorithms new metric of color planes was proposed as extension of Phil Green metric applied to profile' CLUT. The metric of color planes do not requires special images, ramps or optimization coefficients and can be easily computed by using only profile for one and three channels. The new method performed high Pearson correlation with visual judgments and better performance of predicting smoothness than others smoothness metrics (PG, KM).

GSSIM have been shown better performance for predicting difference in smoothness between original image and reproduction. GSSIM have high Pearson correlation with z-scores and gives consistent response.

GSSIM and other image quality metrics can only evaluate result of color transformation applied to concrete image and define difference in smoothness comparing with reference image. So it does not give reason to conclude that particular color transformation give smooth or unsmooth output result. The PML^* and PML^*, a^*, b^* are aimed to predict how smooth results will provide converting to particular profile in general. So in case if it is necessary to evaluate smoothness of output results for particular image using image, and where is no information about profile GSSIM can be used. For evaluating output result of color transformation in general for images with different content PML^* and PML^*, a^*, b^* should be used.

As future perspective human perception of smoothness and ability extract information about smoothness changes should be investigated. How important colors changes on in evaluating smoothness of image? Does smoothness only depends on lightness changes? Thus more work is required in this direction but it will allow improving existed methods of evaluating smoothness

The proposed algorithm of evaluating smoothness of color transformation PML^* or PML^*, a^*, b^* were implemented only in 1 dimension (for planes when R and G primaries are constant, and B changes) . The extension of this method can be considering 3 directions for computing metric. The round-trip-transform test can be considered where L^*, a^*, b^* color planes (AToB# table) can be converted back to device RGB plane using BToA# table and then again back to L^*, a^*, b^* color space. The values of color planes before and after transform should be compared. The proposed method can be also examined on natural images involving more observers.

Bibliography

[1] Adams, R. M. & Weisberg, J. B. 2000. *The GATF Practical Guide to Color Management.* GATFPress, second edition.

[2] P.Green & S.Lindberg. 1985. Methods of quality assessment for large sample sets. *Science and Technology*, 4(49).

[3] Hardeberg, J. Y. 2002. Color image quality for multi-function peripherals. In *Image Quality, Image Capture, Systems Conference PICS2002*, 76–81. Proceedings of IS&T's Image Processing.

[4] Kang, H. R. 1996. *Color Technology For Electronic Imaging Devices*. SPIEThe International Society for Optical Engineering.

[5] Green, P. 2005. Accuracy of colour transforms. In *Color Imaging XI: Processing, Hardcopy, and Application*, R.Eschbach, G., ed, volume 6058, 605802I1–605802I10. Proceedings of SPIEIS&T's Electronic Imaging.

[6] Olson, T. 1999. Smooth ramps: Walking the straight and narrow path through color space. In *The Seventh Color Imaging Conference: Color Science, Systems, and Applications*, volume 6058, 57a–57i. IS&T - The Society for Imaging Science and Technology.

[7] Green, P. 2008. A smoothness metric for colour transforms. In *Color Imaging XIII: Processing, Hardcopy, and Applications.*, R.Eschbach, Gabriel G. Marcu, S. T., ed, volume 6807, 68070I1–68070I5. Proceedings of SPIEIS&T's Electronic Imaging.

[8] Kim, Y. J., Bang, Y., & Choh, H.-K. January-March 2010. Gradient approach to quantify the gradation smoothness for output media. *Journal of Electronic Imaging*, 19(1-011012), 1–9.

[9] Morovic, J., Albarran, A., Arnabat, J., Richard, Y., & Maria, M. November 2008. Accuracypreserving smoothing of color transformation Luts. In *16th Color Imaging Conference Final Program and Proceedings.*, volume 16, 243–245. Society for Imaging Science and Technology.

[10] Garcia, E. & Gupta, M. November 2009. Building accurate and smooth Icc profiles by lattica regression. In *17th Color Imaging Conference Final Program and Proceedings.*, volume 17, 101–106. Society for Imaging Science and Technology.

[11] Sharma, G., ed. 2003. *Digital color imaging handbook*. CRC Press LLC.

[12] Fraser, B., Murphy, C., & Bunting, F. 2005. *Color management. Industrual-strength profduction technoiques.* Peachprint Press.

[13] Westland, S. & Pipamonti, C. 2004. *Computational color science using MATLAB*. John Wiley&Sons Ltd.

[14] Hardeberg, J. Y. & Schmitt, F. November 1997. Color printer characterization using a computational geometry approach. In *Fifth Color Imaging Conference: Color Science, Systems and Applications*, volume 5, 96–99. The Society for Imaging Science and Technology.

[15] Green, P. & MacDonald, L. 2002. *Color engineering. Achieving Device Independent Color.* John Wiley&Sons Ltd.

[16] Poynton, C. 2002. Frequently asked questions about gamma. http://www.poynton.com/notes/colour_and_gamma/GammaFAQ.html. Last access : 17/05/2010.

[17] Sharma, G. 2002. Comparative evaluation of color characterization and gamut of lcds versus crts. In *Color Imaging: Device-Independent Color, Color Hardcopy, and Apllications VII*, Eschbach, R. & Marcu, M., eds, volume 4663, 177–186. Society of Photooptical Instrumentation Engineers (SPIE), Proceedings of SPIE.

[18] Berns, R. S. 1996. Methods for characterizing crt displays. *Displays*, 16(4), 173–181.

[19] ISO 126462008(E). Graphic technology.Displays for colour proofing.Characteristics and viewing conditions.

[20] ISO 3664 2000. Viewing conditions. Graphics technology and photography.

[21] Kasson, J. M., Nin, S. I., Plouffe, W., & L.Hafner, J. 1995. Performing colour space conversions with three-dimensional linear interpolation. *Journal of Electronic Imaging*, 4(3), 226–249.

[22] Balasubramanian, R. July-August 2000. Reducing the cost of lookup table based color transformations. *Journal of Imaging Science and Technology*, 44(4), 321–327.

[23] Specification ICC.1 200410 (profile version 4.2.0.0). Image technology color management – architecture, profile format, and data structure. http://www.color.org/ICC1v42_200605.pdf.

[24] Revie, W. G. 2002. ICC color management for print production. TAGA Annual Technical Conference 2002. http://www.color.org/craigrevie.pdf. Last access : 20/05/2010.

[25] Wallner, D. 2000. *Building ICC Profiles the Mechanics and Engineering*. Sun Microsystems.

[26] Tapp, E. 2006. *Practical color management*. ORELLY.

[27] Johnson, T. & Scott-Taggart, M. 1998. *Guidlines for choosing the correct viewing conditions for color publishing.* Pira International., Surrey, UK.

[28] Pollehn, H. & Roehrig, H. June 1970. Effect of noise on the modulation thansfer function of the visual channel. *Journal of the Optical society of America*, 60(6).

[29] Olson, T. 1996. Deriving digital imaging specifications some requirements for artifact-free continuous tone output. In *Part2 Pixel intensity coding*. IS&T 49th Conference.

[30] Nes, F. V. & A.Bounman, M. 1965. The effects of wavelength and luminance on visual modulation transfer. In *Proceedings of the Symposium, Delf.t, Performance of the Eye at Low Luminance.*, 125.

[31] Burningham, N. & Bouk, T. 1994. Threshold visibility and objectionability of banding in reflection prints. In *IS&Ts Tenth International Congress on Advances in Non-Impact Printing Technologies*.

[32] Olson, T. November 1992. Digital film part2 Good grays and continuous colors. In *134th SMPTE Technical conference*.

[33] Hunt, R. 1995. Why is black-and-white so important in color? In *4th IS&T/SID Color Imaging Conference*, 54–57.

[34] Kitoh, S. & P.Hung. 2005. A new method to quantitatively evaluate gradation smoothness of output media. In *13 th Color Imaging Conference*, 89–94. IS&T.

[35] Brigg, J. C. 2000. Banding characterization for inkject printing. In *Image Processing, Image Quality, Image Capture Systems Conference*. IS&T's PICS.

[36] Arslan, O., Pizlo, Z., & Allebach, J. P. 2007. Softcopy banding visibility assessment. *Journal of Imaging Science and Technology*, 51(3), 271–281.

[37] Bartleson, . J. 1960. Memory colors of familiar objects. *Journal of Optical Society*, 50(1), 73–77.

[38] Green, P. 2005. Advances in color management. In *Proceedings from Gøvik Color Imaging Simposium 2005*, Hardeberg, J. Y., Nussbaum, P., Alsam, A., Skarsbø, S. E., & Farup, I., eds. Institutt for Informatikk og Medieteknikk.

[39] Pedersen, M. & Hardeberg, J. Y. June 2009. Survey of full-reference image quality metrics. The Norwegian Color Research Laboratory, Høgskolen i Gjøvik's rapportserie.

[40] Luo, M. R., Cui, G., & Rigg, B. 2001. The development of the CIE 2000 color-difference formula CIEDE2000. *Color Research & Application*, 26(5), 340–350.

[41] Wang, Z. & Bovik, A. C. March 2002. A universal image quality index. In *IEEE Signal Processing Letters*, volume XX.

[42] Wang, Z., Bovik, A. C., Sheikn, H. R., & Simoncelli, E. P. April 2004. Image quality assessment from error visibility to structural similarity. In *IEEE Transactions on Image Processing*, volume 13, 600–611.

[43] Chen, G., Yang, C., & Xie, S. October 2006a. Gradient-based structural similarity for image quality assessment. In *IEEE International Conference on Image Processing*, 2929–2932, Atlanta, GA,USA.

[44] Li, C. & Bovik, A. C. 2010. Content-partitioned structural similarity index for image quality assessment. *Signal Processing Image Communication. Article in press*, 25, 1–10.

[45] Zhang, X. & Wandell, B. A. March 1997. A spatial extension of CIELABfor digital color-image reproduction. *Journal of the Society for Information Display*, 5(1), 61–63.

[46] Wang, Z. & Hardeberg, J. Y. November 2009. An adaptive bilateral filter for predicting color image. In *17th Color Imaging Conference Final Program and Proceedings Color Science and Engineering Systems, Technologies, and Applications*, 27–31, Norway. Gjøvik Univercity College.

[47] Thomasi, C. & R.Manduchi. 1998. Bilateral filtering for gray and color images. In *Proceedings of the IEEE International Conference on Computer Vision*, Bombay, India.

[48] Silva, E. A., Panetta, K., & Agaian, S. S. April 2007. Quantifying image similarity using measure of enhancement by entropy. In *Mobile Multimedia. Image Processing for Security Applications*, volume 6579. SPIE Security Symposium 2007. Last access: 26/05/2010.

[49] Kratochvil, T. & Simicek, P. 2005. Utilization of matlab for picture quality evaluation. Institute of Radio Electronics, Brno University of Technology.

[50] Wikipedia. April 2010. Minkowski distance. http://en.wikipedia.org/wiki/Minkowski_distance. Last access 26/05/2010.

[51] Ferwerda, J. A. 2008. Psychophysics 101 how to run perception experiments in computer graphics, SIGGRAPH 2008 courses program. In *International Conference on Computer Graphics and Interactive Techniques*, number 87, Los Angeles, California. Munsell Color Science Laboratory,.

[52] Wang, Z., Aristova, A., & Hardeberg, J. Y. 2010. The evaluation of smooth transformation using 3DLUTs. In *CGIV 2010 European Conference on Colour in Graphics, Imaging, and Vision*, Joensuu, Finland.

[53] Wang, Z., Aristova, A., & Hardeberg, J. Y. May, 2010 2010. Quantifying smoothness of the LUTsbased color transformations. In *ICIS2010 The 31st International Congress on Imaging Science Imaging Science and Technology in the Digital Era*, China National Convention Center, Beijing, China.

[54] Spectroradiometer CS-1000A minolta. http://www.tequipment.net/pdf/Minolta/CS-1000A.pdf. Last access: 15/06/2010.

[55] Berns, R. S. 2000. *Bilmeyer and Saltzman Principles of Color Technology*. John Wiley&Sons Ltd, New York, 3 edition.

[56] Standard viewing conditions. http://www.xrite.co.uk/documents/literature/en/StandardViewingNTK_EN.pdf, Xrite color services, UK.

[57] Ruff, M. December 2008. The power of neutral gray. *ScreenPrinting*, 12, 34–38.

[58] Croarkin, C. & Tobias, P., eds. 2010. *Engineering Statistics Handbook*. USA National Institute of Standard and Technology, SIMATECH.

[59] May 2010. Phaser 7760 color tabloid laser printer. http://www.direct.xerox.com/shop/office-equipment/printers/phaser7760. Last Access: 28/05/2010.

[60] User guide Xerox Phaser 7760, Xerox Corporation. http://www.office.xerox.com/userdoc/P7760/pdfs/user_guide_en.pdf. Last access: 28/05/2010.

[61] December 2004. White paper 3 : ICC recommendations for color measurement. http://www.color.org/ICC_white_paper3measurement.pdf. Last access : 28/05/2010.

[62] LOGO, GretagMacbeth Group Company. *Profile Maker Professional Help*, 2004.

[63] Chan, E. July 2007. Perceptual gamut mapping options in eye-one match. http://people.csail.mit.edu/ericchan/dp/i1GamutMapping/index.html. Last access : 29/05/2010.

[64] Adobe System Incorporation. *Adobe Photoshop CS3 help module*, 2007.

[65] Bhattacharya, A. & McGlothlin, J. D., eds. 1996. *Occupational Ergonomics: Theory and Applications*. Marcel Dekker.

[66] Ankrum, D. R. Viewing angle and distance in computer workstations. http://www.allscan.ca/ergo/vangle.htm. Last access: 28/05/2010.

[67] 2010. Color blindness or color vision deficiency. http://www.archimedes-lab.org/colorblindnesstest.html. Last access : 28/05/2010.

[68] Torgerson, W. S. 1960. *Theory and methods of scaling*. Wiley.

A   Display characterization

a)red sample RGB=(255;0;0);

b)green sample RGB=(0;255;0);

c)blue sample RGB=(0;0;255);
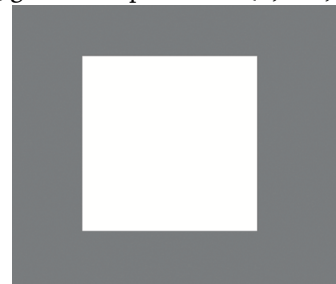
d)white sample
RGB=(255;255;255);

e)black sample RGB=(0;0;0).

Figure 47: Channel-independence test (background is neutral gray RGB=[119;119;119])
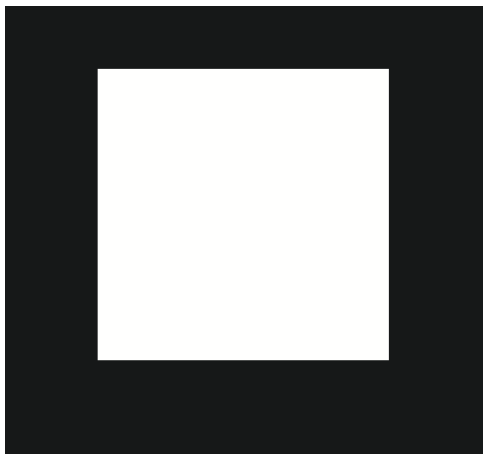
a) white sample RGB=(255;255;255) on black background RGB=(0;0;0);
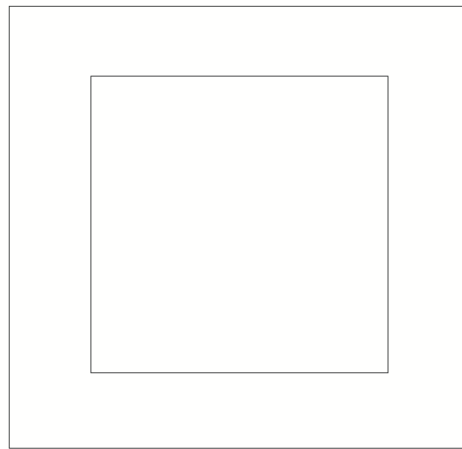
b)white sample RGB=(255;255;255) on white background RGB=(255;255;255).

Figure 48: Spatial independence test

R	G	B
0	0	0
16	16	16
32	32	32
48	48	48
64	64	64
80	80	80
96	96	96
112	112	112
125	125	125
144	144	144
160	160	160
176	176	176
192	192	192
208	208	208
224	224	224
240	240	240
255	255	255

Table 24: Neutral series
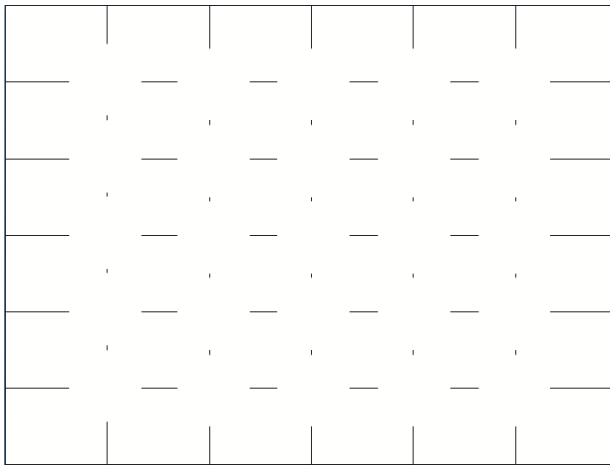
a) white sample RGB=(255; 255; 255);
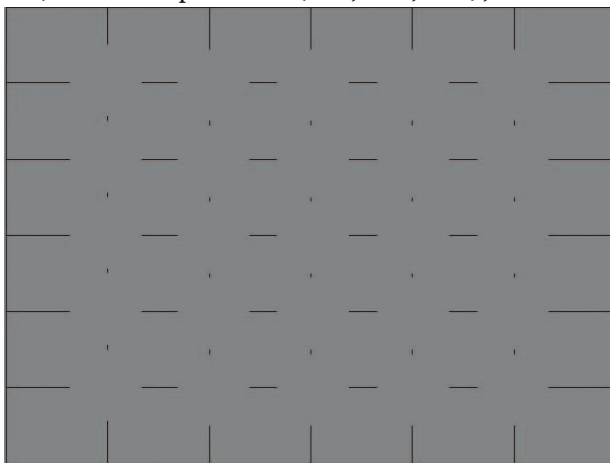
b) gray sample RGB=(127; 127; 127);
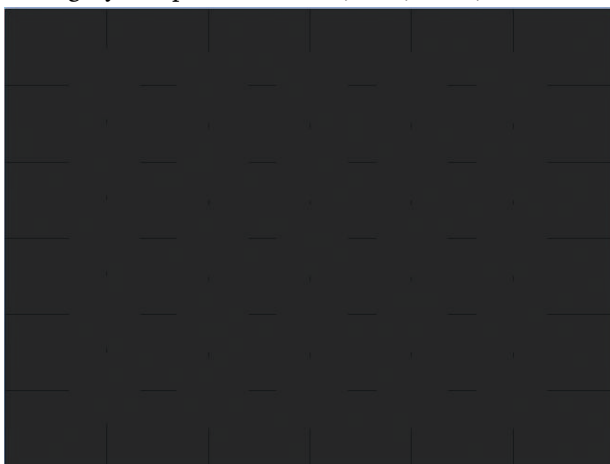
c)black sample RGB=(28; 28; 28).

Figure 49: Spatial-uniformity test

B   Interpolation methods

a)Mapping point P within RGB cub to P'
within Lab cub;

b)CIELAB subcub.
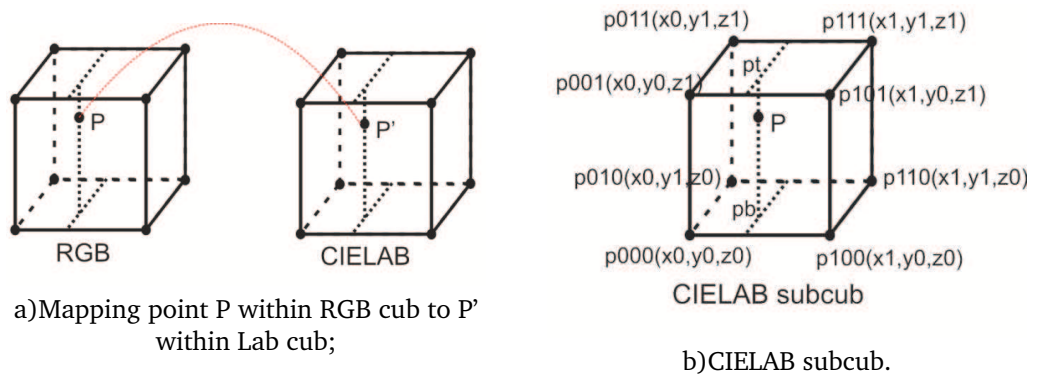
Figure 50: Trilinear interpolation

a) Division of cub on prisms;

b) Mapping point P within RGB prism to
P' within Lab prism.
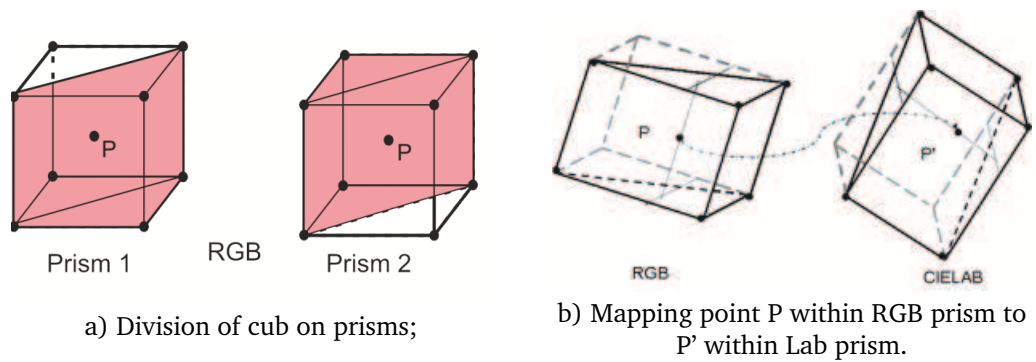
Figure 51: Prism interpolation

99

Tetrahedron 1

Tetrahedron 2

Tetrahedron 3

Tetrahedron 4

Tetrahedron 5

Tetrahedron 6

a)The six tetrahedrons;

b)Mapping point P within RGB tetrahedron to P' within Lab tetrahedron.
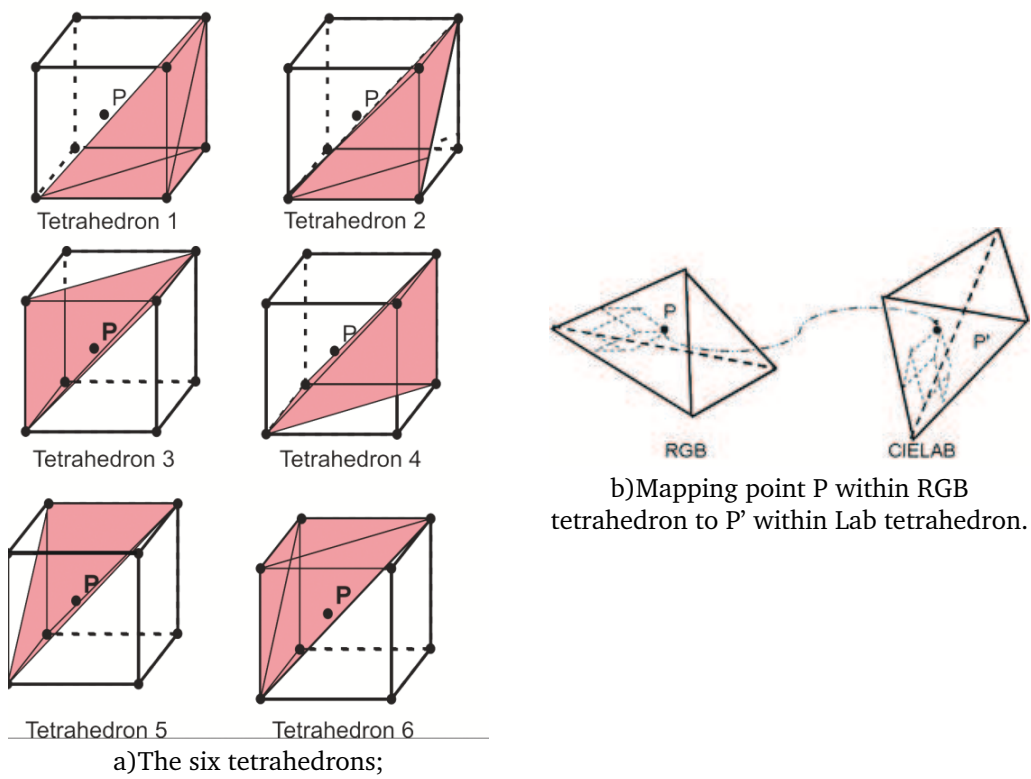
Figure 52: Tetrahedral interpolation

C   Factors affecting on 3DLUT-based color transforms

Table 25: MOS and standard deviation for image data set

Image Name	Type	Observer1	Observer2	Observer3	Observer4	MOS	Stand. deviation
Balloon	90p	2	1	1	1	1.25	0.50
	90tr	1	2	2	2	1.75	0.50
	90tet	2	1	2	2	1.75	0.50
	91p	1	0	1	1	0.75	0.50
	91tr	1	0	2	0	0.75	0.96
	91tet	1	2	1	2	1.5	0.58
	95p	3	5	3	3	3.5	1.00
	95tr	1	0	3	2	1.5	1.29
	95tet	2	2	2	1	1.75	0.50
	910p	3	2	3	3	2.75	0.50
	910tr	1	4	4	4	3.25	1.50
	910tet	3	5	3	5	4	1.15
	920p	3	4	1	5	3.25	1.71
	920tr	3	5	5	5	4.5	1.00
	920tet	3	4	4	3	3.5	0.58
	170p	1	0	1	2	1	0.82
	170tr	1	0	1	0	0.5	0.58
	170tet	1	0	0	3	1	1.41
	171p	2	0	3	2	1.75	1.26
	171tr	1	3	1	1	1.5	1.00
	171tet	2	3	4	1	2.5	1.29
	175p	3	4	4	3	3.5	0.58
	175tr	4	6	5	6	5.25	0.96
	175tet	3	3	4	2	3	0.82
	1710p	3	4	6	4	4.25	1.26
	1710tr	1	4	6	6	4.25	2.36
	1710tet	4	5	6	5	5	0.82
	1720p	4	6	6	5	5.25	0.96
	1720tr	5	7	7	7	6.5	1.00
	1720tet	4	7	7	6	6	1.41
Bows and threads	90p	1	1	1	1	1	0.00
	90tr	1	2	4	3	2.5	1.29
	90tet	2	2	3	2	2.25	0.50
	91p	1	2	3	3	2.25	0.96

Image Name	Type	Observer1	Observer2	Observer3	Observer4	MOS	Stand. deviation
	91tr	3	4	6	4	4.25	1.26
	91tet	1	2	5	3	2.75	1.71
	95p	3	5	4	4	4	0.82
	95tr	3	3	5	3	3.5	1.00
	95tet	4	6	5	6	5.25	0.96
	910p	3	4	6	2	3.75	1.71
	910tr	2	5	5	4	4	1.41
	910tet	3	7	4	6	5	1.83
	920p	4	7	6	6	5.75	1.26
	920tr	5	7	7	7	6.5	1.00
	920tet	5	6	6	5	5.5	0.58
	170p	0	2	1	1	1	0.82
	170tr	2	2	3	0	1.75	1.26
	170tet	2	2	1	1	1.5	0.58
	171p	0	3	2	2	1.75	1.26
	171tr	5	5	3	4	4.25	0.96
	171tet	2	5	5	4	4	1.41
	175p	5	6	6	6	5.75	0.50
	175tr	4	5	5	5	4.75	0.50
	175tet	3	5	5	5	4.5	1.00
	1710p	5	7	6	6	6	0.82
	1710tr	4	7	6	6	5.75	1.26
	1710tet	5	6	6	7	6	0.82
	1720p	4	7	7	5	5.75	1.50
	1720tr	6	7	6	6	6.25	0.50
	1720tet	4	7	7	7	6.25	1.50
Picnic	90p	2	2	2	2	2	0.00
	90tr	1	1	1	2	1.25	0.50
	90tet	1	2	1	2	1.5	0.58
	91p	2	1	1	2	1.5	0.58
	91tr	2	3	1	2	2	0.82
	91tet	2	1	1	1	1.25	0.50
	95p	1	1	3	2	1.75	0.96
	95tr	3	1	2	1	1.75	0.96
	95tet	2	1	1	0	1	0.82
	910p	2	2	3	2	2.25	0.50
	910tr	3	4	5	4	4	0.82
	910tet	3	2	4	2	2.75	0.96
	920p	3	2	5	3	3.25	1.26
	920tr	3	5	4	5	4.25	0.96
	920tet	3	3	6	1	3.25	2.06

Image Name	Type	Observer1	Observer2	Observer3	Observer4	MOS	Stand. deviation
	170p	2	1	2	1	1.5	0.58
	170tr	1	2	2	2	1.75	0.50
	170tet	1	1	2	2	1.5	0.58
	171p	2	2	1	2	1.75	0.50
	171tr	2	0	2	0	1	1.15
	171tet	2	1	2	1	1.5	0.58
	175p	7	3	5	7	5.5	1.91
	175tr	4	5	4	3	4	0.82
	175tet	2	2	2	0	1.5	1.00
	1710p	5	4	3	5	4.25	0.96
	1710tr	2	6	3	5	4	1.83
	1710tet	3	4	1	1	2.25	1.50
	1720p	6	7	7	7	6.75	0.50
	1720tr	7	7	6	7	6.75	0.50
	1720tet	7	7	7	7	7	0.00
RGB	90p	0	1	1	1	0.75	0.50
	90tr	2	3	2	1	2	0.82
	90tet	1	3	1	1	1.5	1.00
	91p	3	0	1	0	1	1.41
	91tr	4	4	5	2	3.75	1.26
	91tet	2	1	4	3	2.5	1.29
	95p	3	2	5	2	3	1.41
	95tr	3	5	5	3	4	1.15
	95tet	3	4	4	3	3.5	0.58
	910p	3	5	4	3	3.75	0.96
	910tr	3	3	5	2	3.25	1.26
	910tet	3	3	4	4	3.5	0.58
	920p	3	4	6	4	4.25	1.26
	920tr	4	6	5	5	5	0.82
	920tet	2	3	5	2	3	1.41
	170p	1	3	2	1	1.75	0.96
	170tr	3	0	0	0	0.75	1.50
	170tet	0	0	1	0	0.25	0.50
	171p	2	2	4	1	2.25	1.26
	171tr	3	2	4	1	2.5	1.29
	171tet	1	2	3	2	2	0.82
	175p	4	4	5	4	4.25	0.50
	175tr	3	3	6	3	3.75	1.50
	175tet	3	4	6	5	4.5	1.29
	1710p	1	3	6	1	2.75	2.36
	1710tr	6	5	6	6	5.75	0.50

Image Name	Type	Observer1	Observer2	Observer3	Observer4	MOS	Stand. deviation
	1710tet	4	3	5	3	3.75	0.96
	1720p	3	4	5	4	4	0.82
	1720tr	5	7	7	7	6.5	1.00
	1720tet	2	4	6	3	3.75	1.71

a) Balloon

b) Bows and threads

c) Picnic

d) RGB

Figure 53: Experimental images set

a) Prism interpolation 3DLUT 17x17x17
with noise ratio 0;

b) Prism interpolation 3DLUT 17x17x17
with noise ratio 1;

c) Prism interpolation 3DLUT 17x17x17
with noise ratio 5;

d) Prism interpolation 3DLUT 17x17x17
with noise ratio 10;
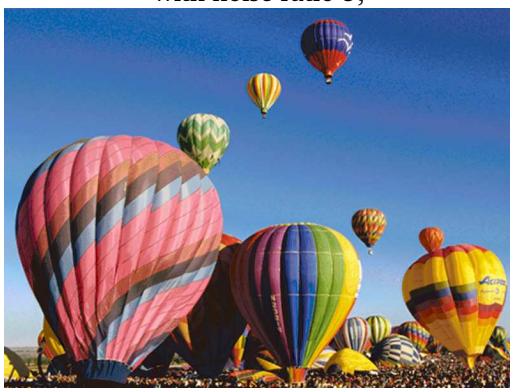
d) Prism interpolation 3DLUT 17x17x17
with noise ratio 20;

Figure 54: Reproductions of Balloon image (different noise ratio)

a) Trilinear interpolation 3DLUT
17x17x17with noise ratio 0;

b) Prism interpolation 3DLUT 17x17x17
with noise ratio 0;

c) Tetrahedral interpolation 3DLUT
17x17x17 with noise ratio 0;

Figure 55: Reproductions of Picnic image (different interpolation method)

a) Trilinear interpolation 3DLUT 9x9x9with noise ratio 10;

b) Prism interpolation 3DLUT 9x9x9 with noise ratio 10;

c) Tetrahedral interpolation 3DLUT 9x9x9 with noise ratio 10;

Figure 56: Reproductions of RGB image (different interpolation method, noise ratio 10)

a) Trilinear interpolation 3DLUT 9x9x9 with noise ratio 0;

b) Trilinear interpolation 3DLUT 17x17x17 with noise ratio 0;

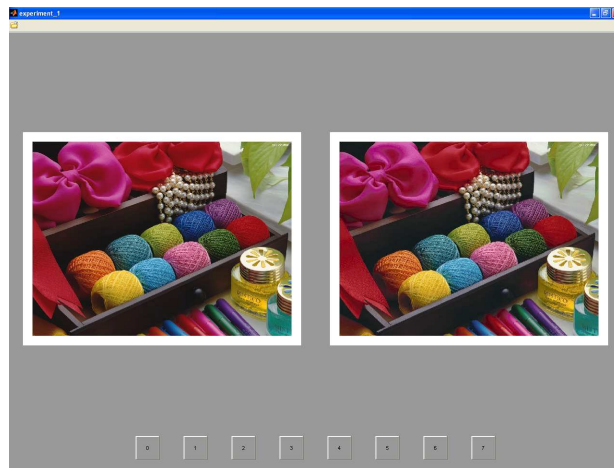Figure 57: Reproductions of Bows and threads image (different LUTs size)

Figure 58: GUI for conducting experiment
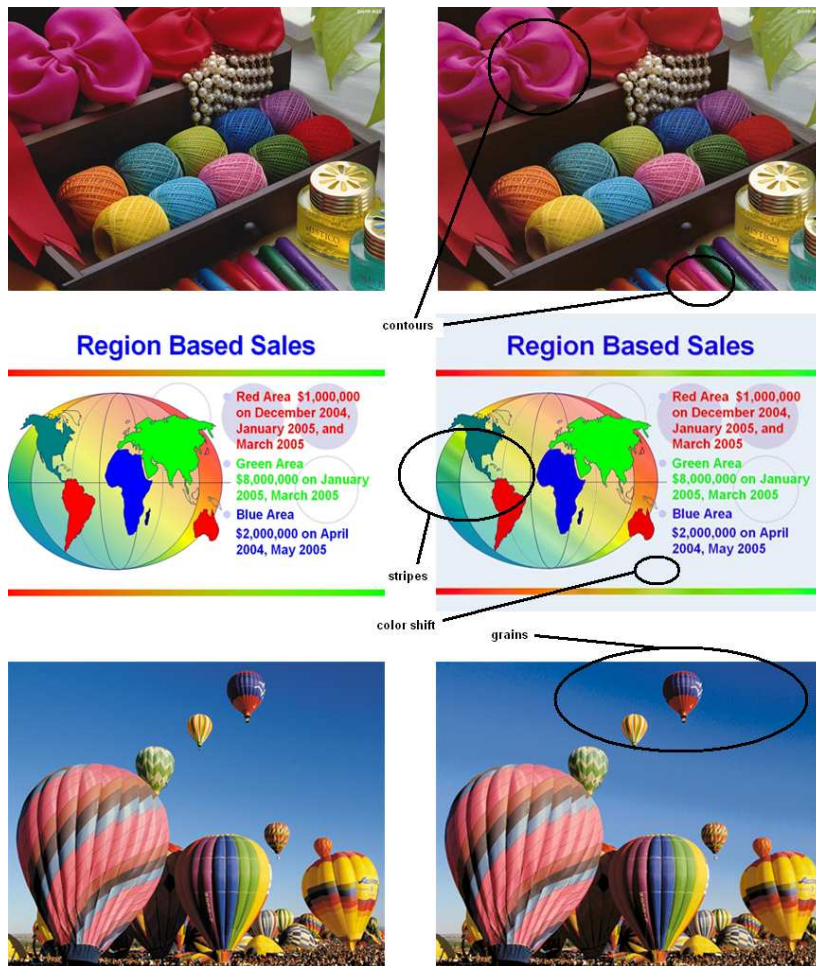

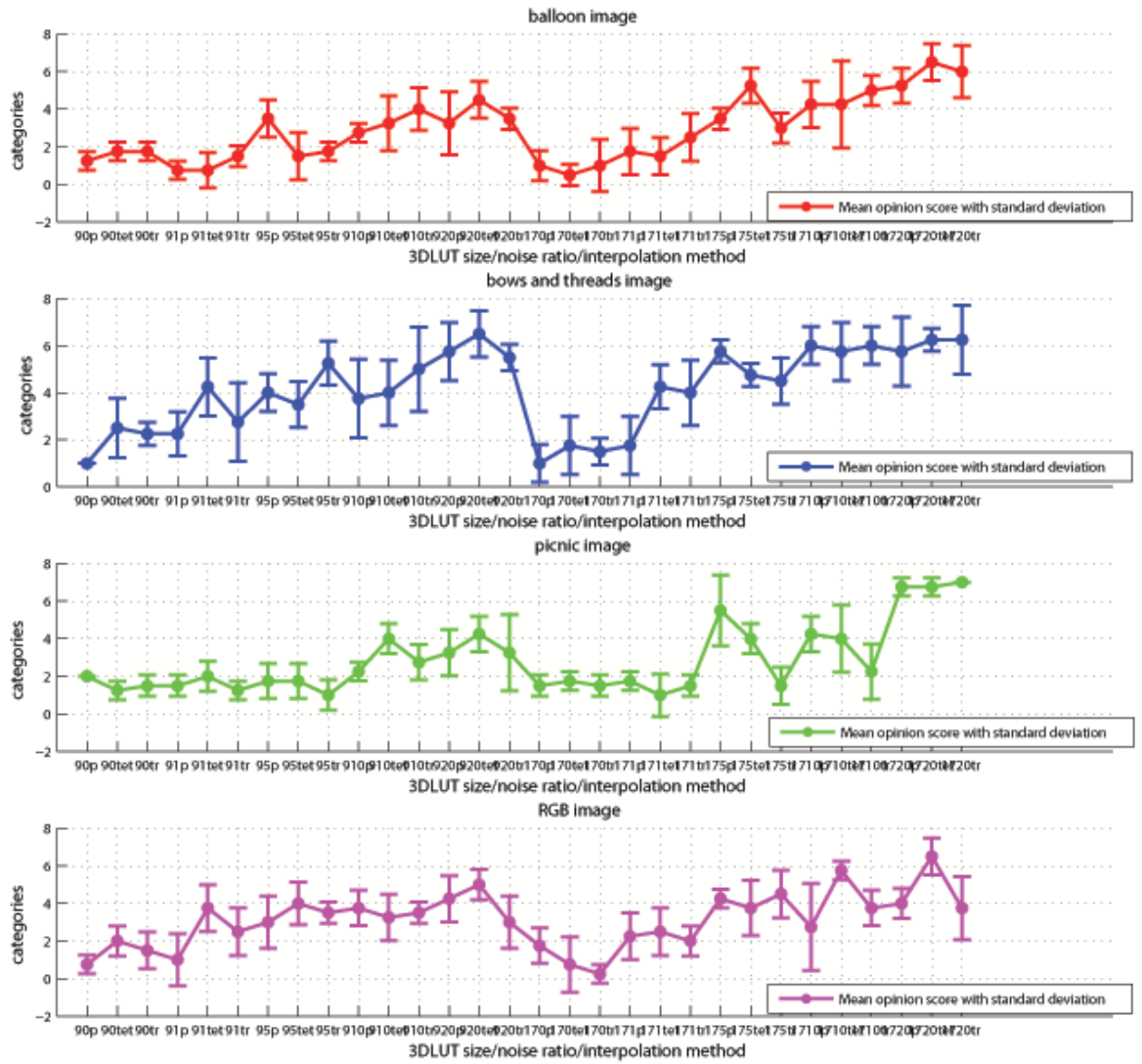Figure 59: Examples of post-processed images' artifacts

Figure 60: MOSs with 95% confidence interval for set of images
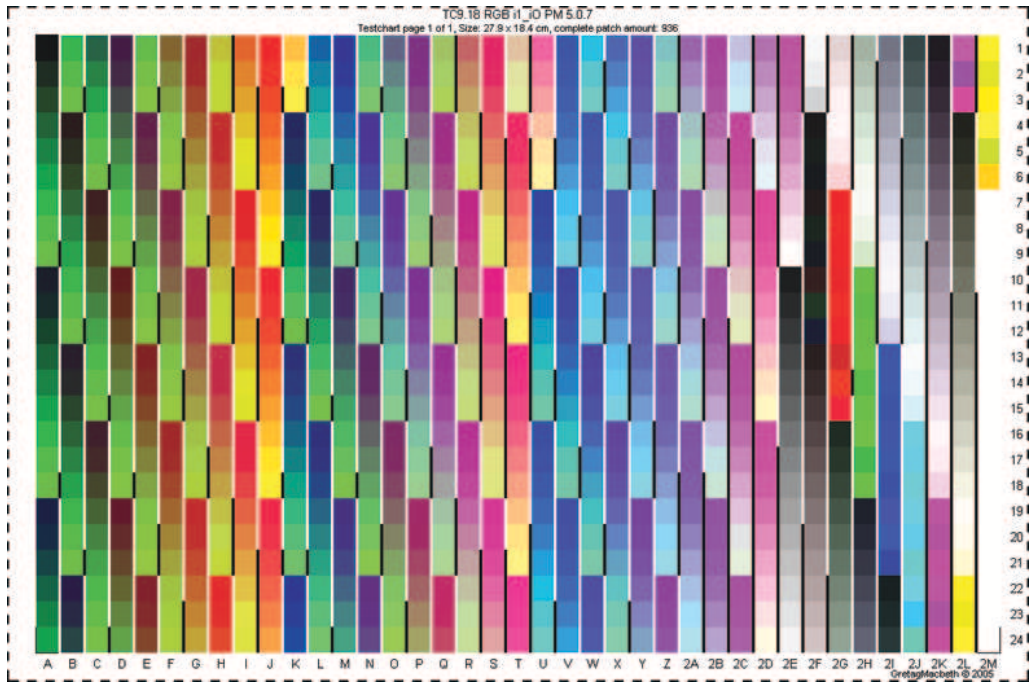
D Profiles Generation

Figure 61: TC9 18 RGB i1 iO color test chart for GretagMacbeth Eye-One i1 iO (MeasureTool)

Measurement	Average delta CIELAB	Max delta CIELAB	Average of average
1	1.38	6.24	0.863
2	0.86	3.35	0.863
3	0.81	5.57	0.863
4	1.05	6.57	0.863
5	0.64	5.52	0.863
6	0.76	3.27	0.863
7	0.96	6.6	0.863
8	0.61	0.38	0.863
9	0.83	4.32	0.863
10	0.7	4.77	0.863
11	0.68	5.1	0.863
12	0.87	5.28	0.863
13	0.63	4.39	0.863
14	0.86	6.29	0.863
15	0.92	11.96	0.863
16	0.83	4.65	0.863
17	0.92	4.86	0.863
18	0.82	5.39	0.863
19	1.16	6.97	0.863
20	0.97	5.73	0.863

Table 26: The color difference between average and single measurement(20 successive)

Measurement	Average delta CIELAB	L^*	a^*	b^*	Average of average
1	2.25	47.04	58.82	34.92	2.058
2	0.74	45.23	59.66	36.99	2.058
3	1.73	44.65	59.78	37.88	2.058
4	0.99	46.37	58.92	36.13	2.058
5	0.52	45.87	59.31	37.13	2.058
6	1.8	44.77	60.49	37.77	2.058
7	0.44	45.95	59.48	36.28	2.058
8	1.59	46.4	60.02	38.14	2.058
9	1.57	44.96	60.66	37.36	2.058
10	1.02	45.72	60.3	37.42	2.058
11	1.49	46.75	58.5	37.25	2.058
12	2.12	44.86	60.36	38.38	2.058
13	1.85	45	60.45	38.06	2.058
14	0.66	46.3	59.25	36.3	2.058
15	11.96	49.24	52.3	27.83	2.058
16	2.88	44.99	61.55	38.6	2.058
17	1.09	46.72	59.31	37.33	2.058
18	1.74	45.72	60.92	37.81	2.058
19	2.89	45.41	61.56	38.76	2.058
20	1.83	45.66	61.16	37.6	2.058
av.	-	45.9	59.59	36.69	-

Table 27: The color difference between average and single measurement(20 successive, patch J1)

112

Measurement	Average delta CIELAB	L*	a*	b*	Average of average
1	2.34	44.02	60.9	29.59	1.0085
2	0.99	43.45	62.26	31.04	1.0085
3	1	43.81	61.66	31.17	1.0085
4	0.75	45.08	62.49	31.55	1.0085
5	0.62	45	62.45	31.26	1.0085
6	0.84	44.61	62.98	31.91	1.0085
7	1.17	44.11	61.48	31.84	1.0085
8	0.58	43.92	62.34	30.93	1.0085
9	0.82	43.64	62.38	30.92	1.0085
10	1.37	44.81	63.05	32.43	1.0085
11	0.61	44.09	62.05	31.59	1.0085
12	0.51	43.89	62.31	31.27	1.0085
13	0.82	43.77	62.31	31.79	1.0085
14	0.83	45.2	62.58	31.22	1.0085
15	1.76	45.49	61.23	30.72	1.0085
16	1.04	44.57	63.5	31.36	1.0085
17	0.79	44.84	63.12	31.28	1.0085
18	1.03	44.29	63.35	30.75	1.0085
19	1.24	44.21	63.7	31.24	1.0085
20	1.06	44.66	63.48	31.51	1.0085
av.	-	44.38	62.48	31.28	-

Table 28: The color difference between average and single measurement(20 successive, patch T4)

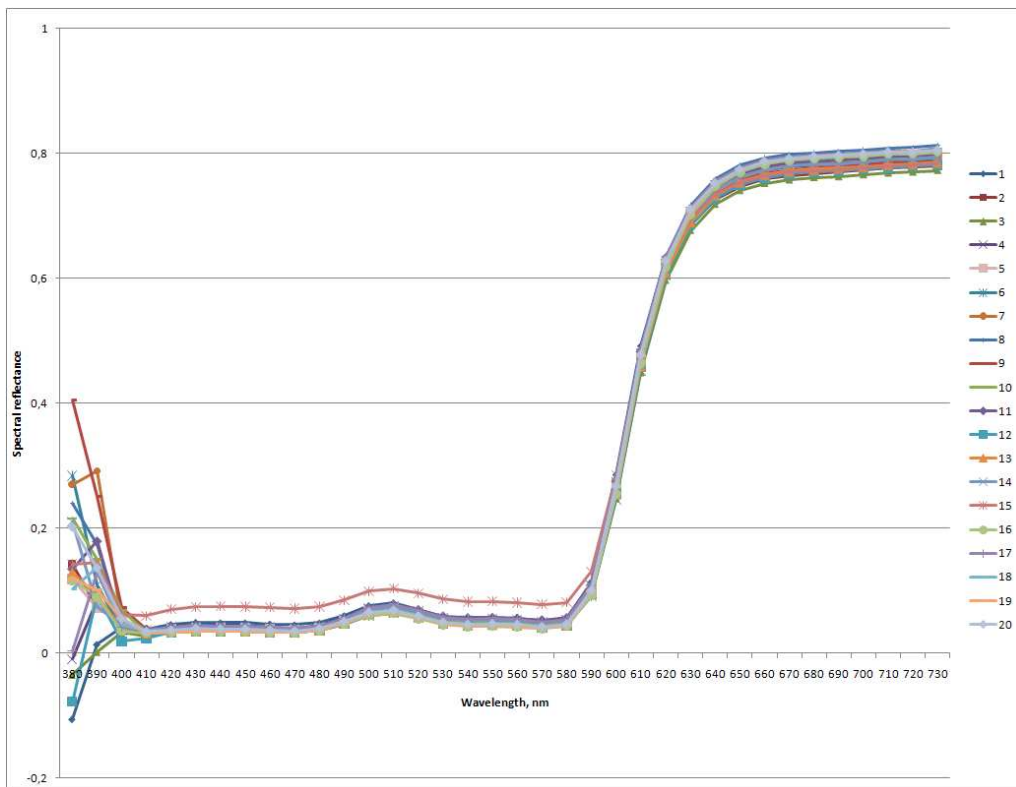Figure 62: ΔE^*_{ab} for 20 successive measurements for color patch J1

113
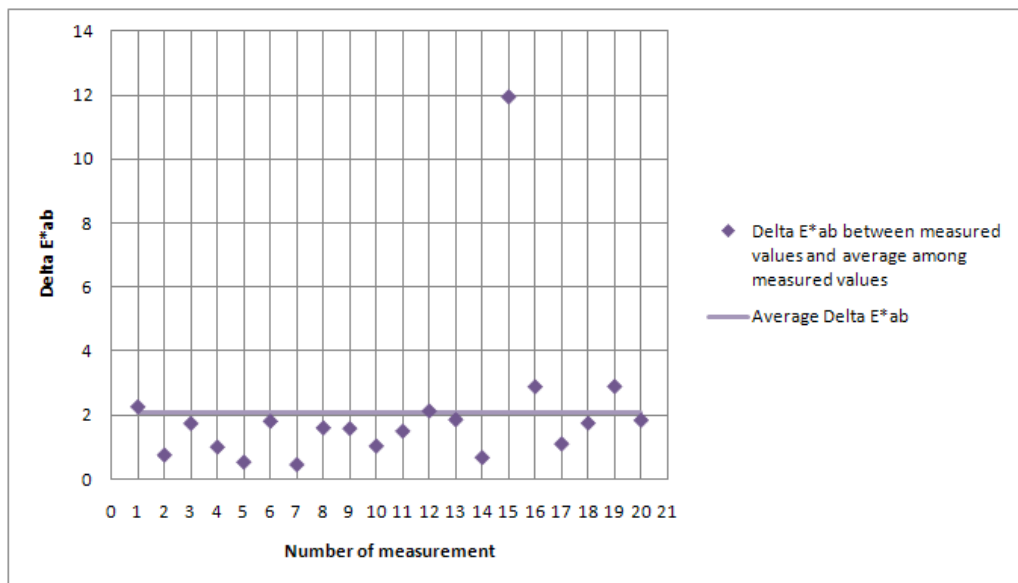
Figure 63: Spectral reflectance for patch J1(20 successive)
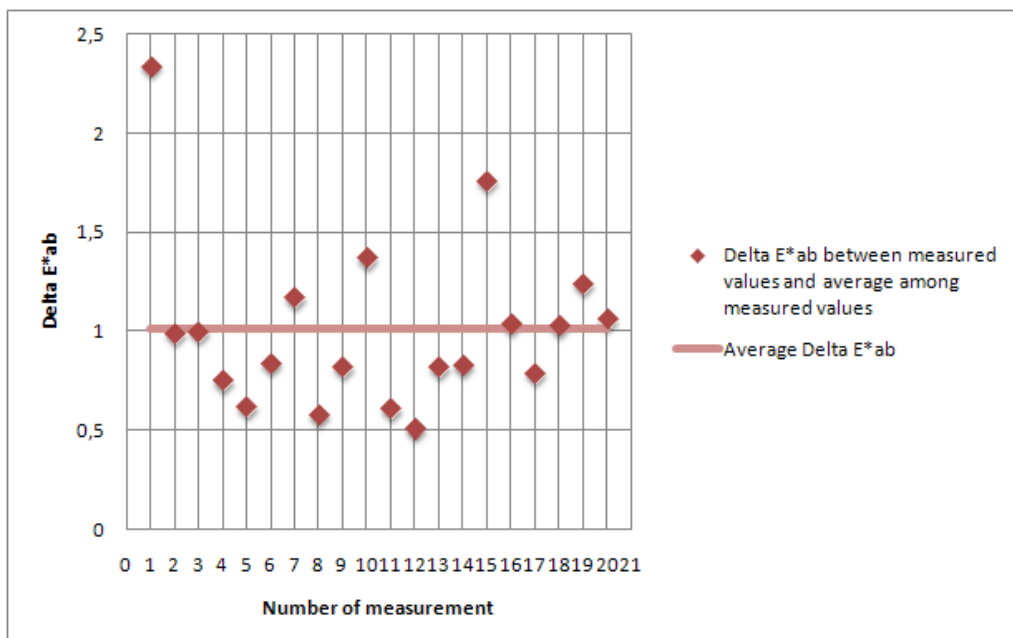
Figure 64: ΔE_{ab}^* for 20 successive measurements for color patch T4

114
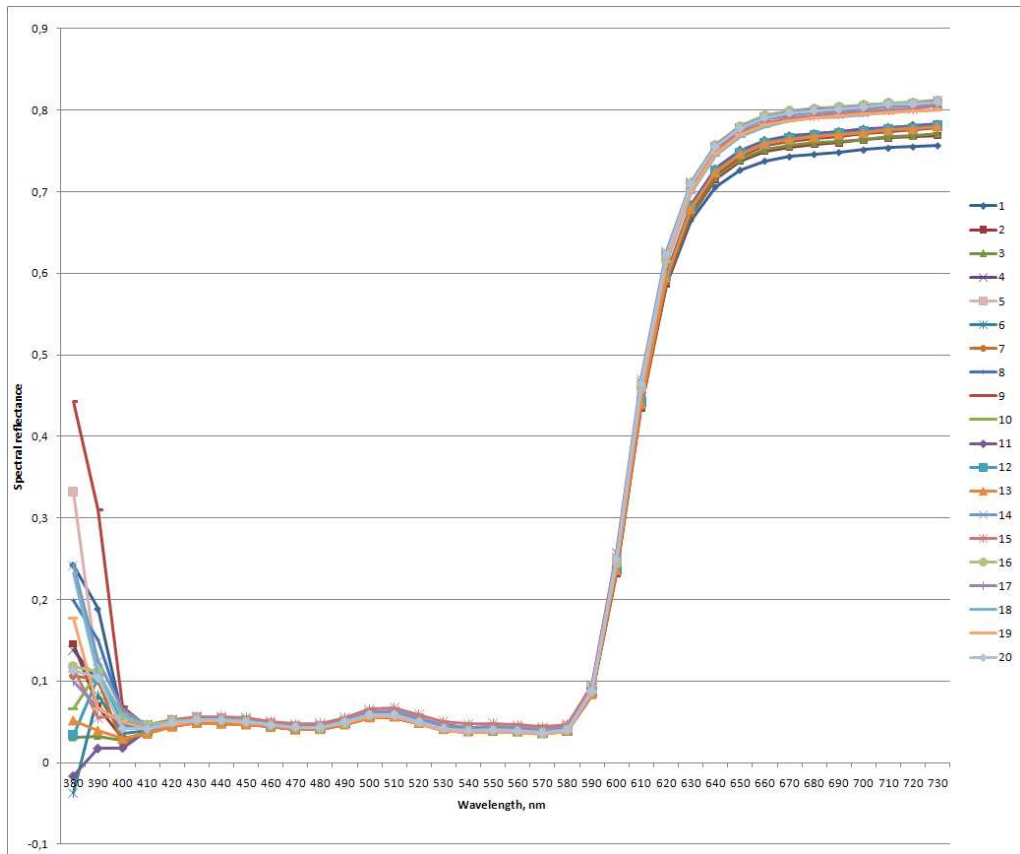
Figure 65: Spectral reflectance for patch T4(20 successive)

Measurement	Average delta CIELAB	Max delta CIELAB	Average of average
1	1.15	11.57	1.007
2	1.2	10.88	1.007
3	0.94	11.22	1.007
4	0.79	11.36	1.007
5	0.81	11.36	1.007
6	0.92	11.79	1.007
7	0.79	11.55	1.007
8	0.73	11.47	1.007
9	0.97	10.62	1.007
10	1.37	33.14	1.007
11	0.89	11.96	1.007
12	0.88	10.47	1.007
13	0.72	11.77	1.007
14	2.91	89.5	1.007
15	0.76	12	1.007
16	0.77	12.23	1.007
17	0.97	11.83	1.007
18	0.85	12.28	1.007
19	0.82	1.74	1.007
20	0.9	11.96	1.007

Table 29: The color difference between average and single measurement(20 substrates)

Measurement	Average delta CIELAB	L^*	a^*	b^*	Average of average
1	3.58	41.69	64.63	45.72	3.4195
2	1.05	43.13	64.18	43.37	3.4195
3	0.4	43.09	63.62	42.15	3.4195
4	2.25	42.1	64.3	44.5	3.4195
5	3.13	42.11	64.89	45.27	3.4195
6	1.88	43.33	63.71	44.3	3.4195
7	2.22	42.03	64.63	44.33	3.4195
8	2.73	42.03	64.73	44.86	3.4195
9	0.58	43.05	64.15	42.82	3.4195
10	23.85	50.67	49	25.4	3.4195
11	3.3	42.05	65.07	45.38	3.4195
12	1.3	42.8	64.55	43.46	3.4195
13	1.25	42.51	64.69	43.16	3.4195
14	2.58	41.87	65.07	44.44	3.4195
15	2.77	42.02	64.95	44.82	3.4195
16	2.02	42.9	64.72	44.23	3.4195
17	3.81	41.87	65.59	45.65	3.4195
18	3.8	41.92	65.52	45.69	3.4195
19	1.96	42.76	64.79	44.12	3.4195
20	3.93	42.01	65.55	45.86	3.4195
av.	-	42.86	63.72	42.47	-

Table 30: The color difference between average and single measurement(20 substrates, patch J1)

Figure 66: ΔE_{ab}^* for 20 substrates measurements for color patch J1
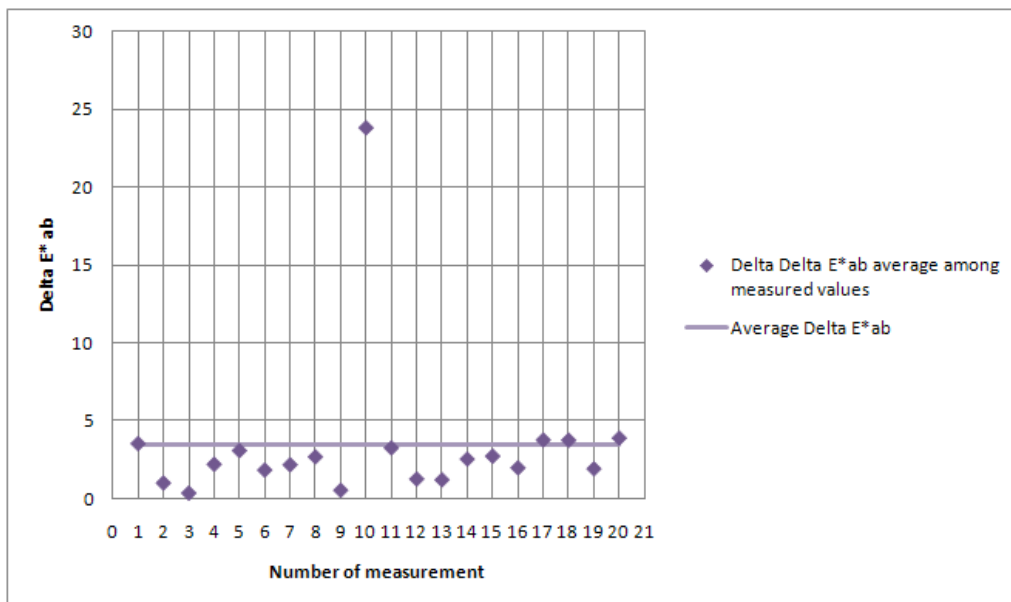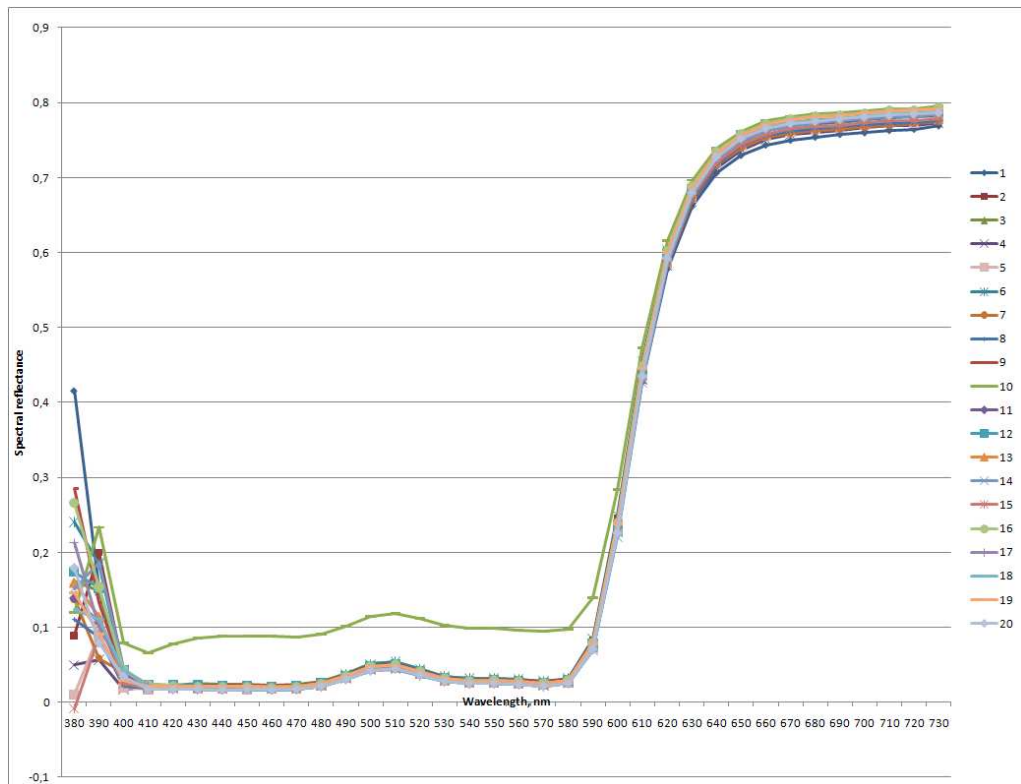
Figure 67: Spectral reflectance for patch J1(20 substrates)

Measurement	Average delta CIELAB	Max delta CIELAB	Average of average
1	0.41	1.54	0.586
2	0.38	1.51	0.586
3	0.38	8.16	0.586
4	0.45	1.74	0.586
5	0.38	1.82	0.586
6	2.45	12.79	0.586
7	0.38	1.37	0.586
8	0.36	1.61	0.586
9	0.33	1.34	0.586
10	0.34	1.7	0.586

Table 31: The color difference between average and single measurement(1 hour interval)

Measurement	Average delta CIELAB	L^*	a^*	b^*	Average of average
1	0.94	44.58	63.15	36.81	1.388
2	0.65	44.57	63.05	36.47	1.388
3	0.7	44.67	63.07	35.94	1.388
4	0.91	44.78	63.28	36.3	1.388
5	0.63	44.66	62.99	36.35	1.388
6	6.83	39.86	57.84	33.88	1.388
7	0.69	44.62	63.06	36.46	1.388
8	0.75	44.68	63.02	35.78	1.388
9	0.94	44.55	63.09	36.89	1.388
10	0.84	44.58	63.15	36.66	1.388
av.	-	44.19	62.61	36.17	-

Table 32: The color difference between average and single measurement(1 hour interval, patch J1)
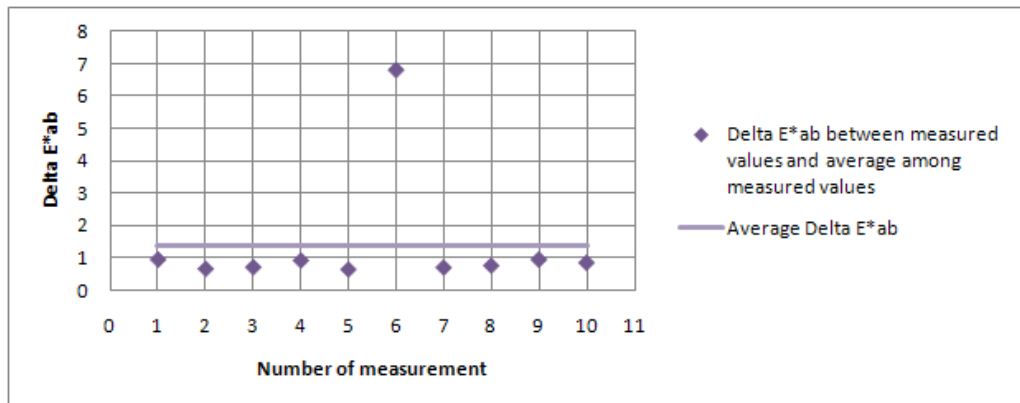
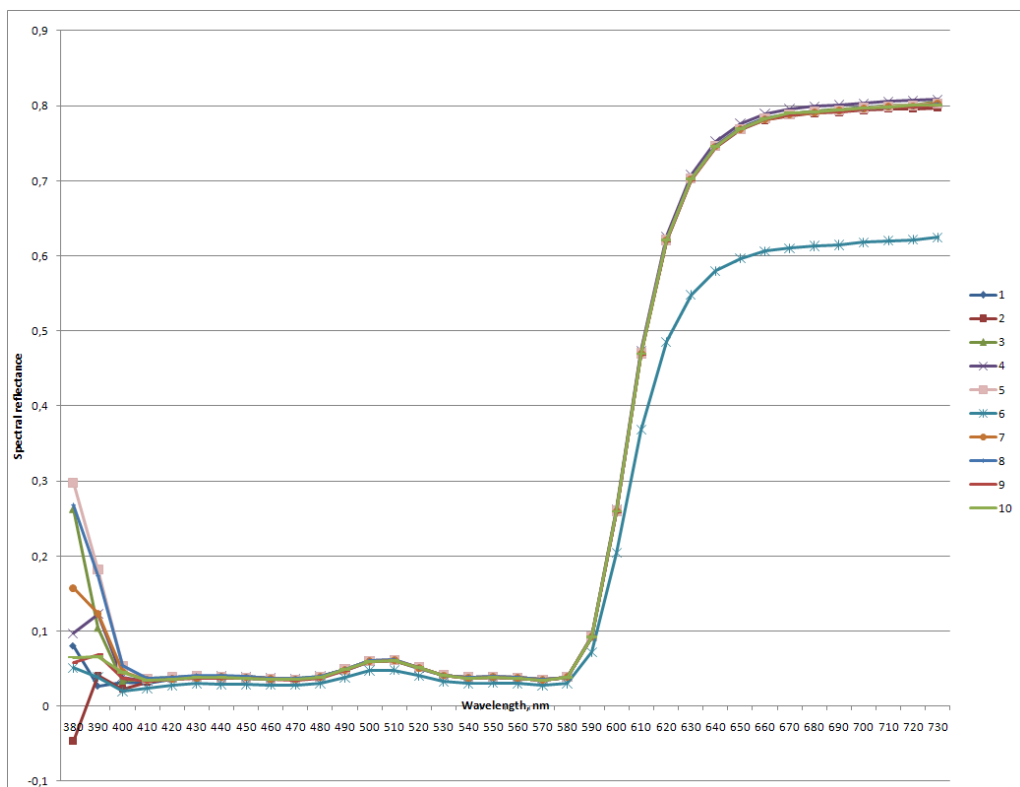Figure 68: ΔE_{ab}^* for 20 measurements with 1 hour repeatability for J1

Figure 69: Spectral reflectance for patch J1(1 hour repeatability)

Measurement	Average delta CIELAB	Max delta CIELAB	Average of average
1	0.4	7.36	0.2725
2	0.31	2.43	0.2725
3	0.22	1.97	0.2725
4	0.25	2.02	0.2725
5	0.27	1.84	0.2725
6	0.41	23.25	0.2725
7	0.24	2.06	0.2725
8	0.21	1.9	0.2725
9	0.29	1.99	0.2725
10	0.41	6.09	0.2725
11	0.24	2.2	0.2725
12	0.26	2.09	0.2725
13	0.27	1.89	0.2725
14	0.23	1.78	0.2725
15	0.19	1.82	0.2725
16	0.28	2.03	0.2725
17	0.39	17.22	0.2725
18	0.19	1.85	0.2725
19	0.19	1.99	0.2725
20	0.2	1.61	0.2725

Table 33: The color difference between average and single measurement(30 minutes interval)

Measurement	Average delta CIELAB	L^*	a^*	b^*	Average of average
1	1.94	44.92	62.35	34.91	0.5875
2	0.32	44.71	63.47	36.34	0.5875
3	0.37	44.89	63.53	36.41	0.5875
4	0.51	44.82	63.52	37	0.5875
5	0.43	44.82	63.57	36.88	0.5875
6	0.77	45.01	63.24	35.89	0.5875
7	0.76	44.7	63.57	37.29	0.5875
8	0.74	44.73	63.55	37.27	0.5875
9	1.12	44.77	63.7	37.64	0.5875
10	0.95	44.49	62.78	35.79	0.5875
11	0.46	44.46	63.1	36.23	0.5875
12	0.28	44.49	63.08	36.58	0.5875
13	0.29	44.45	63.11	36.52	0.5875
14	0.45	44.51	63.14	36.98	0.5875
15	0.48	44.56	63.25	37.05	0.5875
16	0.64	44.68	63.49	37.2	0.5875
17	0.3	44.66	63.36	36.29	0.5875
18	0.36	44.64	63.26	36.22	0.5875
19	0.37	44.53	63.32	36.93	0.5875
20	0.21	44.66	63.34	36.39	0.5875
av.	-	44.67	63.29	36.54	-

Table 34: The color difference between average and single measurement(30 hour interval, patch J1)
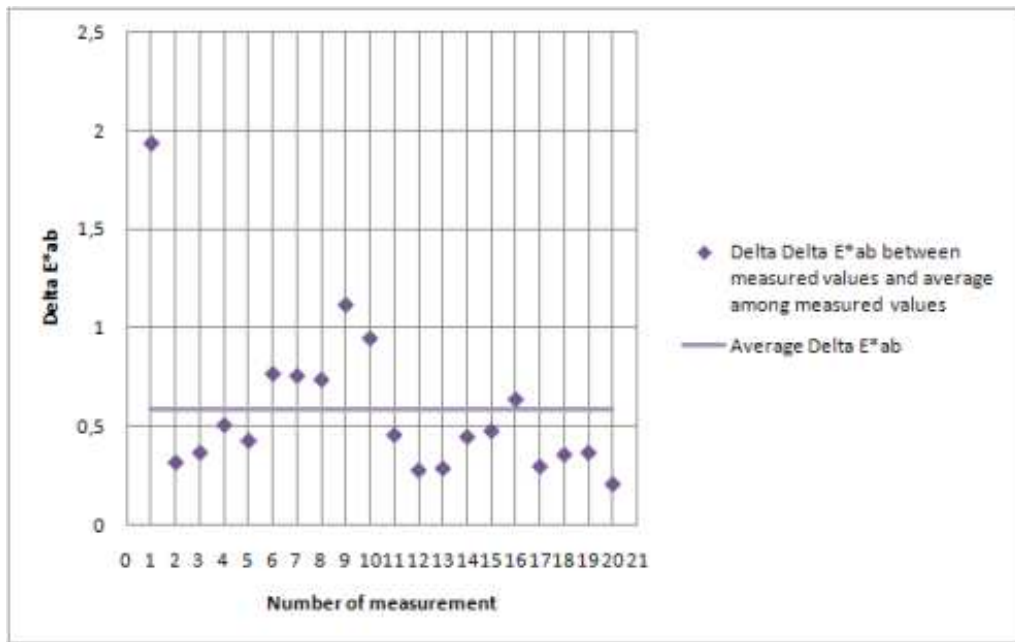
Figure 70: ΔE_{ab}^* for 20 measurements with 30 min repeatability for J1
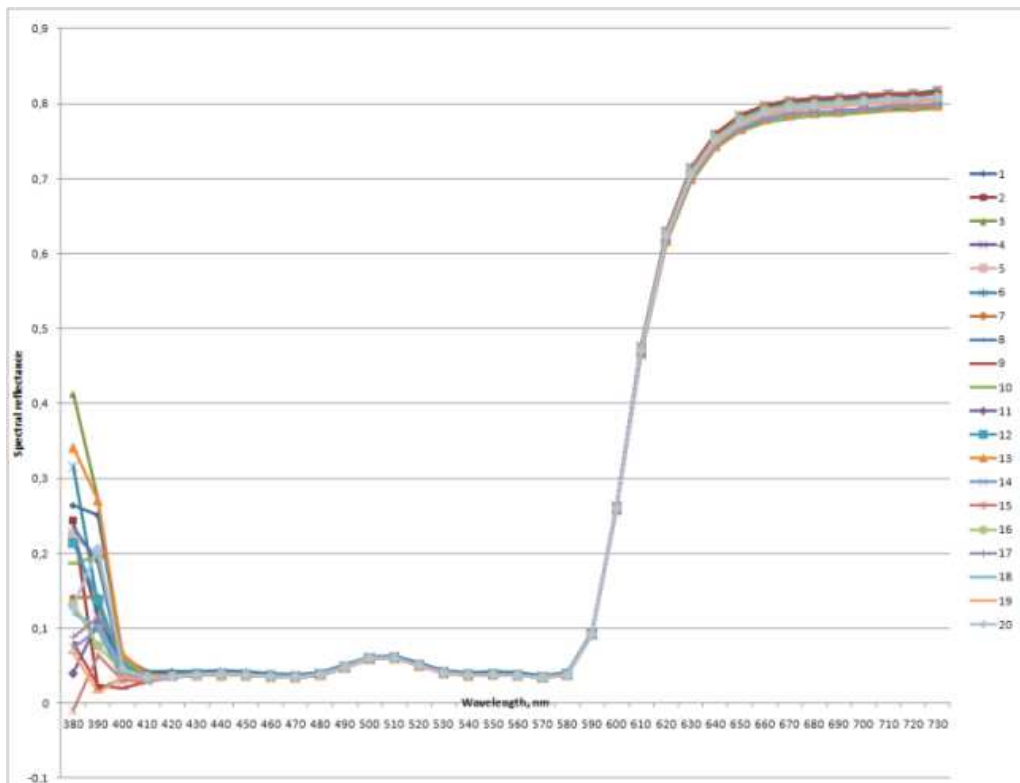

Figure 71: Spectral reflectance for patch J1(30 minutes repeatability)

E   Testing images samples
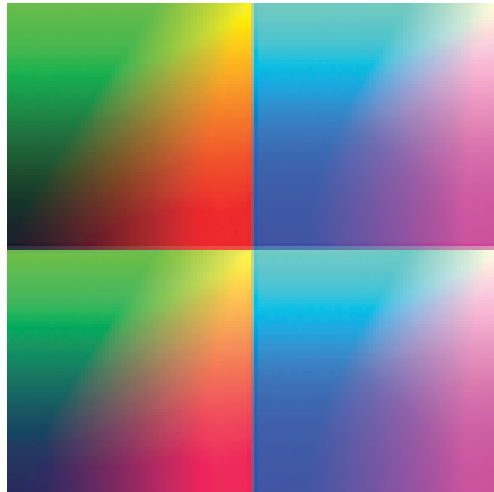
a) Four cubes
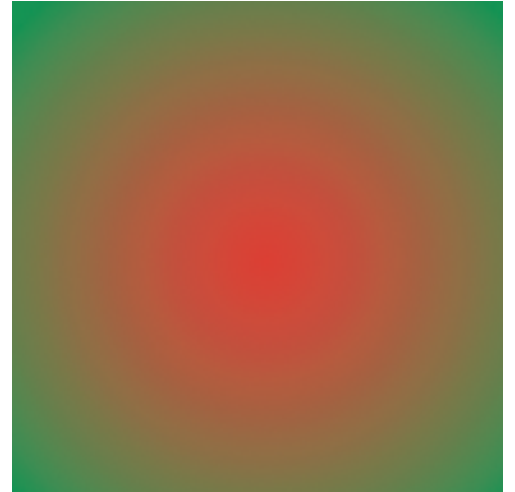
b) Red and green ball
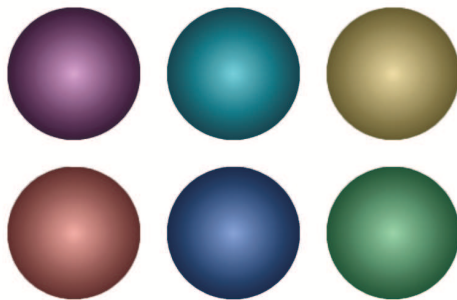
c) Six color balls
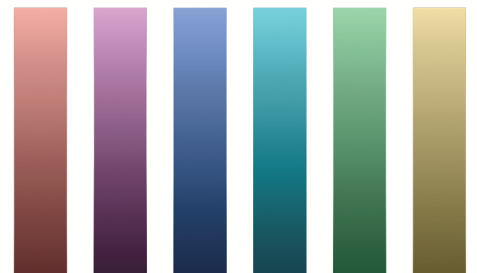
d) Six color stripes

Figure 72: Experimental images set
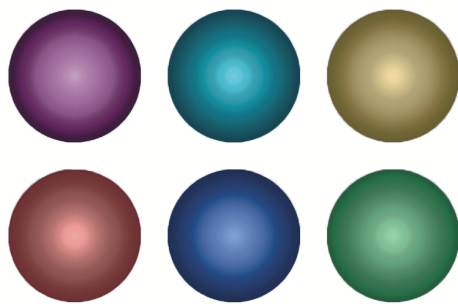
a) Six balls image converted to 3rd profile of 20 successive measurements
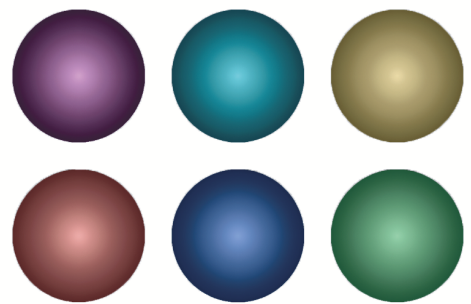
b) Red and green ball image converted to 3rd profile of 20 substrates measurements
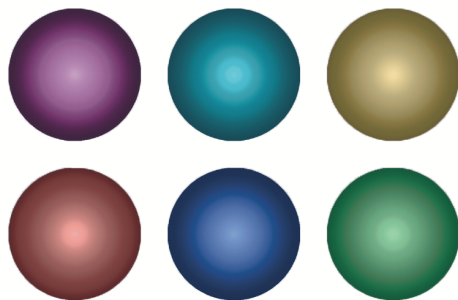
c) Six color balls image converted to 16th profile of 20 measurements(30 min. interval)
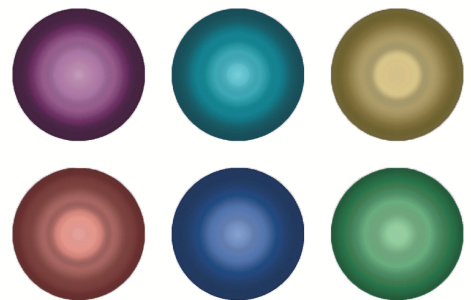
d) Six color balls image converted to 6th profile of 10 measurements(1 hour interval)

Figure 73: Examples of image Six color balls converted to different profiles
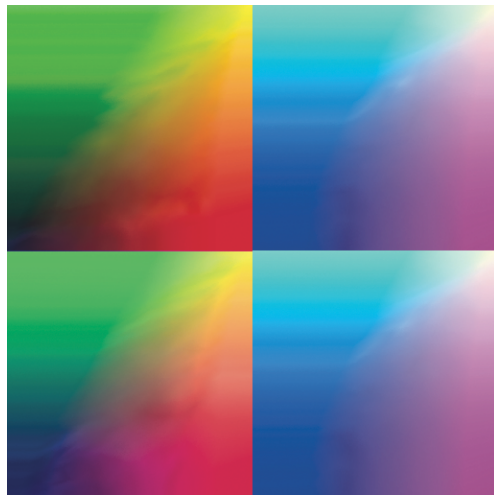
a) Four color cubes image converted to 7th profile of 20 successive measurements

b)Red and green ball image converted to 7th profile of 20 successive measurements
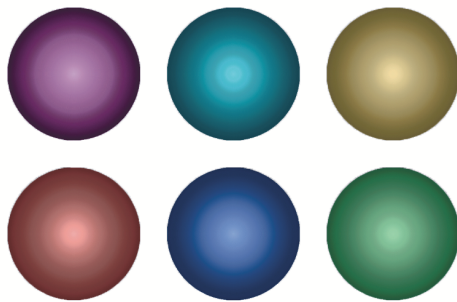
c) Six color balls image converted to converted to 7th profile of 20 successive measurements
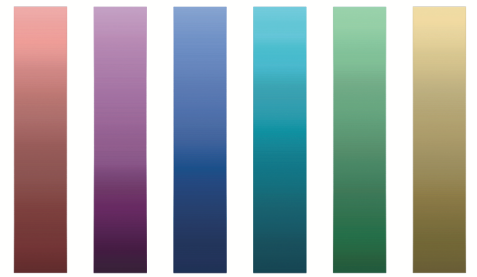
d) Six color stripes image converted to converted to 7th profile of 20 successive measurements

Figure 74: Examples of different images converted to 7th profile of 20 successive measurements
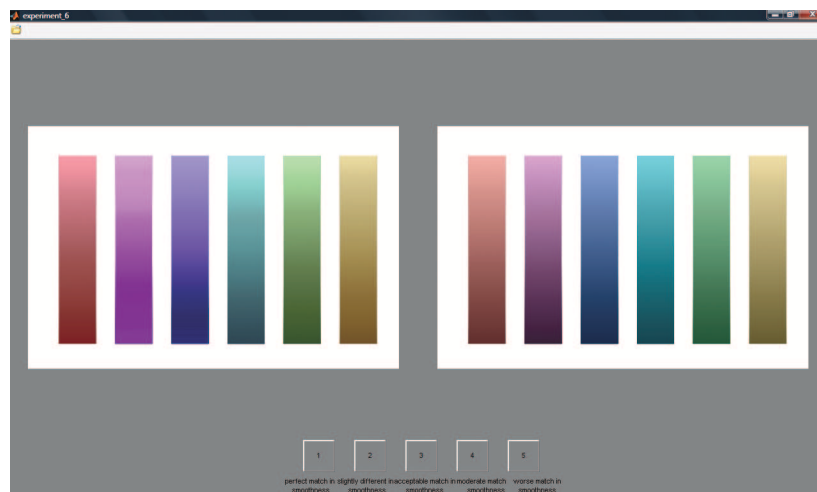
Figure 75: GUI for conducting psychophysical experiment

F   Visual judgements analysis

Table 35: Z-scores, MOSs, frequencies of each image in categories

Image	Z-scores	MOS	Cat.1	Cat.2	Cat.3	Cat.4	Cat.5
1	0.6745	4.25	0	0	0	15	5
2	-0.1257	4.55	0	0	0	9	11
3	0.3853	4.35	0	0	0	13	7
4	-0.5483	3.95	0	1	3	12	4
5	-1.0151	4.60	0	0	1	6	13
6	-0.6958	4.35	0	0	1	11	8
7	-0.1226	4.05	0	0	2	15	3
8	-0.3256	4.20	0	0	3	10	7
9	-1.0174	4.40	0	1	1	7	11
10	-0.6689	4.05	0	1	2	12	5
11	-0.6689	4.05	0	1	2	12	5
12	-0.8224	4.45	0	0	1	9	10
13	-1.0547	4.35	0	1	0	10	9
14	-0.7596	4.40	0	0	1	10	9
15	-1.2336	4.35	1	0	0	9	10
16	-0.3915	4.25	0	0	3	9	8
17	0.2533	4.40	0	0	0	12	8
18	0.1257	4.45	0	0	0	11	9
19	-0.4481	4.25	0	0	2	11	7
20	-0.1257	4.55	0	0	0	9	11
21	0.2751	3.25	0	4	9	5	2
22	-0.0844	3.60	0	1	7	11	1
23	0.4519	3.15	0	5	8	6	1
24	0.1184	3.50	0	3	5	11	1
25	-0.1961	3.20	1	4	7	6	2
26	-0.4208	3.30	0	4	6	10	0
27	-0.2868	2.75	2	6	7	5	0
28	0.0561	3.00	2	4	7	6	1
29	-0.1284	3.65	0	1	6	12	1
30	0.0000	4.00	0	0	3	14	3
31	-0.4272	2.90	2	3	10	5	0
32	-0.1630	3.60	0	1	8	9	2
33	-0.6689	3.05	1	2	12	5	0
34	-0.6745	4.75	0	0	0	5	15

Image	z-scores	MOS	Cat.1	Cat.2	Cat.3	Cat.4	Cat.5
35	0.0561	3.00	2	4	7	6	1
36	-0.5483	2.95	1	4	10	5	0
37	0.1707	3.35	0	6	4	7	3
38	0.4983	3.10	0	5	9	5	1
39	0.6348	2.95	0	9	4	6	1
40	-0.2744	3.20	0	5	6	9	0
41	-0.2533	4.60	0	0	0	8	12
42	-1.1114	4.25	1	0	1	9	9
43	-1.1039	4.50	0	1	1	5	13
44	-0.3256	4.20	0	0	3	10	7
45	-0.1257	4.55	0	0	0	9	11
46	-0.3065	3.80	0	2	3	12	3
47	-0.0974	4.05	0	0	3	13	4
48	-0.7201	3.90	2	0	2	10	6
49	-0.7444	4.15	0	1	3	8	8
50	0.0000	4.00	0	0	3	14	3
51	-0.8572	3.95	1	0	5	7	7
52	-0.3580	4.25	0	0	4	7	9
53	-0.9218	4.20	0	1	0	13	6
54	-0.5478	4.00	0	2	1	12	5
55	-0.5793	4.05	0	2	2	9	7
56	-0.4976	4.00	0	3	1	9	7
57	-0.7190	4.10	0	1	2	11	6
58	-0.7004	4.10	0	1	3	9	7
59	-1.0174	4.40	0	1	1	7	11
60	-1.0599	4.45	0	1	1	6	12
61	0.0000	4.00	0	0	5	10	5
62	-0.6298	4.30	0	0	1	12	7
63	-0.3035	4.15	0	0	2	13	5
64	-0.7653	4.15	0	1	2	10	7
65	-0.6958	4.35	0	0	1	11	8
66	0.3372	1.75	10	5	5	0	0
67	0.7004	1.90	7	9	3	1	0
68	0.5182	1.65	10	7	3	0	0
69	0.4829	2.05	5	11	2	2	0
70	0.5236	2.00	7	8	3	2	0
71	0.7051	2.15	7	7	3	2	1
72	0.5676	1.95	8	7	3	2	0
73	0.7004	1.90	7	9	3	1	0
74	0.3915	1.75	8	9	3	0	0
75	0.4463	2.45	2	11	4	2	1

Image	z-scores	MOS	Cat.1	Cat.2	Cat.3	Cat.4	Cat.5
76	0.7869	1.80	9	7	3	1	0
77	0.8853	1.50	11	8	1	0	0
78	0.4735	2.05	7	7	4	2	0
79	-0.5043	3.70	3	1	2	7	7
80	0.7077	1.80	10	6	2	2	0
81	0.8519	1.75	9	8	2	1	0
82	0.4836	1.65	11	5	4	0	0
83	0.8519	1.75	9	8	2	1	0
84	0.6020	1.90	10	4	4	2	0
85	0.1446	1.90	7	8	5	0	0
86	-0.8365	4.05	2	0	1	9	8
87	-0.9274	4.10	1	1	1	9	8
88	-0.6449	4.45	0	0	3	5	12
89	0.1257	4.45	0	0	0	11	9
90	-0.2941	4.20	0	0	4	8	8
91	-0.2744	2.20	5	6	9	0	0
92	0.3522	2.25	4	8	7	1	0
93	0.7316	2.15	4	12	2	1	1
94	-0.3915	2.25	3	9	8	0	0
95	0.2101	2.30	3	10	5	2	0
96	0.6386	1.95	8	6	5	1	0
97	0.0073	2.40	1	12	5	2	0
98	-0.4554	2.30	3	8	9	0	0
99	0.7431	2.20	4	10	5	0	1
100	-0.0419	2.55	2	7	9	2	0
101	0.0419	2.45	3	8	6	3	0
102	0.0027	2.45	2	10	5	3	0
103	0.0723	2.90	1	6	8	4	1
104	-0.1184	2.50	1	11	5	3	0
105	0.0000	2.50	2	8	8	2	0
106	0.0000	2.50	2	8	8	2	0
107	-0.5779	2.35	2	9	9	0	0
108	-0.0844	2.60	2	6	10	2	0
109	0.2028	2.40	3	7	9	1	0
110	-0.0817	2.55	2	8	7	3	0
111	1.0222	1.55	13	4	2	1	0
112	0.3580	1.75	9	7	4	0	0
113	1.0599	1.55	12	6	1	1	0
114	0.8938	1.70	10	7	2	1	0
115	0.6408	1.60	10	8	2	0	0
116	1.1810	1.50	12	7	0	1	0

Image	z-scores	MOS	Cat.1	Cat.2	Cat.3	Cat.4	Cat.5
117	0.9336	1.70	9	9	1	1	0
118	1.1385	1.55	11	8	0	1	0
119	0.5141	1.70	8	10	2	0	0
120	0.6447	1.95	7	8	4	1	0
121	0.8707	1.70	11	5	3	1	0
122	0.5779	1.65	9	9	2	0	0
123	0.4554	1.70	9	8	3	0	0
124	0.4276	2.15	3	12	4	1	0
125	0.2744	1.80	9	6	5	0	0
126	0.9491	1.45	12	7	1	0	0
127	0.8007	1.85	6	12	1	1	0
128	0.5182	1.65	10	7	3	0	0
129	0.3372	1.75	10	5	5	0	0
130	0.2941	1.80	8	8	4	0	0
131	-0.2282	2.15	4	9	7	0	0
132	0.0073	2.40	1	12	5	2	0
133	0.2024	2.35	5	5	8	2	0
134	0.1446	1.90	7	8	5	0	0
135	0.0844	2.40	3	9	5	3	0
136	-0.7426	3.90	1	2	2	8	7
137	0.0578	3.00	2	5	5	7	1
138	-0.2379	3.25	1	3	8	6	2
139	0.0750	3.95	0	0	6	9	5
140	-0.3580	3.25	0	4	7	9	0
141	0.2049	2.80	2	5	9	3	1
142	0.2495	3.30	0	2	11	6	1
143	-0.1053	3.15	1	4	7	7	1
144	-0.3015	2.80	3	5	5	7	0
145	-0.0419	3.55	0	1	8	10	1
146	0.3762	2.65	3	4	11	1	1
147	-0.4519	2.85	1	6	8	5	0
148	-0.3918	2.90	3	3	7	7	0
149	-0.1284	3.65	0	1	6	12	1
150	0.0908	2.95	2	6	4	7	1
151	-0.4983	2.90	1	5	9	5	0
152	-0.6132	4.00	0	1	2	13	4
153	-0.1510	3.30	2	2	5	10	1
154	0.0419	3.45	0	2	9	7	2
155	-0.3786	3.20	0	2	12	6	0
156	-0.4983	2.90	1	5	9	5	0
157	-0.2943	2.75	2	7	5	6	0

Image	z-scores	MOS	Cat.1	Cat.2	Cat.3	Cat.4	Cat.5
158	-0.2126	2.70	3	6	5	6	0
159	-0.1494	2.65	3	5	8	4	0
160	0.0419	2.45	5	6	4	5	0
161	-0.3096	2.70	1	8	7	4	0
162	0.0287	2.45	4	8	3	5	0
163	0.4746	2.45	3	9	5	2	1
164	0.4258	2.50	3	9	4	3	1
165	0.2411	2.70	4	6	4	4	2
166	0.0817	2.45	3	7	8	2	0
167	0.2518	2.75	3	6	5	5	1
168	-0.3522	2.75	1	7	8	4	0
169	0.0185	3.05	2	3	8	6	1
170	0.1173	2.95	3	3	7	6	1
171	-0.0419	2.55	4	5	7	4	0
172	-0.2311	2.70	2	6	8	4	0
173	-0.2442	2.70	2	7	6	5	0
174	-0.0557	2.55	4	6	5	5	0
175	-0.0419	2.55	3	6	8	3	0
176	-0.1662	3.65	0	2	6	9	3
177	0.0419	3.45	0	1	10	8	1
178	-1.3647	4.55	1	0	0	5	14
179	0.0280	3.60	0	3	3	13	1
180	0.0000	3.50	0	2	8	8	2

profile	z-score	MOS	Cat.1	Cat.2	Cat.3	Cat.4	Cat.5
1	-0.4282	3.5375	6	10	14	35	15
2	-0.5373	3.4625	6	13	15	30	16
3	-0.2476	3.7375	7	15	12	30	16
4	-0.4347	3.5625	3	11	20	29	17
5	-0.4888	3.4125	3	14	16	31	16
6	-0.7399	3.7625	11	11	20	22	16
7	-0.4673	3.625	1	14	22	30	13
8	-0.4016	3.5625	4	13	19	30	14
9	-0.7016	3.6625	7	18	12	26	17
10	-0.5365	3.4625	2	11	21	33	13
11	-0.5201	3.4125	6	16	20	25	13
12	-0.3753	3.575	3	17	16	28	16
13	-0.6338	3.5375	4	11	18	30	17
14	-0.3254	3.2625	1	13	13	32	21
15	-0.5266	3.5	5	15	13	24	23
16	-0.4894	3.4625	3	13	25	26	13
17	-0.1963	3.35	2	10	12	37	19
18	-0.5596	3.55	4	8	17	36	15
19	-0.4084	3.2875	3	10	22	29	16
20	-0.2854	3.5625	2	10	20	29	19
21	0.6206	2.3625	24	18	25	11	2
22	0.2030	2.375	18	24	19	18	1
23	0.3152	3.4125	25	24	17	13	1
24	0.5597	2.3875	18	26	17	18	1
25	0.1330	2.175	23	26	16	13	2
26	-0.3270	2.3875	20	26	16	17	1
27	0.5928	2.3	23	30	14	13	0
28	0.3384	2.2875	23	30	15	10	2
29	0.5516	2.3625	19	29	15	15	2
30	0.7239	2.5	13	25	15	21	6
31	0.7262	2.2625	25	22	24	9	0
32	0.5658	2.475	23	24	16	14	3
33	0.1461	2.3125	18	24	27	11	0
34	0.7433	2.4125	8	16	14	19	23
35	0.5815	2.2125	24	19	21	14	2
36	0.6431	2.225	26	24	20	10	0
37	0.6279	2.4	19	29	17	12	3
38	0.2809	2.775	21	27	20	11	1
39	0.7137	2.2125	24	24	18	13	1
40	0.5742	2.3875	18	27	23	12	0
41	-0.4906	3.6125	6	11	14	26	23
42	-0.5030	3.55	3	14	17	28	18
43	-0.7423	3.9625	6	6	12	17	39
44	-0.4164	3.5375	7	11	11	34	17
45	-0.5913	3.6625	3	11	17	28	21

Table 36: Z-scores, MOSs, frequencies for each profile

Observer	Chi-square	dF	Critical Chi-square	Result
1	169.3355	176	146.317937	$\chi_c^2 < \chi_{emp}^2$ H0 is rejected
2	176.3118	176	146.317937	$\chi_c^2 < \chi_{emp}^2$ H0 is rejected
3	199.5038	176	146.317937	$\chi_c^2 < \chi_{emp}^2$ H0 is rejected
4	123.0876	88	67.373234	$\chi_c^2 < \chi_{emp}^2$ H0 is rejected
5	185.8632	176	146.317937	$\chi_c^2 < \chi_{emp}^2$ H0 is rejected
6	78.96465	132	106.458637	$\chi_c^2 > \chi_{emp}^2$ H0 is not rejected
7	175.2363	176	146.317937	$\chi_c^2 < \chi_{emp}^2$ H0 is rejected
8	181.905	176	146.317937	$\chi_c^2 < \chi_{emp}^2$ H0 is rejected
9	194.1223	176	146.317937	$\chi_c^2 < \chi_{emp}^2$ H0 is rejected
10	154.8573	176	146.317937	$\chi_c^2 < \chi_{emp}^2$ H0 is rejected
11	161.0763	176	146.317937	$\chi_c^2 < \chi_{emp}^2$ H0 is rejected
12	167.7949	176	146.317937	$\chi_c^2 < \chi_{emp}^2$ H0 is rejected
13	196.1439	176	146.317937	$\chi_c^2 < \chi_{emp}^2$ H0 is rejected
14	154.2132	176	146.317937	$\chi_c^2 < \chi_{emp}^2$ H0 is rejected
15	48.49778	88	67.373234	$\chi_c^2 > \chi_{emp}^2$ H0 is not rejected
16	199.0695	176	146.317937	$\chi_c^2 < \chi_{emp}^2$ H0 is rejected
17	173.4735	176	146.317937	$\chi_c^2 < \chi_{emp}^2$ H0 is rejected
18	177.8974	176	146.317937	$\chi_c^2 < \chi_{emp}^2$ H0 is rejected
19	164.4286	176	146.317937	$\chi_c^2 < \chi_{emp}^2$ H0 is rejected
20	219.9936	176	146.317937	$\chi_c^2 < \chi_{emp}^2$ H0 is rejected

Table 37: Chi-square Pearson criterion for first 20 observers
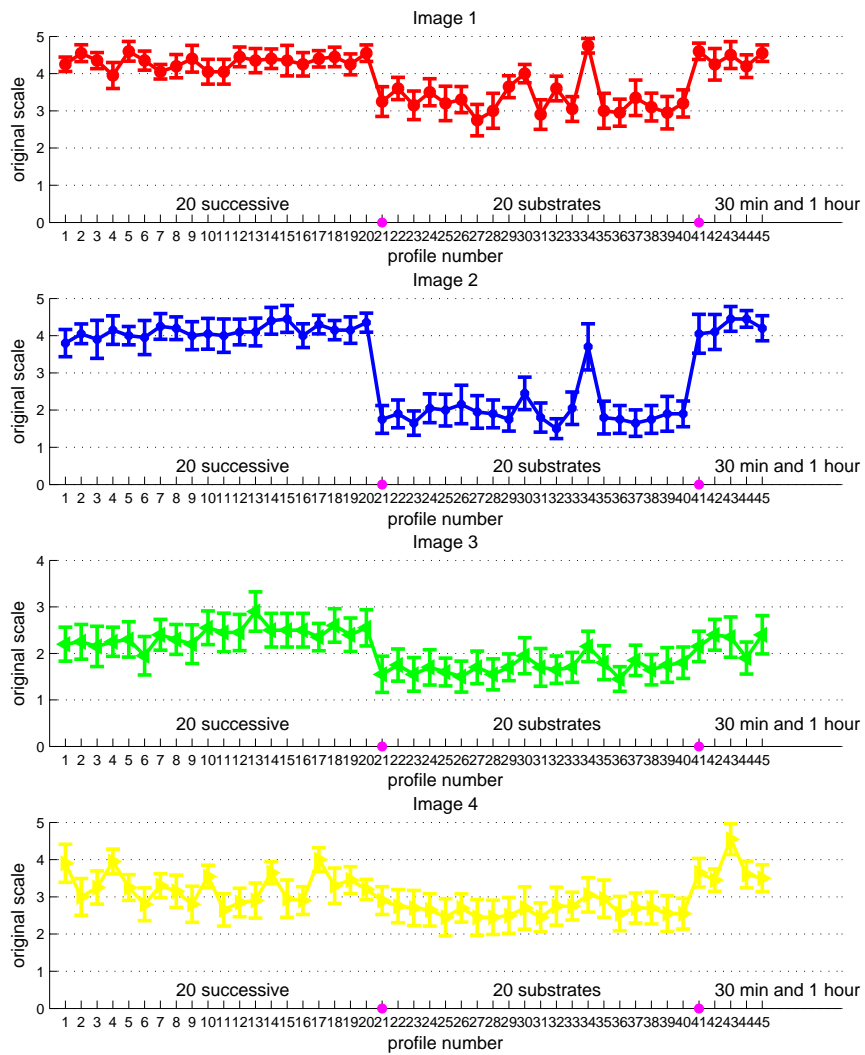
Figure 76: MOS and 95% confidence interval of images
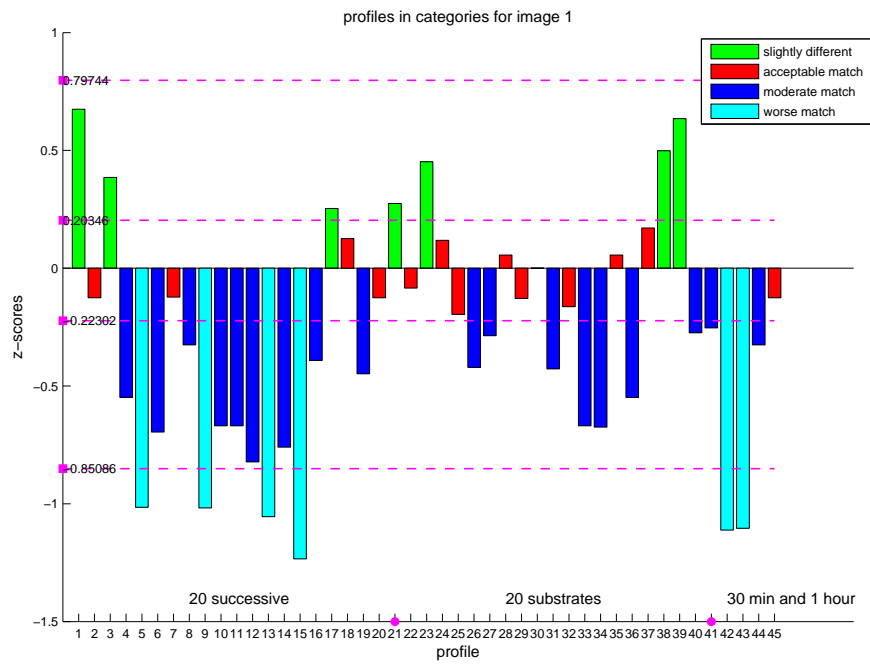
Figure 77: Image 1 reproductions categories
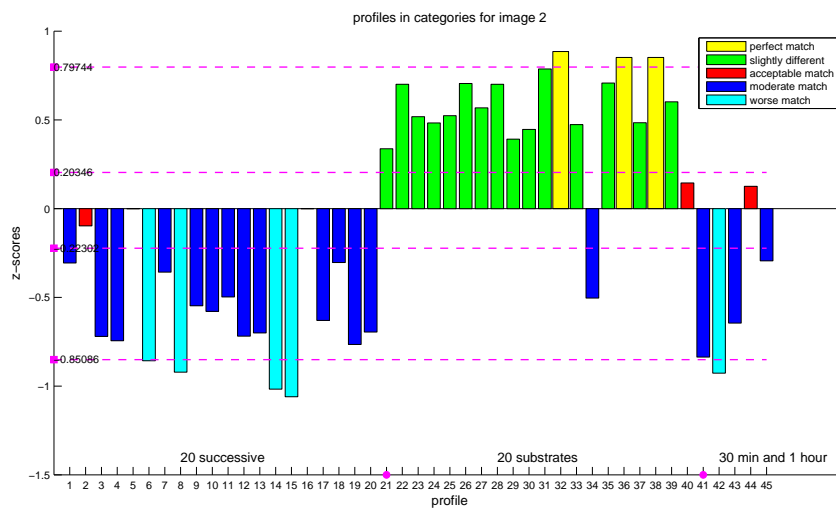
Figure 78: Image 2 reproductions categories
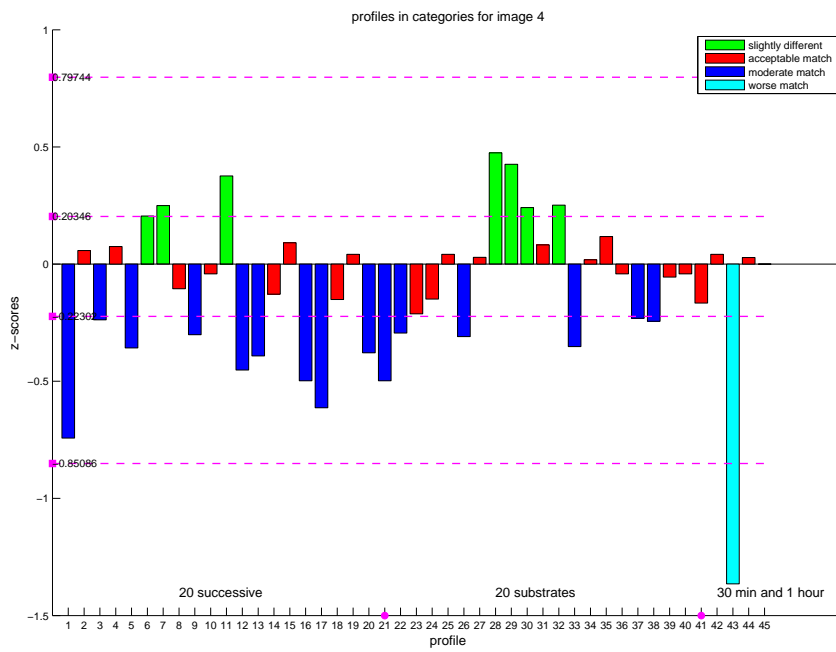
135
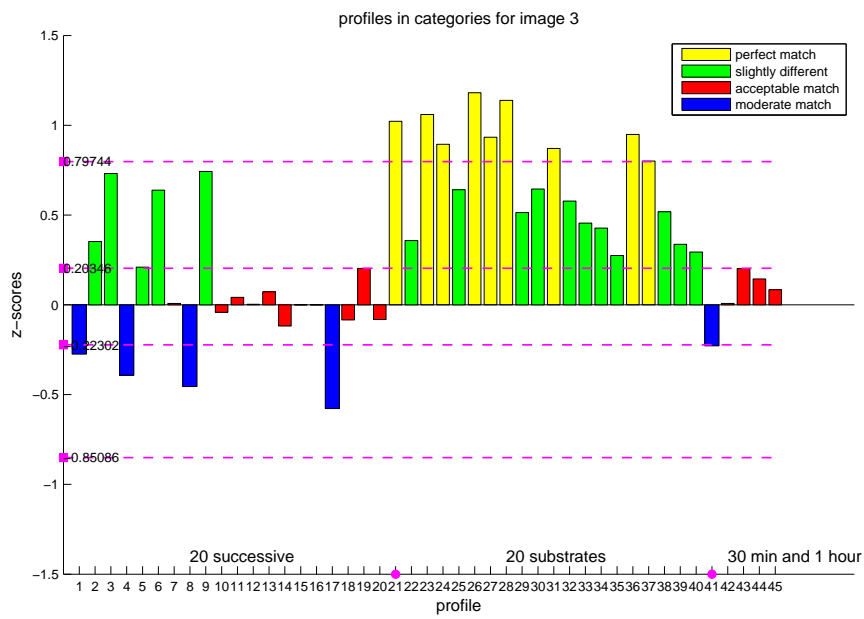
Figure 79: Image 3 reproductions categories

Figure 80: Image 4 reproductions categories

136
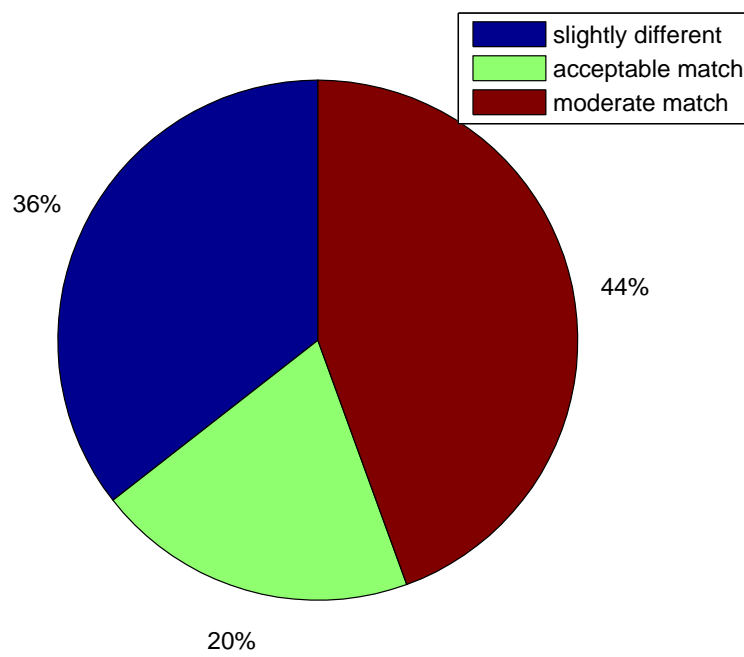
36%

44%

20%

slightly different
acceptable match
moderate match

Figure 81: Percentage of profiles in categories

G   Metrics and algorithms implementation

a)Entire RGBLUT;

b)Entire L*a*b*LUT;

c)Entire L*a*b*LUT;

d)Entire L*a*b*LUT
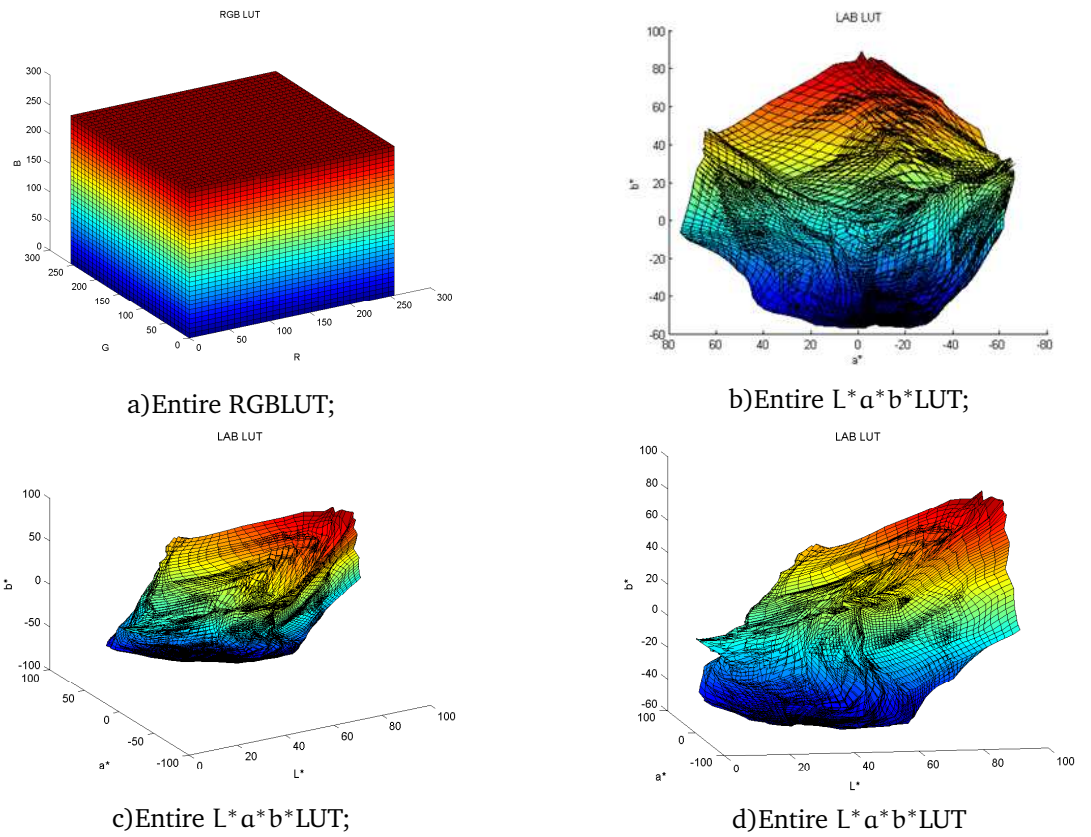
Figure 82: 3DLUTs RGB L*a*b*
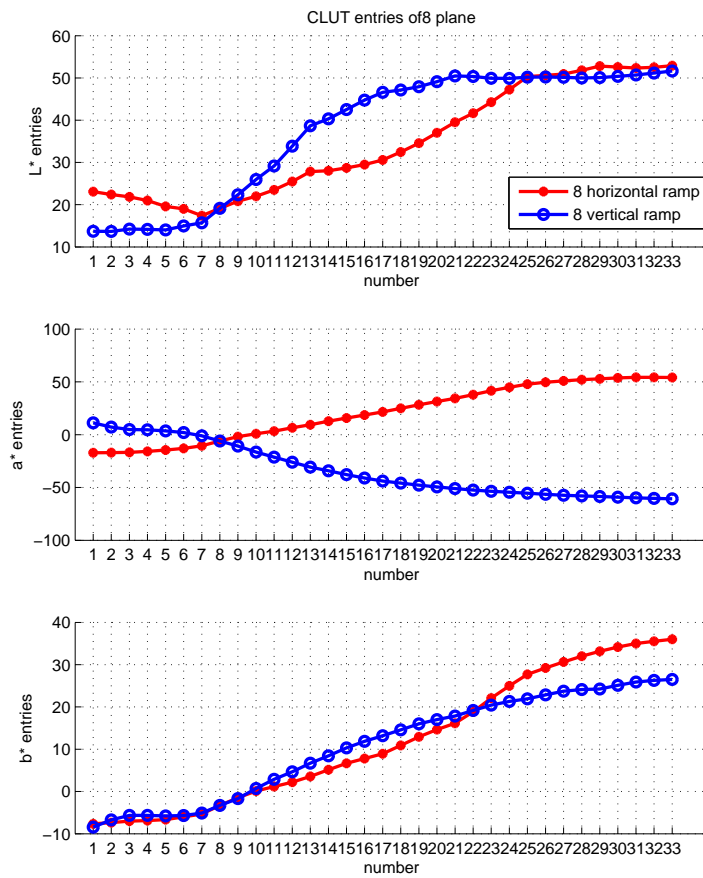
Figure 83: CLUT entries of 8th color plane
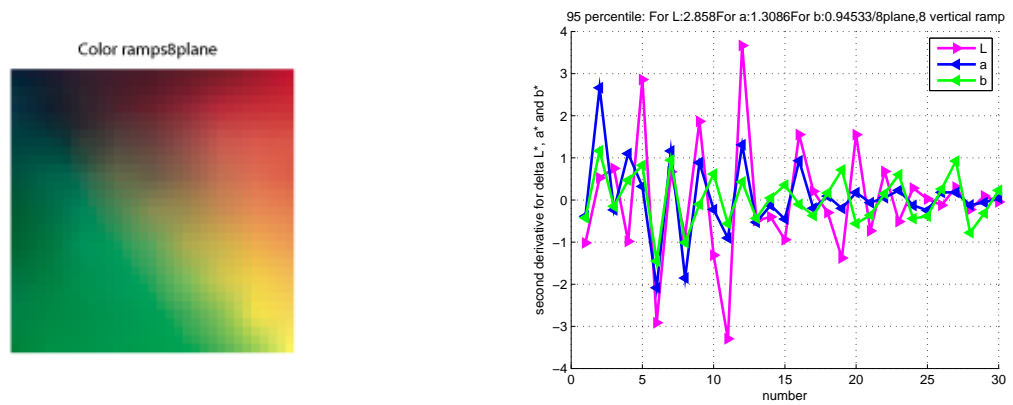
a)Eighth color plane;
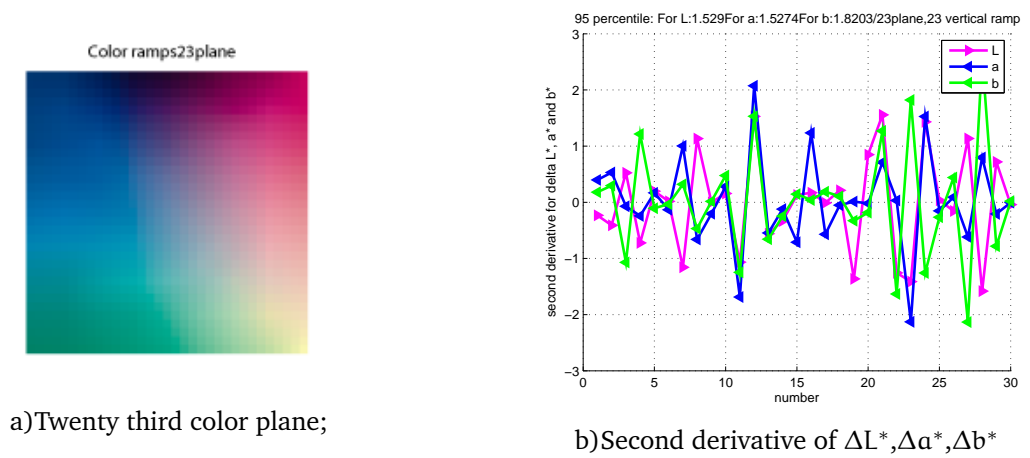
b)Second derivative of $\Delta L^*, \Delta a^*, \Delta b^*$

Figure 84: Eighth color plane and second derivative
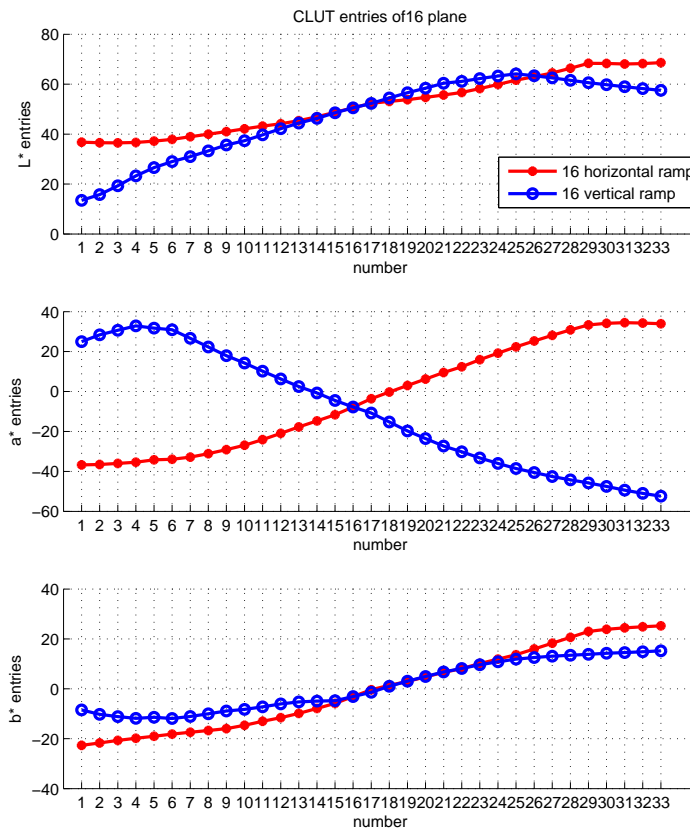
Figure 85: CLUT entries of 16th color plane
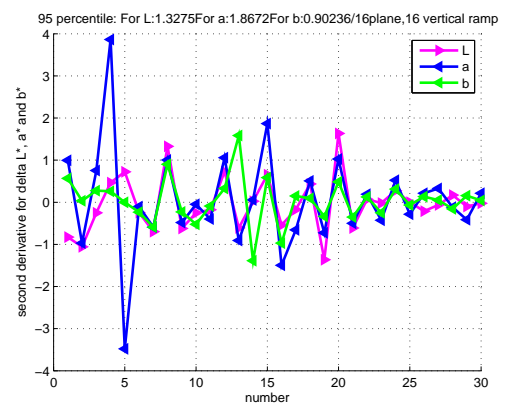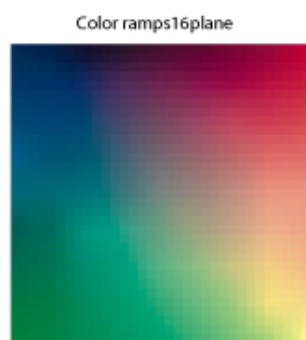
a)Sixteenth color plane;

b)Second derivative of $\Delta L^*, \Delta a^*, \Delta b^*$

Figure 86: Eighth color plane and second derivative
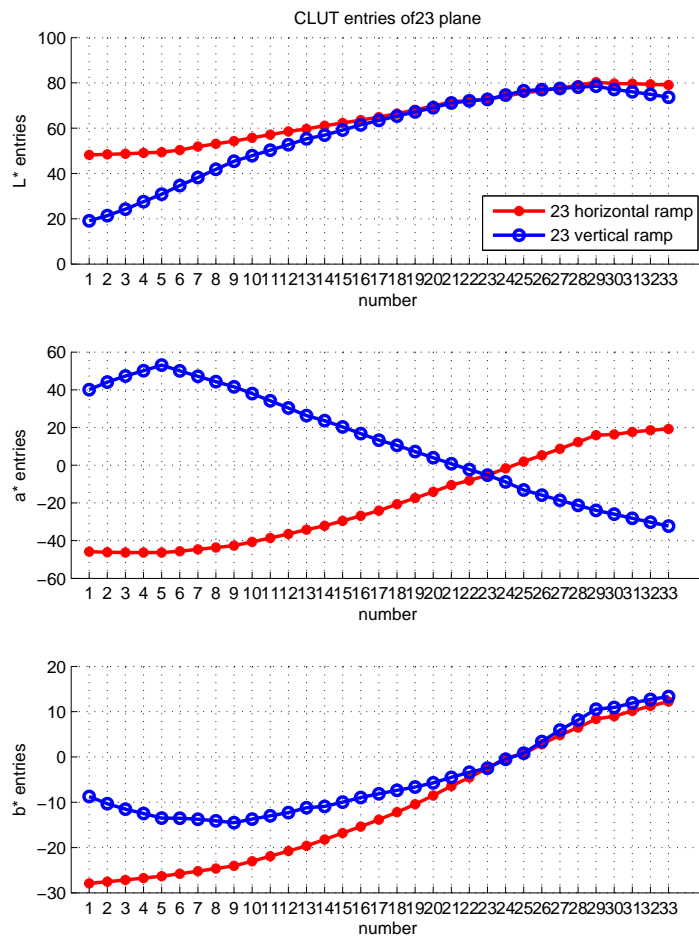
Figure 87: CLUT entries of 23d color plane

a)Twenty third color plane;

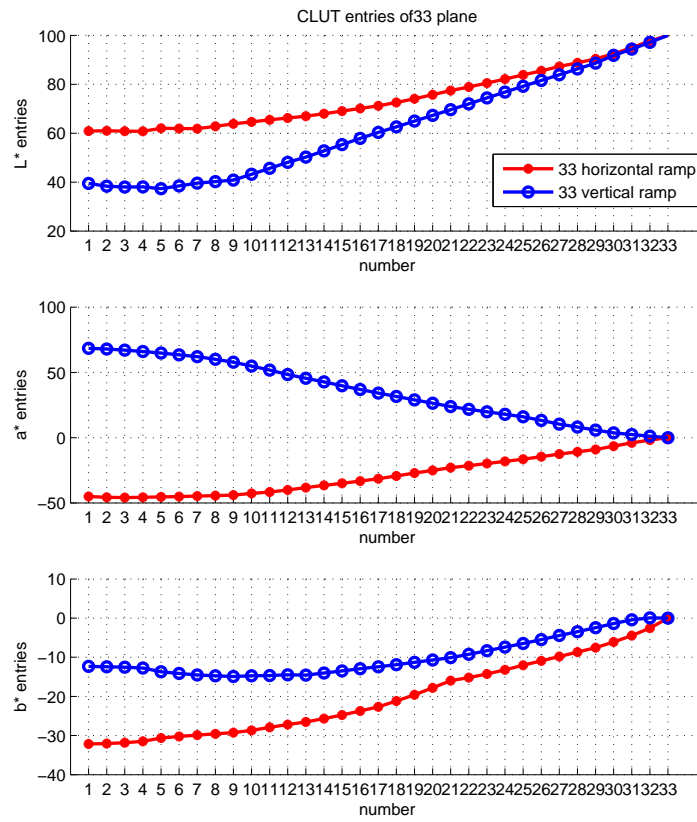b)Second derivative of $\Delta L^*, \Delta a^*, \Delta b^*$

Figure 88: Twenty third color plane and second derivative

Figure 89: CLUT entries of 33d color plane

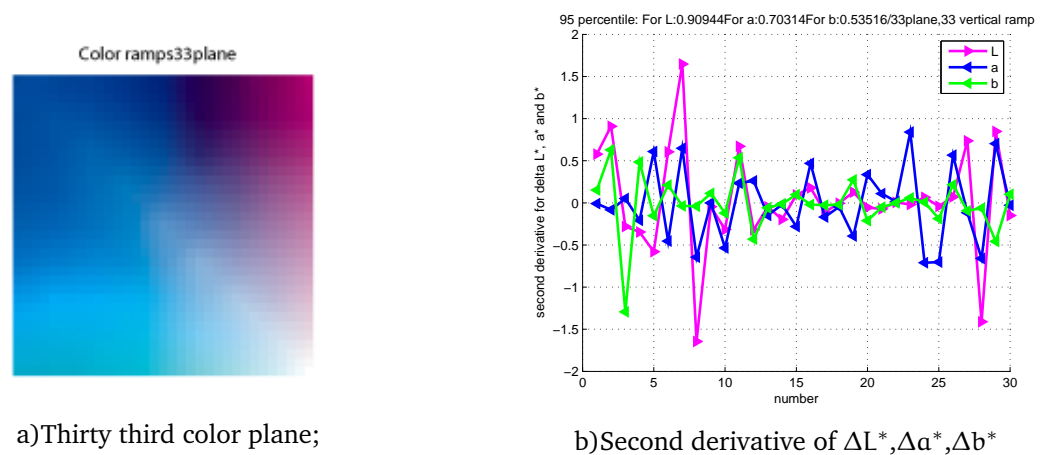a)Thirty third color plane;

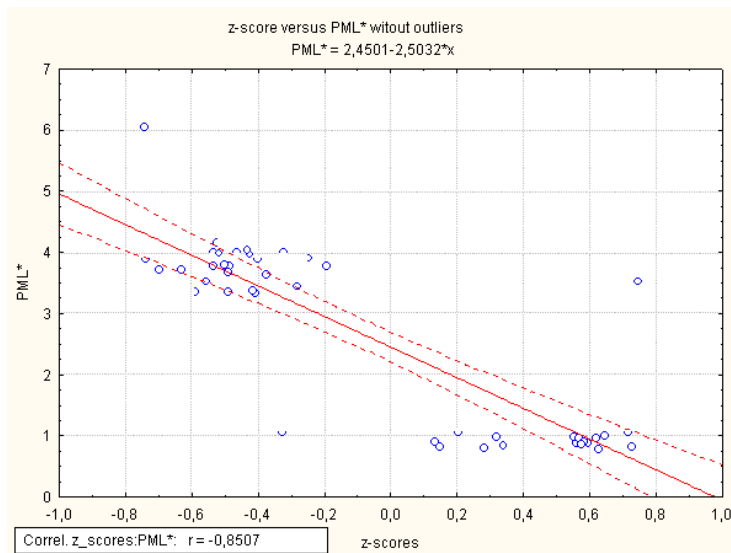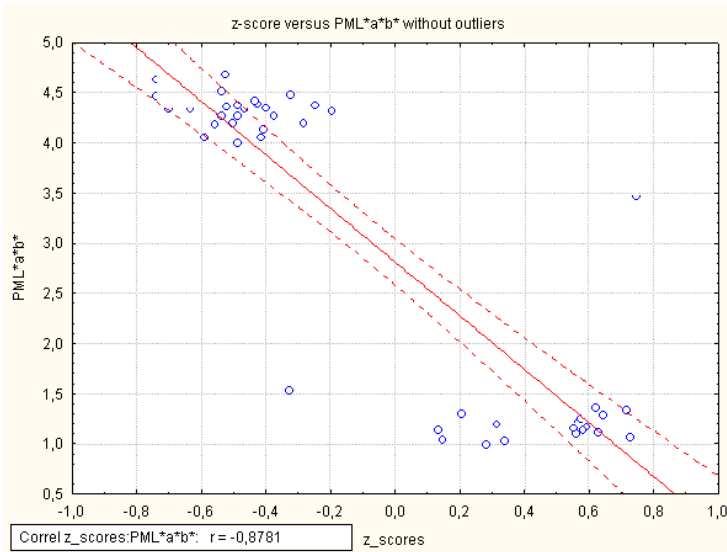b)Second derivative of $\Delta L^*, \Delta a^*, \Delta b^*$

Figure 90: Thirty third color plane and second derivative

H Algorithms and metrics comparison

a) Z-score versus PML* without outliers;

b) Z-score versus PML*a*b* without outliers

Figure 91: Scatter plot z-score versus PML* and PML*a*b*

Table 38: ΔE_{ab}^*, Adaptive bilateral filter, GSSIM, SSIM, SCIELAB, EdgeSim values

Image	z-score	ΔE_{ab}^*	ADF	GSSIM	SSIM	sCIELAB	EdgeSim	SC
1	0.6745	22.1304	21.9634	0.7880	0.9606	24.4707	9.1138	0.7826
2	-0.1257	21.2759	21.1052	0.8075	0.9634	24.0924	8.6177	0.7896
3	0.3853	21.4518	21.2875	0.8069	0.9621	24.1376	8.3777	0.7889
4	-0.5483	22.0300	21.8668	0.8069	0.9606	24.0886	8.6845	0.7832
5	-1.0151	21.4553	21.2871	0.8022	0.9619	23.9192	8.6757	0.7856
6	-0.6958	21.3438	21.1744	0.7993	0.9622	23.9209	8.7460	0.7869
7	-0.1226	21.9337	21.7683	0.8036	0.9611	24.1973	9.2948	0.7854
8	-0.3256	21.4781	21.3082	0.7988	0.9614	23.9608	8.7329	0.7851
9	-1.0174	21.1866	21.0183	0.7950	0.9617	23.8349	8.6668	0.7892
10	-0.6689	21.4322	21.2668	0.8002	0.9615	23.6160	8.9211	0.7847
11	-0.6689	21.5725	21.4053	0.7999	0.9608	23.8963	9.0572	0.7874
12	-0.8224	21.1651	20.9970	0.8054	0.9636	23.5927	8.7980	0.7891
13	-1.0547	21.3544	21.1885	0.7942	0.9607	23.7727	9.1378	0.7862
14	-0.7596	21.7864	21.6150	0.7891	0.9576	23.7893	9.4986	0.7805
15	-1.2336	21.5364	21.3607	0.7636	0.9534	23.5660	9.1696	0.7820
16	-0.3915	21.3363	21.1718	0.8044	0.9631	23.5456	8.7198	0.7884
17	0.2533	21.6404	21.4796	0.8026	0.9607	23.6197	9.7153	0.7878
18	0.1257	21.2705	21.1068	0.8017	0.9622	23.4738	9.4016	0.7882
19	-0.4481	21.2908	21.1277	0.8062	0.9622	23.5291	9.9632	0.7887
20	-0.1257	21.4947	21.3308	0.8015	0.9613	23.4669	9.8408	0.7848
21	0.2751	17.8583	17.7465	0.9207	0.9816	20.6537	8.3539	0.8108
22	-0.0844	18.6650	18.5648	0.9142	0.9800	21.1374	8.1683	0.8093
23	0.4519	18.3973	18.2985	0.9201	0.9821	20.9764	8.1483	0.8114
24	0.1184	18.3363	18.2380	0.9218	0.9825	21.0845	8.3203	0.8131
25	-0.1961	18.4577	18.3591	0.9200	0.9819	20.9989	8.3155	0.8098
26	-0.4208	18.3360	18.2344	0.9154	0.9815	20.9807	8.1882	0.8112
27	-0.2868	18.2844	18.1847	0.9181	0.9821	21.0096	7.9739	0.8139
28	0.0561	18.4777	18.3764	0.9218	0.9816	21.0900	8.9587	0.8114
29	-0.1284	18.8184	18.7185	0.9194	0.9810	21.2167	8.3203	0.8076
30	0	20.6530	20.5209	0.8277	0.9465	25.2024	7.9105	0.7793
31	-0.4272	18.2275	18.1283	0.9197	0.9819	20.9921	8.1433	0.8133
32	-0.163	18.7437	18.6465	0.9198	0.9806	21.2075	8.1982	0.8087
33	-0.6689	18.4763	18.3781	0.9214	0.9820	21.0070	8.4763	0.8116
34	-0.6745	20.0358	19.8893	0.8387	0.9493	23.2646	10.1478	0.7928
35	0.0561	18.4716	18.3725	0.9182	0.9815	21.0548	8.1783	0.8098
36	-0.5483	18.3656	18.2659	0.9196	0.9816	20.9287	8.0208	0.8106
37	0.1707	18.3521	18.2542	0.9193	0.9822	21.0727	8.4484	0.8132
38	0.4983	18.4235	18.3236	0.9221	0.9818	20.9861	8.4108	0.8119
39	0.6348	18.7026	18.6042	0.9203	0.9812	21.1126	8.4437	0.8085
40	-0.2744	18.1241	18.0265	0.9205	0.9822	20.8704	8.0620	0.8133

image	z-score	ΔE^*_{ab}	ADF	GSSIM	SSIM	sCIELAB	EdgeSim	SC
41	-0.2533	21.6596	21.4934	0.8140	0.9608	23.6126	9.9295	0.7898
42	-1.1114	21.9632	21.8028	0.8068	0.9616	23.4947	9.7785	0.7862
43	-1.1039	22.2524	22.0621	0.7577	0.9382	26.5374	10.3447	0.7798
44	-0.3256	21.5286	21.3582	0.8230	0.9644	23.5877	9.7329	0.7865
45	-0.1257	21.6636	21.4926	0.8168	0.9628	23.6482	10.3447	0.7878
46	-0.3065	2.1017	1.9907	0.9553	0.9915	0.9106	5.5613	0.9688
47	-0.0974	2.2538	2.1661	0.9537	0.9908	0.9380	5.3368	0.9721
48	-0.7201	2.3198	2.2285	0.9521	0.9896	0.9967	5.6041	0.9709
49	-0.7444	2.2378	2.1297	0.9576	0.9918	0.9850	5.7083	0.9715
50	0	2.2434	2.1394	0.9584	0.9918	0.9591	5.4626	0.9726
51	-0.8572	2.2924	2.2044	0.9613	0.9917	0.9853	5.7790	0.9720
52	-0.358	2.2246	2.1151	0.9529	0.9901	0.9472	5.6357	0.9704
53	-0.9218	2.2091	2.1042	0.9560	0.9910	0.9726	5.4288	0.9722
54	-0.5478	2.1768	2.0828	0.9537	0.9906	0.9335	5.1172	0.9719
55	-0.5793	2.1009	1.9952	0.9509	0.9905	0.9352	6.2231	0.9725
56	-0.4976	2.2276	2.1314	0.9506	0.9904	0.9647	5.1676	0.9717
57	-0.719	2.0840	1.9837	0.9537	0.9904	0.9185	5.4514	0.9725
58	-0.7004	2.1051	1.9966	0.9542	0.9900	0.9049	5.2171	0.9714
59	-1.0174	1.9602	1.8296	0.9571	0.9910	0.8753	5.7890	0.9723
60	-1.0599	2.5430	2.4403	0.9492	0.9865	0.9774	5.4514	0.9673
61	0	2.1123	2.0057	0.9570	0.9909	0.9505	5.4737	0.9722
62	-0.6298	2.2731	2.1429	0.9466	0.9871	0.9573	5.6252	0.9674
63	-0.3035	2.0231	1.8964	0.9525	0.9910	0.9349	5.5613	0.9726
64	-0.7653	1.9665	1.8196	0.9543	0.9905	0.8699	5.7890	0.9733
65	-0.6958	1.9543	1.8019	0.9489	0.9900	0.8688	6.2145	0.9718
66	0.3372	0.9204	0.8507	0.9815	0.9967	0.4182	4.0817	0.9893
67	0.7004	1.3808	1.3355	0.9789	0.9959	0.6374	4.7177	0.9853
68	0.5182	1.4293	1.3855	0.9780	0.9957	0.6489	5.0528	0.9854
69	0.4829	1.3915	1.3496	0.9801	0.9964	0.6368	5.2656	0.9866
70	0.5236	1.3761	1.3319	0.9804	0.9961	0.6326	5.0916	0.9859
71	0.7051	1.4780	1.4352	0.9804	0.9962	0.6715	4.4814	0.9853
72	0.5676	1.4695	1.4304	0.9806	0.9964	0.6617	4.2727	0.9865
73	0.7004	1.3747	1.3290	0.9785	0.9959	0.6410	5.6671	0.9856
74	0.3915	1.3783	1.3304	0.9808	0.9963	0.6369	5.2896	0.9864
75	0.4463	2.7449	2.7063	0.9483	0.9819	1.0709	7.5886	0.9666
76	0.7869	1.4081	1.3648	0.9798	0.9963	0.6437	4.8488	0.9862
77	0.8853	1.4069	1.3645	0.9792	0.9962	0.6599	4.7027	0.9856
78	0.4735	1.3465	1.3021	0.9817	0.9965	0.6328	5.4959	0.9863
79	-0.5043	3.2743	3.1843	0.9404	0.9668	0.9373	8.0000	0.9695
80	0.7077	1.3361	1.2886	0.9800	0.9961	0.6168	5.0788	0.9853
81	0.8519	1.4371	1.3926	0.9796	0.9957	0.6511	4.9597	0.9855

image	z-score	ΔE^*_{ab}	ADF	GSSIM	SSIM	sCIELAB	EdgeSim	SC
82	0.4836	1.4544	1.4145	0.9815	0.9965	0.6624	5.2171	0.9856
83	0.8519	1.3776	1.3276	0.9793	0.9960	0.6356	5.6671	0.9856
84	0.602	1.4389	1.3975	0.9809	0.9961	0.6657	4.5789	0.9852
85	0.1446	1.3723	1.3312	0.9806	0.9963	0.6293	4.2727	0.9860
86	-0.8365	2.0975	1.9503	0.9515	0.9899	0.8535	6.7092	0.9673
87	-0.9274	2.1776	2.0160	0.9500	0.9900	0.9069	7.0607	0.9665
88	-0.6449	2.2406	1.9887	0.8799	0.9601	1.0609	6.6343	0.9451
89	0.1257	1.9489	1.7931	0.9514	0.9898	0.7219	6.8328	0.9695
90	-0.2941	1.9795	1.8276	0.9521	0.9900	0.7311	6.8256	0.9696
91	-0.2744	2.1148	2.0752	0.9542	0.9968	1.2608	7.6174	0.9814
92	0.3522	2.2141	2.1783	0.9513	0.9963	1.2762	8.1028	0.9835
93	0.7316	2.2923	2.2574	0.9517	0.9963	1.3371	7.8079	0.9838
94	-0.3915	2.2376	2.1992	0.9531	0.9968	1.3341	7.8188	0.9839
95	0.2101	2.2513	2.2157	0.9530	0.9966	1.3188	7.5244	0.9838
96	0.6386	2.2495	2.2156	0.9500	0.9966	1.3122	7.8079	0.9833
97	0.0073	2.2195	2.1825	0.9522	0.9964	1.2817	7.8188	0.9832
98	-0.4554	2.2163	2.1777	0.9509	0.9965	1.3042	7.4889	0.9837
99	0.7431	2.1833	2.1439	0.9502	0.9963	1.2672	8.0415	0.9836
100	-0.0419	2.1234	2.0844	0.9501	0.9964	1.2643	7.6631	0.9841
101	0.0419	2.2215	2.1820	0.9517	0.9964	1.2951	8.0415	0.9839
102	0.0027	2.1181	2.0792	0.9528	0.9966	1.2619	7.6631	0.9841
103	0.0723	2.1529	2.1154	0.9510	0.9964	1.2640	8.1028	0.9838
104	-0.1184	2.0327	1.9872	0.9515	0.9966	1.2417	7.5595	0.9840
105	0	2.4829	2.4444	0.9423	0.9947	1.2935	8.2327	0.9802
106	0	2.1654	2.1261	0.9547	0.9967	1.3058	7.5828	0.9839
107	-0.5779	2.2806	2.2433	0.9513	0.9957	1.2933	7.5712	0.9821
108	-0.0844	2.1079	2.0682	0.9508	0.9966	1.2769	7.9264	0.9839
109	0.2028	2.0446	2.0020	0.9536	0.9966	1.2170	7.2177	0.9842
110	-0.0817	2.0267	1.9851	0.9534	0.9965	1.2084	7.4530	0.9829
111	1.0222	0.8918	0.8419	0.9681	0.9982	0.5094	5.0397	0.9935
112	0.358	1.4835	1.4600	0.9674	0.9980	0.9163	5.0658	0.9908
113	1.0599	1.5013	1.4788	0.9685	0.9979	0.9217	5.1426	0.9909
114	0.8938	1.4805	1.4569	0.9683	0.9981	0.9124	5.3832	0.9916
115	0.6408	1.4598	1.4349	0.9673	0.9980	0.9021	5.3133	0.9910
116	1.181	1.5624	1.5403	0.9688	0.9978	0.9611	5.8480	0.9902
117	0.9336	1.5362	1.5149	0.9693	0.9981	0.9361	5.5178	0.9914
118	1.1385	1.4694	1.4454	0.9664	0.9981	0.9172	5.7890	0.9908
119	0.5141	1.4621	1.4365	0.9686	0.9981	0.9070	5.5397	0.9915
120	0.6447	2.4923	2.4893	0.9433	0.9891	1.2967	7.0068	0.9772
121	0.8707	1.4938	1.4702	0.9671	0.9981	0.9136	5.5178	0.9913
122	0.5779	1.5095	1.4864	0.9677	0.9981	0.9450	5.7489	0.9907

image	z-score	ΔE_{ab}^*	ADF	GSSIM	SSIM	sCIELAB	EdgeSim	SC
123	0.4554	1.4475	1.4227	0.9676	0.9982	0.8998	4.4480	0.9913
124	0.4276	2.7940	2.7756	0.9429	0.9902	1.1927	7.8188	0.9876
125	0.2744	1.4315	1.4058	0.9665	0.9980	0.8816	5.1676	0.9908
126	0.9491	1.5151	1.4917	0.9679	0.9978	0.9158	5.6877	0.9905
127	0.8007	1.5442	1.5223	0.9704	0.9981	0.9419	5.5613	0.9907
128	0.5182	1.4694	1.4438	0.9677	0.9981	0.9017	4.9324	0.9909
129	0.3372	1.5261	1.5036	0.9668	0.9979	0.9446	5.7083	0.9902
130	0.2941	1.4458	1.4218	0.9681	0.9980	0.8777	5.1426	0.9908
131	-0.2282	2.0890	2.0511	0.9533	0.9964	1.2051	7.3434	0.9809
132	0.0073	2.1891	2.1511	0.9504	0.9962	1.2599	7.8079	0.9800
133	0.2024	2.3562	2.3055	0.9196	0.9896	1.4689	11.8831	0.9778
134	0.1446	1.9327	1.8882	0.9539	0.9964	1.1342	7.3061	0.9832
135	0.0844	1.9688	1.9274	0.9548	0.9964	1.1592	6.9932	0.9832
136	-0.7426	3.8212	3.7396	0.9738	0.9921	6.7846	28.5936	0.9870
137	0.0578	3.1227	3.0264	0.9805	0.9943	5.9440	28.4428	0.9925
138	-0.2379	3.4754	3.3880	0.9817	0.9945	6.1433	29.0909	0.9912
139	0.075	3.4738	3.3891	0.9765	0.9931	6.0911	29.1345	0.9886
140	-0.358	2.9857	2.8790	0.9792	0.9942	5.5054	29.7599	0.9924
141	0.2049	3.0298	2.9412	0.9781	0.9947	5.1987	28.9853	0.9932
142	0.2495	3.7434	3.6594	0.9774	0.9938	6.1215	29.7136	0.9874
143	-0.1053	3.0390	2.9370	0.9755	0.9936	5.5217	29.6587	0.9916
144	-0.3015	2.8806	2.7793	0.9773	0.9944	5.0009	29.8526	0.9931
145	-0.0419	3.0881	2.9917	0.9783	0.9947	5.0374	29.5744	0.9911
146	0.3762	2.9498	2.8482	0.9757	0.9946	5.3293	29.2027	0.9910
147	-0.4519	3.0638	2.9651	0.9797	0.9948	5.2762	29.7964	0.9924
148	-0.3918	3.2562	3.1670	0.9795	0.9956	4.9522	29.8709	0.9924
149	-0.1284	3.6873	3.6045	0.9767	0.9936	6.0544	29.8769	0.9887
150	0.0908	3.4386	3.3393	0.9771	0.9939	5.5443	29.5770	0.9900
151	-0.4983	2.8668	2.7657	0.9796	0.9953	4.7975	29.4115	0.9931
152	-0.6132	4.1037	4.0333	0.9767	0.9931	6.9859	29.7347	0.9862
153	-0.151	2.9278	2.8266	0.9779	0.9946	4.7334	30.7521	0.9921
154	0.0419	3.0483	2.9481	0.9784	0.9943	5.0790	30.3489	0.9917
155	-0.3786	3.2511	3.1677	0.9791	0.9944	5.4140	30.0831	0.9904
156	-0.4983	2.8166	2.7373	0.9890	0.9950	5.8233	28.6992	0.9944
157	-0.2943	3.3525	3.3030	0.9868	0.9943	5.7931	27.3881	0.9931
158	-0.2126	3.6657	3.6239	0.9874	0.9951	5.8360	26.9280	0.9944
159	-0.1494	3.6371	3.5981	0.9867	0.9951	5.6936	26.5220	0.9942
160	0.0419	3.6000	3.5606	0.9871	0.9945	5.8880	27.0155	0.9935
161	-0.3096	3.6814	3.6387	0.9869	0.9950	5.7476	26.4078	0.9940
162	0.0287	3.8490	3.8085	0.9882	0.9951	5.8685	26.3498	0.9943
163	0.4746	3.7305	3.6919	0.9874	0.9945	5.8983	27.4510	0.9935

image	z-score	ΔE_{ab}^*	ADF	GSSIM	SSIM	sCIELAB	EdgeSim	SC
164	0.4258	3.3719	3.3193	0.9864	0.9944	5.7756	26.8967	0.9938
165	0.2411	4.3946	4.3424	0.9752	0.9925	6.7576	28.6193	0.9911
166	0.0817	3.5003	3.4565	0.9875	0.9949	5.6220	27.4387	0.9941
167	0.2518	3.2000	3.1463	0.9860	0.9941	5.7771	27.0438	0.9931
168	-0.3522	3.5667	3.5218	0.9854	0.9947	5.8127	26.3157	0.9939
169	0.0185	3.4278	3.3752	0.9836	0.9956	4.8212	27.5739	0.9957
170	0.1173	3.5037	3.4600	0.9889	0.9948	5.7439	27.7334	0.9939
171	-0.0419	3.4507	3.4028	0.9875	0.9947	5.6907	29.6701	0.9939
172	-0.2311	3.7108	3.6707	0.9864	0.9947	5.8769	26.5466	0.9939
173	-0.2442	3.6118	3.5704	0.9875	0.9948	5.8952	27.3805	0.9942
174	-0.0557	3.4236	3.3791	0.9873	0.9945	5.7720	26.1398	0.9936
175	-0.0419	3.5801	3.5376	0.9870	0.9944	5.8413	27.6225	0.9935
176	-0.1662	3.7136	3.6413	0.9798	0.9924	6.3758	29.9826	0.9883
177	0.0419	3.7573	3.6835	0.9795	0.9925	6.3908	29.9172	0.9883
178	-1.3647	4.6678	4.6050	0.9721	0.9893	6.6172	28.7900	0.9842
179	0.028	4.3004	4.2394	0.9791	0.9928	7.0852	29.0712	0.9871
180	0	4.3192	4.2636	0.9808	0.9929	6.8734	28.9639	0.9870

profile	z-score	PG	KM	PML*	PML*a*b*
1	-0.4282	1.1966	2.0479	3.9785	4.3934
2	-0.5373	1.2473	1.9617	4.0054	4.5132
3	-0.2476	1.2706	2.0769	3.9106	4.3771
4	-0.4347	1.1298	1.7818	4.0566	4.4253
5	-0.4888	1.2330	2.0769	3.7788	4.3752
6	-0.7399	1.3712	2.3146	3.8926	4.4666
7	-0.4673	1.2416	1.8592	4.0121	4.3372
8	-0.4016	1.2114	1.7818	3.8985	4.3580
9	-0.7016	1.0654	1.6382	3.7277	4.3385
10	-0.5365	1.3208	2.1774	3.7730	4.2733
11	-0.5201	1.1749	2.0169	3.9924	4.3636
12	-0.3753	1.1108	1.6382	3.6376	4.2751
13	-0.6338	1.0966	1.7818	3.7285	4.3420
14	-0.3254	1.1433	1.8592	4.0188	4.4851
15	-0.5266	1.3169	2.2856	4.1631	4.6839
16	-0.4894	1.1453	2.0007	3.6906	4.2667
17	-0.1963	1.1449	2.0169	3.7765	4.3209
18	-0.5596	1.1043	1.9237	3.5319	4.1909
19	-0.4084	1.4196	2.3146	3.3278	4.1413
20	-0.2854	1.6683	2.3146	3.4613	4.1942
21	0.6206	1.1389	1.6382	0.9624	1.3575
22	0.2030	1.0012	1.6380	1.0654	1.2960
23	0.3152	1.0875	1.6382	0.9866	1.1937
24	0.5597	0.9566	1.6090	0.8835	1.0983
25	0.1330	0.9566	1.6382	0.9137	1.1369
26	-0.3270	0.9121	1.6087	1.0620	1.5329
27	0.5928	0.7538	1.5076	0.8838	1.1687
28	0.3384	1.1513	1.7818	0.8396	1.0265
29	0.5516	1.1079	2.0779	0.9856	1.1593
30	0.7239	1.0048	1.6090	7.9096	51.6103
31	0.7262	1.0889	1.6382	0.8209	1.0684
32	0.5658	0.9278	1.5076	0.9575	1.2225
33	0.1461	1.2185	2.0169	0.8245	1.0426
34	0.7433	1.0875	1.6382	3.5226	3.4747
35	0.5815	1.0989	2.2314	0.9020	1.1311
36	0.6431	1.0726	1.6170	1.0046	1.2926
37	0.6279	0.9773	1.6382	0.7949	1.1075
38	0.2809	1.0124	1.6382	0.8085	0.9902
39	0.7137	1.0834	1.8844	1.0700	1.3346
40	0.5742	1.0769	1.6382	0.8634	1.2593
41	-0.4906	1.8081	2.3146	3.3582	3.9984
42	-0.5030	1.2082	1.6382	3.7940	4.2009
43	-0.7423	1.1010	1.6090	6.0530	4.6394
44	-0.4164	1.1822	1.9617	3.3840	4.0554
45	-0.5913	1.2881	2.0169	3.3554	4.0619

Table 39: PG,KM,PM L^*,PM $L^*a^*b^*$ values of each profile
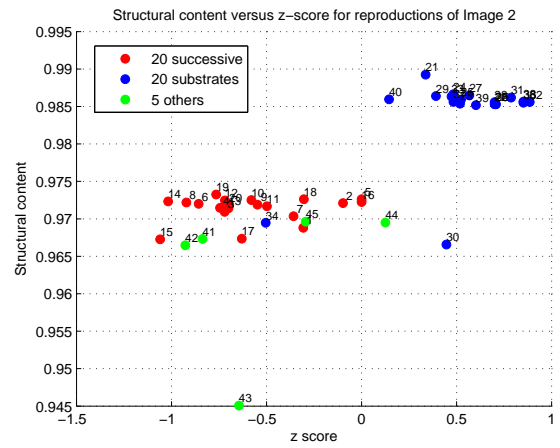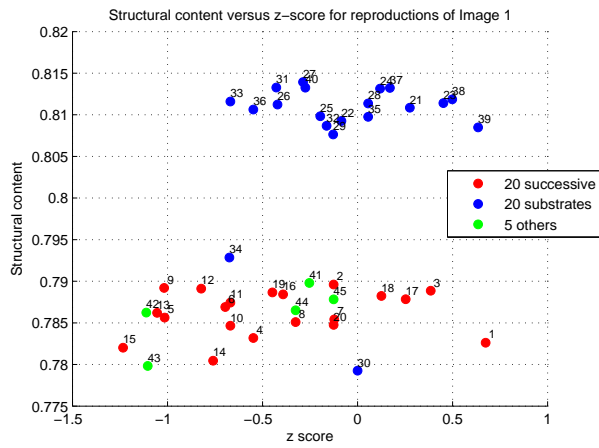
a)for 45 reproductions of image 1(corr=0.41));

b)for 45 reproductions of image 2(corr=0.77);
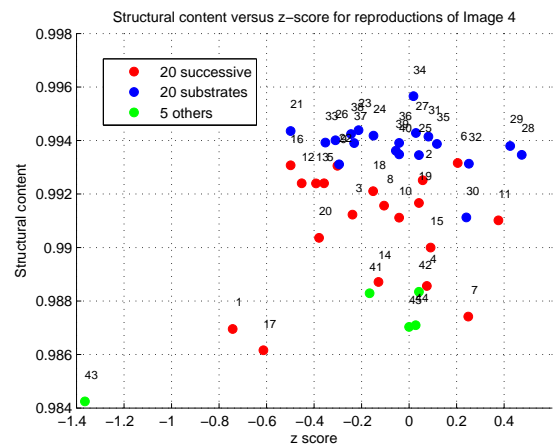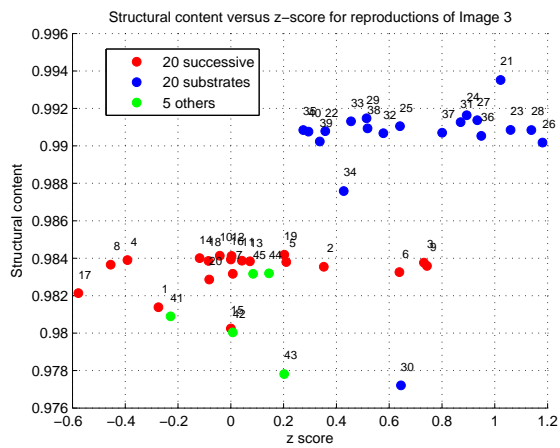
c)for 45 reproductions of image 3(corr=0.65);

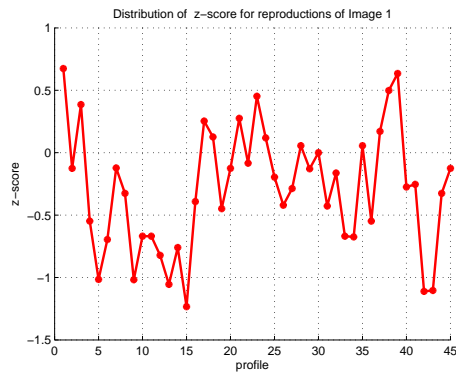d)for 45 reproductions of image 4(corr=0.31).

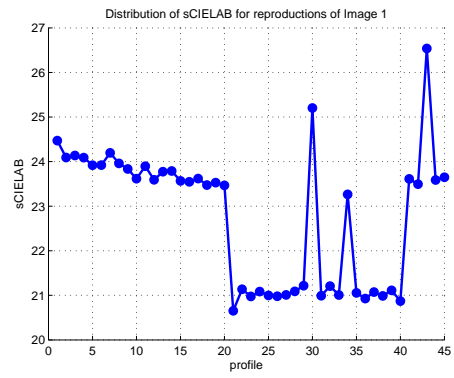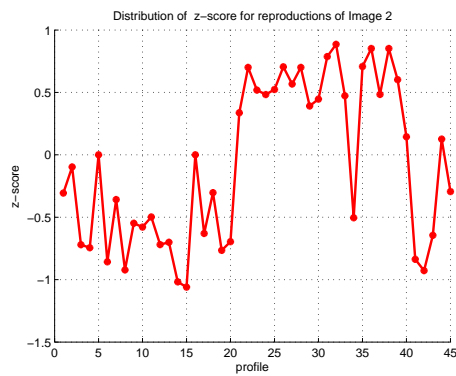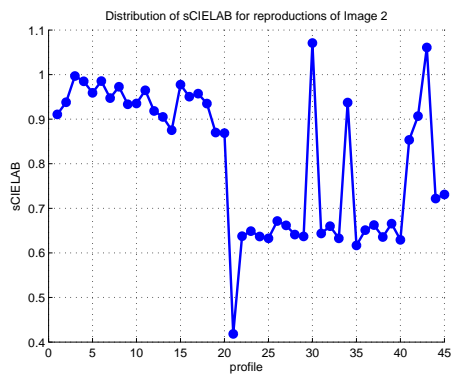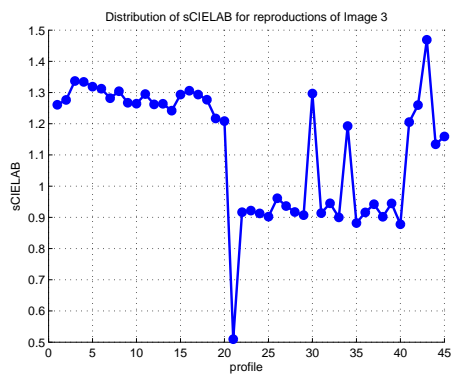Figure 92: Structural content versus z scores for reproductions of images
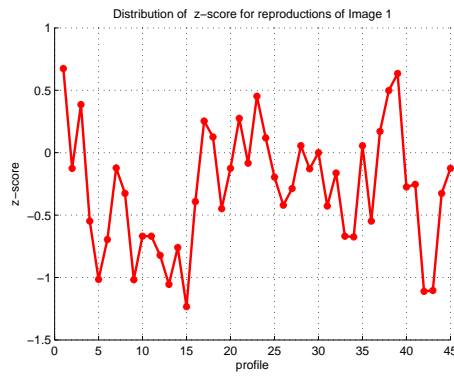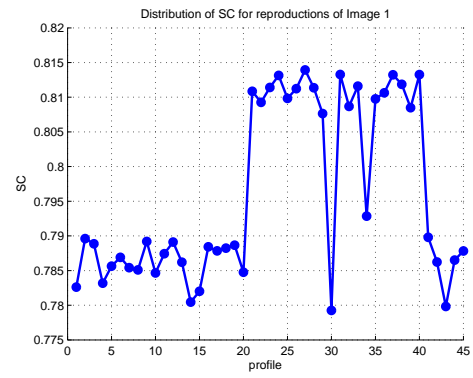
Image 1
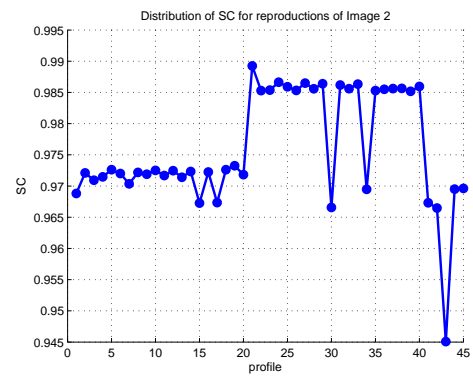
Image 1
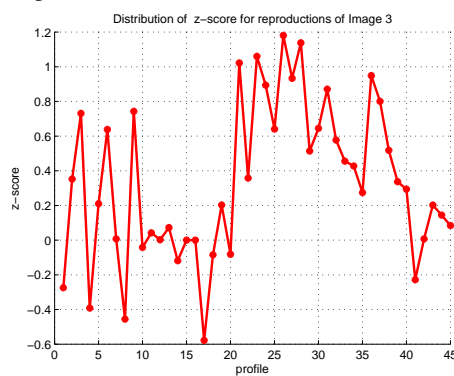
Image 2
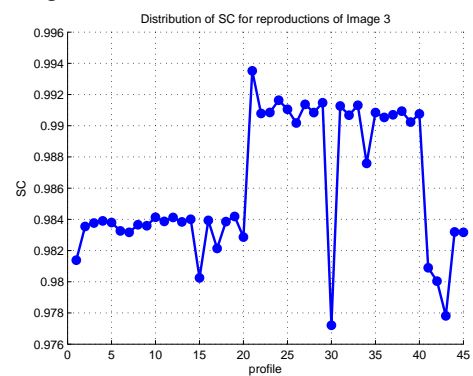
Image 2
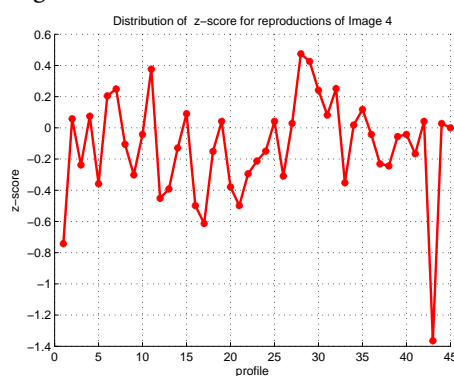
Image 3
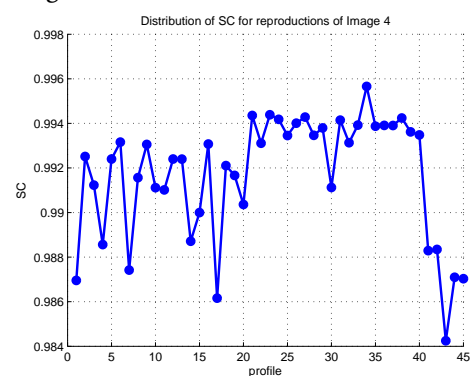
Image 3

Image 4

Image 4
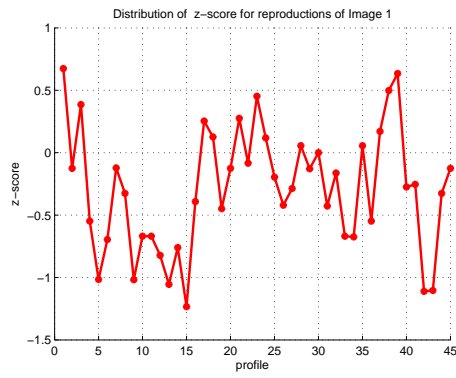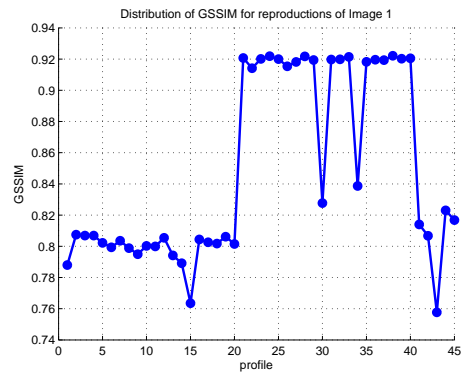
Figure 93: Structural content and z scores values distributions for 45 reproductions of images
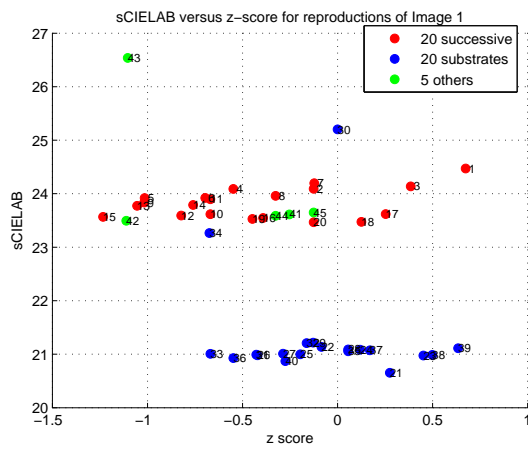
a)for 45 reproductions of image 1(corr=-0.38);
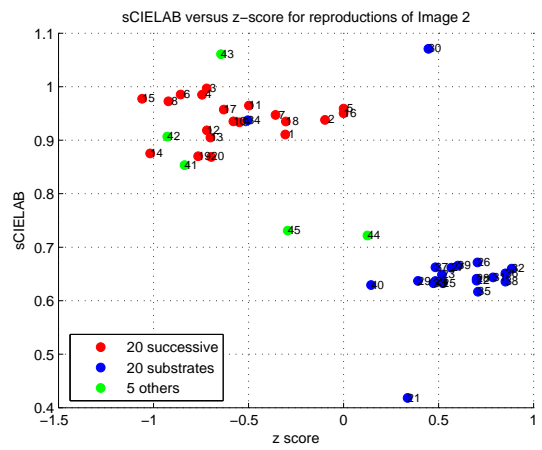
b)for 45 reproductions of image 2(corr=-0.78);
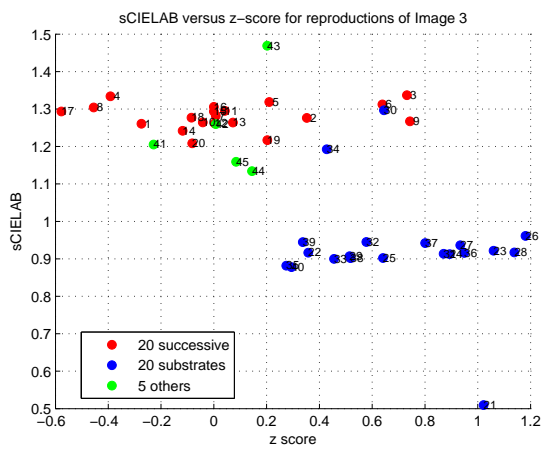
c)for 45 reproductions of image 3(corr=-0.65);
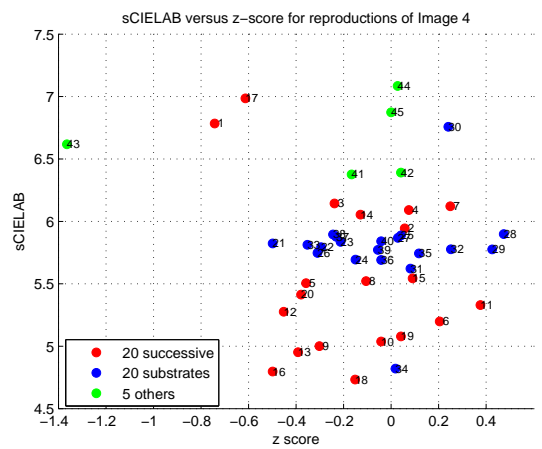
d)for 45 reproductions of image 4(corr=-0.12).

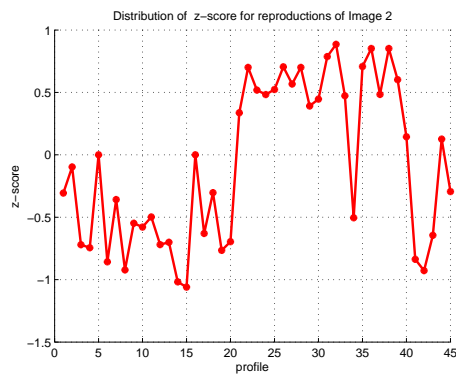Figure 94: sCIELAB versus z scores for reproductions of images
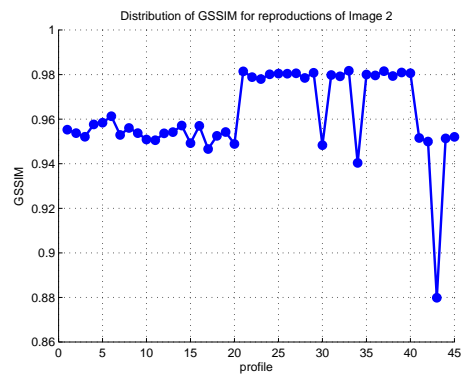
Image 1

Image 1
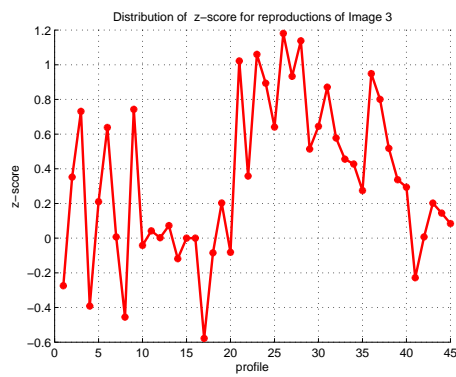
Image 2

Image 2
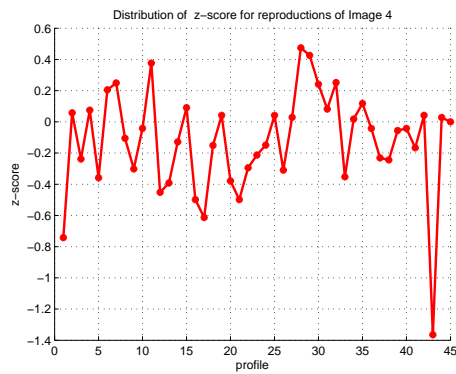
Image 3
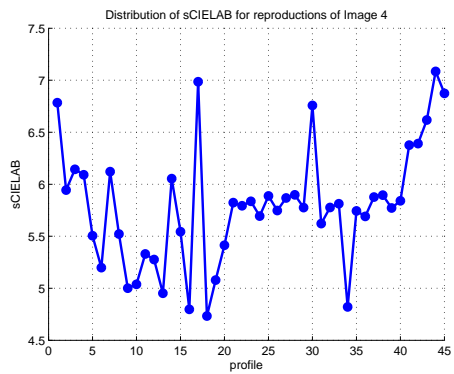
Image 3

Image 4

Image 4

Figure 95: sCIELAB and z scores values distributions for 45 reproductions of images

155
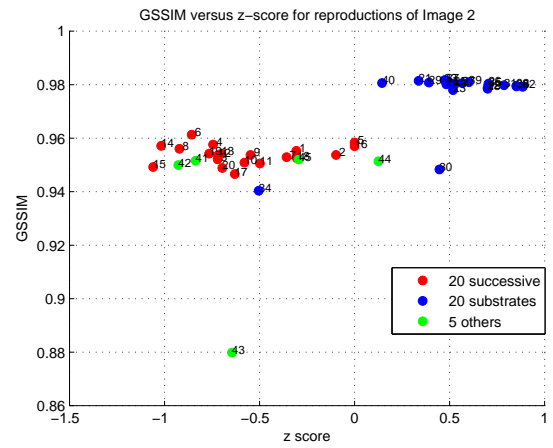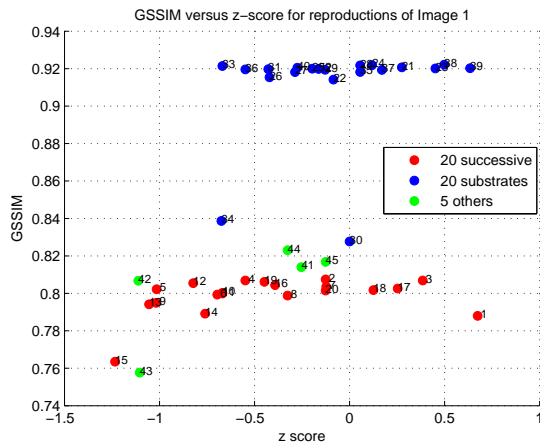
a)for 45 reproductions of image 1(corr=0.46); b)for 45 reproductions of image 2(corr=0.70);
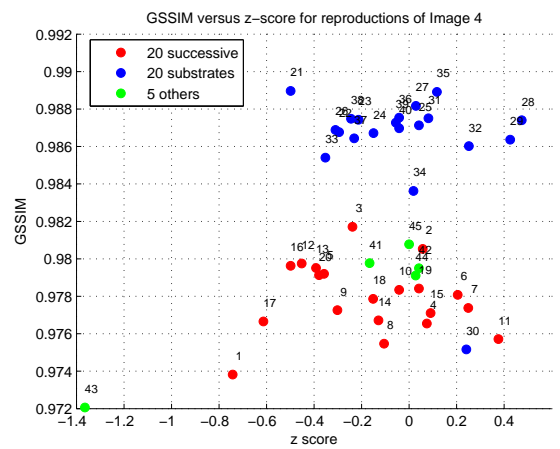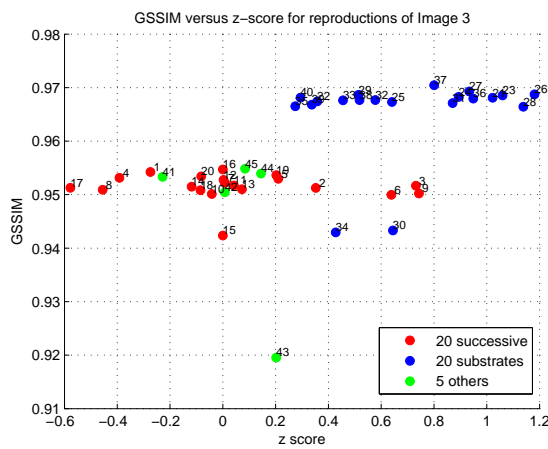
c)for 45 reproductions of image 3(corr=0.54); d)for 45 reproductions of image 4(corr=0.25).

Figure 96: GSSIM versus z scores for reproductions of images
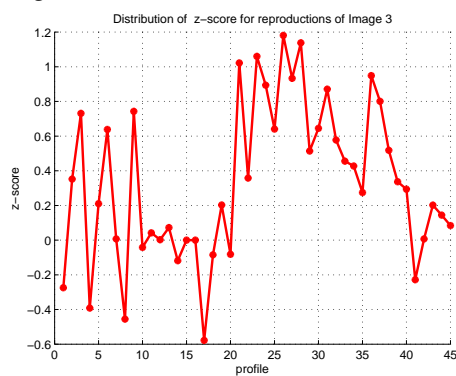
Image 1

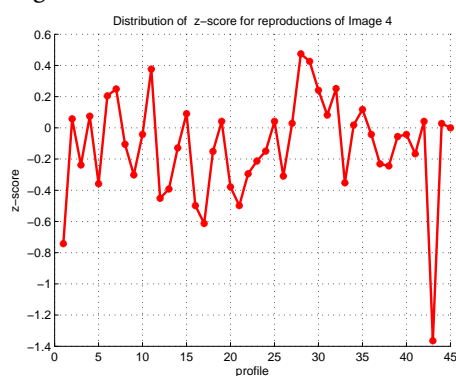Image 1

Image 2

Image 2

Image 3

Image 3

Image 4

Image 4

Figure 97: GSSIM and z scores values distributions for 45 reproductions of images